University of Stavanger

Faculty of Science and Technology

MASTER'S THESIS

Study program/ Specialization: Master of Science in Environmental Technology – Offshore Environmental Engineering	Spring semester, 2011 Open / ~~Restricted access~~
Writer: Kristin Torgersen Ravndal	..... (Writer's signature)
Faculty supervisor: Roald Kommedal External supervisor(s):	
Titel of thesis: Pressure effect on biodegradation of hydrocarbons: Naphthalene and BTEX	
Credits (ECTS): 30	
Key words: Biodegradation, deep-sea, pressure, naphthalene, BTEX, bacterial community	Pages: 88 + enclosure: 8 Stavanger, 29.06.2011 Date/year

Frontpage for master thesis
Faculty of Science and Technology
Decision made by the Dean October 30th 2009

Master's Thesis in Environmental Technology 2011

Pressure Effect on Biodegradation of Hydrocarbons: Naphthalene and BTEX

Kristin T. Ravndal

Abstract

Oil and gas are the most important energy resources in the global economy today. Even though there is a growing concern for global heating, no real alternatives have been found. Current political disturbances in the Arab Countries give an increased interest in oil and gas coming from the Western producers. However in these areas the volumes and current reserves are in decline and new areas must be opened for explorations. This will in turn increase exploration and production in deep-sea environments.

These deep-sea environments are vulnerable due to harsh weather conditions and vast fish resources. Hence, it is paramount that production of oil and gas is done in a way that not damage this environment. Last year the oil spill by Deepwater Horizon was a warning of the possibility of damaging oil spills that the industry must prepare for, and even more important, the industry must understand the possible environmental effects of future incidents.

This thesis sheds new light on biodegradation in the deep-sea environment. This process is one of the important parts of natural remediation of environments polluted by hydrocarbons. It is first and foremost a part of nature's own defence mechanism to cope with vast amounts of organic pollutants released to a vulnerable part of the ocean.

Experiments were performed to assess the effect of pressure on biodegradation of naphthalene and BTEX in seawater. Substrate removal and growth of bacterial cells were analysed. Removal of naphthalene was detected for samples at atmospheric pressure, but not for pressurised samples after 34 days. BTEX degradation was not detected in samples at 1 bar after 28 days, but seen after 35 days. At 80 bars degradation started between day 42 and 52. No degradation was detected after 56 days for 170 bar and 60 days for 340 bar. This indicates that increased pressure slows down the degradation process by prolonging the lag phase, hence prolonging the time needed by natural processes to remove a potential oil spill in the deep-sea.

Weathering processes for oil released to surface waters include evaporation to the atmosphere and degradation by UV radiation from sun light, neither of which is possible weathering processes in the deep-sea. Biodegradation is thus even more important as a natural process for removal of oil in the deep parts of the ocean. A prolonged lag phase, and hence a higher concentration of hydrocarbons in the ocean for a longer period could thus have large consequences for the ecosystem in the deep-sea. With the possibility of oil spreading to a large geographical area by ocean currents, and uptake and bioaccumulation of xenobiotics in food chains, a vast oil spill could have catastrophical effects on the aquatic environment.

Analysis of bacterial diversity shows that diversity decreases when the bacterial community is exposed to BTEX. The species found in samples incubated at 340 bar are also very different from samples from lower pressures, indicating that pressure affect which species that grow. Fewer species from seawater collected at 80 meters depth will tolerate being compressed to a pressure of 340 bar, than to 80 or 170 bar.

There are weaknesses in the methods used in this experiment. The lack of continuous monitoring renders it impossible to detect the exact moment the exponential phase starts. It also makes sampling at the right moments in the growth difficult. The seawater used in the experiment was collected from 80 meters depth, hence the bacteria used at elevated pressures are not initially piezophilic. Different behaviour can thus not be excluded for an inoculum collected from the deep-sea.

More experiments should be done to check if the data found indicating this pressure effect is reproducible. Further work should also focus on extending the numbers of substrates tested, and to improve the experimental method utilised in this work. Seawater collected from the arctic could be used to get closer to the actual ecology in the deep-sea, because of similarities between psychrophilic and piezophilic bacteria. The number of pressures analysed should also be expanded, and research should be done to find out at what depth pressure starts to affect biodegradation.

Contents

List of figures

List of tables

Abbreviations

BOD	Biological oxygen demand
BTEX	Benzene, toluene, ethylbenzene and xylene
DAPI	4,6-diamidino-2-phenylidole
DGGE	Denaturing gradient gel electrophoresis
DOC	Dissolved organic carbon
FEP	Fluorinated ethylene propylene
FID	Flame ionisation detector
GC	Gas chromatograph
HS-GC	Static headspace gas chromatograph
MUFA	Monounsaturated fatty acid
Omp	Outer membrane protein
POC	Particulate organic carbon
POM	Particulate organic matter
PUFA	Polyunsaturated fatty acid
TMAO	Trimethylamine N-oxide
TOC	Total organic carbon

1 Introduction

Already in the mid 1970s there was a growing concern about hydrocarbons being released to the deep-sea and the environmental effect this had (Schwartz et al., 1974). Even though more than 35 years has passed since then, the question is still not solved.

Oil and gas are the most important energy sources in the global economy, and even with the growing concern for global heating, there are no real alternatives in the foreseeable future. With the current political disturbance in the Arab Countries an increased interest in oil and gas coming from the Western producers can be expected. However, the production volumes and current reserves are in decline. New and deeper areas have to be opened for exploration, and this will in turn increase exploration and production in more deep-sea environments.

These environments are vulnerable due to harsh weather conditions and vast fish resources. Hence it is paramount that the oil and gas industry are capable of producing energy without seriously damaging the environment.

Last year the largest offshore oil spill in history took place in the deep-sea of the Gulf of Mexico following the Deepwater Horizon blowout (Camilli et al., 2010). This was a warning that the possibility of damaging oil spills is a threat the offshore oil and gas industry must prepare for, and even more important, the industry must understand the possible environmental effect of future incidents. Another industry of concern is the shipping industry. Oil and gas are transported across the oceans in big tankers. Should an accident happen, these ships can sink to huge ocean depths where oil and gas can be released for extended periods of time. This type of accident happened outside the coast of Spain in 2002 when the tanker Prestige sank to 3850 m sea depth, and fuel oil spilled out from the tanker for months (Uad et al., 2010).

Exploration for oil and gas in deeper and deeper water, and accidents like these two make it even more important to understand the deep-sea environment, its inhabitants and their ability to cope with oil contamination. It is important to study and characterise the physical, chemical and biological factors significant for this biome and get an understanding of what will happen to hydrocarbons released there.

Biodegradation is one of the most important processes the natural environment has to cope with oil spill. Since the deep-sea is also characterized by low temperature, an effect on biodegradation in the deep-sea might be a temperature effect similar to arctic environments, and not a pressure effect. Hence looking at pressure as a factor in the biodegradation process is important to get a clearer

picture of this process in the deep-sea. Both research on degradation of complex hydrocarbon solutions like crude oil or fuel oil, and on specific hydrocarbons found in oil are important to get a wider understanding of the fate of hydrocarbons released to the oceanic deepwater environment.

The goal of this research is to assess whether pressure has an effect on biodegradation of hydrocarbons in seawater. The experiments will be performed as biodegradation experiments of naphthalene, and benzene, toluene, ethylbenzene and xylene (BTEX). Experiments will be performed at constant low temperatures (simulating the psycrophilic deep water environment), while ocean depths are simulated by incubation at 1 bar, 80 bar, 170 bar and 340 bar.

2 Theory

When looking at biodegradation of hydrocarbons in extreme environments it is important to have an understanding of the environment and the chemicals that are studied. This chapter is meant to present the special physical, chemical and biological characteristics of the deep-sea. Possible biodegradation pathways under normal conditions of the hydrocarbons used in this experiment is described, and current knowledge of biodegradation of hydrocarbons in the deep-sea is reviewed.

2.1 The deep-sea environment

The oceans have an average depth of about 3800 m (Bartlett, 2002). The deep-sea, also called the piezosphere, is generally considered as the volume of the sea with depths greater than 1000 m (Kaneko et al., 2000; Fang et al., 2010). This is about 75 % of the total global ocean volume (Fang et al., 2010).

The ocean can be divided into zones by depth. From 0-200 meters sea depth is the epipelagic zone, the mesopelagic zone follows from 200-1000 meters, the bathypelagic zone from 1000-3000 meters, the abyssal zone from 3000-6000 meters, and the hadal zone from 6000 meters and downwards (Nagata et al., 2010; Lauro and Bartlett, 2008; Arístegui et al., 2009). The limits between zones are not strictly defined, and the bathypelagic zone is defined down to 4000 meters in Arístegui et al. (2009) and 5000 meters in Nagata et.al. (2010).

Common for deep-sea environments is the high hydrostatic pressure, from 100 bar at 1000 meters water depth, to about 1100 bars in the deepest part of the ocean in the Marian Trench (Kato et al., 1998; Kaneko et al., 2000). The temperature is low and very stable between -1 and 4 °C, except for areas around hydrothermal vents where it locally can be up to about 400 °C (Kaneko et al., 2000; Nagata et al., 2010; Fang et al., 2010). There is a high availability of inorganic nutrients (Arístegui et al., 2009; Hewson et al., 2006), while availability of organic matter is limited (Fang et al., 2010). For heterothrops this makes the deep-sea an oligotrophic and often carbon limited environment.

The bathypelagic zone is in general oxygenated (Nagata et al., 2010). There are high amounts of oxygenated inorganic nutrients like NO_3 and PO_4 available, while the availability of reduced compounds including ammonium is limited (Nagata et al., 2010). Compared to the surface, the physical conditions are stable while concentration and composition of organic compounds are variable (Nagata et al., 2010).

Localised large inputs of food occurs in the areas around the hydrothermal vents (Prieur et al., 1995), cold seeps (Elvert et al., 2000) and whale falls (Lundsten et al., 2010). Hydrothermal vents and cold

seeps are characterized by availability of reduced inorganic compounds and chemoautotrophs dominates (Lauro and Bartlett, 2008).

Organic carbon is supplied discontinuously by transportation of complex polymers (Simonato et al., 2006), and particulate organic matter (POM) from surface waters (Arístegui et al., 2009), where particles greater than 0.5 mm are known as marine snow (Lampitt, 2001). A connection between bacterioplankton processes and flux of sinking particulate organic carbon (POC) in deep waters have been found (Nagata et al., 2000), indicating that a substantial transformation of organic carbon occurs via a route from sinking POC to dissolved organic carbon (DOC) to assimilation in bacteria. Chrenarcheota in the deep-sea fix carbon by nitrification (Herndl et al., 2005) providing an autochthonous carbon source. This will act as an additional source of organic carbon for heterotrophic prokaryotes.

Bathypelagic, abyssal and hadal zones have water-mass residence times of centuries (Arístegui et al., 2009). Organic carbon that is respired to CO_2 in the deep sea is hence stored for centuries, before water circulation return the carbon to the upper ocean and the atmosphere above (Arístegui et al., 2009).

Grazing of prokaryotes by nanoflagellates is important in the bathypelagic ocean, even if the abundance of nanoflagellates is found to decrease with depth (Fukuda et al., 2007). Fukuda et al. (2007) found a negative correlation between prokaryote turnover time and biomass of nanoflagellates, indicating a significant grazing pressure on prokaryotes in the deep-sea exerted by nanoflagellates.

2.1.1 Biological adaptations

Piezophiles, also called barophiles, are bacteria or archaea that have optimal growth rate at pressures greater than atmospheric pressure (Yano et al., 1998; Delong and Yayanos, 1987). The word barophilic was first introduced to describe bacteria growing under increased pressure by ZoBell and Johnson (1949). Later Yayanos (1995) proposed to change the nomenclature used, and instead of barophile use the word piezophile. He reasoned that while barophile is Greek for *weight lover*, piezo is the Greek verb to press, and thus piezophile is a better suited description of this type of prokaryotes. This would also be consistent with chemistry and physics, as piezo is widely used as a prefix for pressure. Figure 2-1 illustrates the difference of piezosensitive, piezotolerant, piezophilic and hyperpiezophilic prokaryotes.

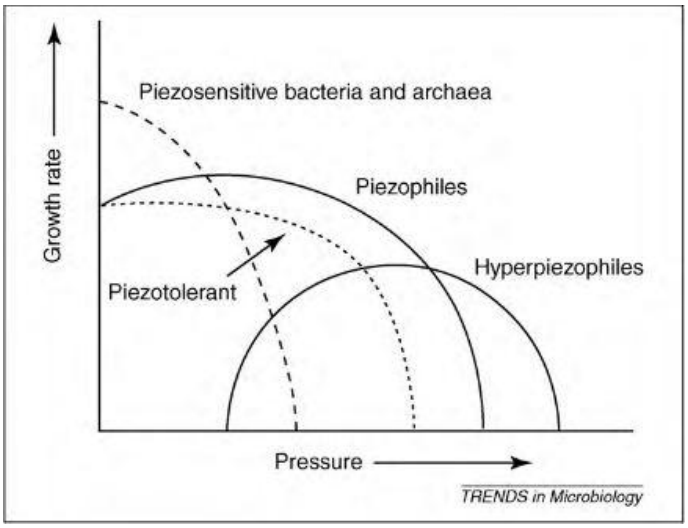

Figure 2-1: Growth rates of prokaryotes depending on pressure (Fang et al., 2010).

Prokaryotes in the deep-sea are further divided into groups depending on their optimal growth temperature (Table 2-1). For a specific bacterium, the optimum hydrostatic pressure for growth will be shifted to a higher value if the bacterium is grown at an increased temperature (Kaneko et al., 2000).

Table 2-1: Definitions of prokaryotes depending on both optimal growth pressure (P_{opt}) and optimal growth temperature (T_{opt}) (Fang et al., 2010).

P_{opt}\T_{opt}	<15 °C	15-45 °C	45-80 °C	> 80 °C
< 100 bar	Psychro-piezotolerant	Meso-piezotolerant	Thermo-piezotolerant	Hyperthermo-piezotolerant
100-500 bar	Psychro-piezophile	Meso-piezophile	Thermo-piezophile	Hyperthermo-piezophile
> 500 bar	Psycro-hyperpiezophile	Meso-hyperpiezophile	Thermo-hyperpiezophile	Hyperthermo-hyperpiezophile

Several of the effects that high hydrostatic pressure has on the cell are shown to be similar to the effect of low temperature (Kaneko et al., 2000; Lauro et al., 2007). How high pressure has to be for prokaryotes to adapt to it is hard to say, but Tholosan et al. (1999) concluded that bacteria collected from 800 m depth are adapted to living under high pressure.

The effect of high pressure on a cell is associated with volume changes induced by chemical reactions (Abe, 2007). Reactions that induce a volume decrease will be stimulated by an increasing pressure, while reactions that induce a volume increase will be inhibited.

2.1.1.1 Membrane lipids

Membranes in piezophilic microorganisms contain large amount of both monounsaturated fatty acids (MUFAs) and long chain polyunsaturated fatty acids (PUFAs) (Delong and Yayanos, 1986; Yano et al., 1998; Allen et al., 1999; Kaneko et al., 2000; Kato et al., 2008). This is to preserve functionality of the cell membrane at high hydrostatic pressures and low temperatures (Delong and Yayanos, 1986; Simonato et al., 2006). The effect on membranes from 1000 bar pressure at 2 °C is similar to the effect of -18 °C at 1 bar pressure (Simonato et al., 2006).

Several hypotheses have been proposed for the special membrane composition. One proposed explanation is that it is to maintain the fluidity of the membrane (homeoviscous adaption), similar to membrane adaptations in psychrophiles (Delong and Yayanos, 1986; Yano et al., 1998; Kaneko et al., 2000). It may also be due to piezophiles effort to maintain the membrane within a liquid-crystalline phase (homeophasic adaption) (Bartlett, 2002). Other explanations that have come up are optimisation of ion permeability across the membrane for proton translocation and ATP synthesis, and to adjust the membrane curvature due to elastic stress (Reviewed in Bartlett (2002) and Simonato et al. (2006)).

Addition of MUFAs in the membrane is found to be required for growth at high pressure (Allen et al., 1999). 16:1 fatty acid is found in all piezophilic and psychrophilic bacteria analysed, hence this fatty acid seems to be a requirement for growth at high pressure (Kato et al., 2008). Production of long-chain PUFAs doesn't seem to be a requirement, but it is a common property for piezophiles (Kato et al., 2008).

2.1.1.2 Membrane proteins

In *Photobacterium profundum* strain SS9, ToxR regulates the gene expression of the two outer membrane protein (Omp) genes; *OmpH* (induced by high pressure) and *OmpL* (induced by low pressure) (Welch and Bartlett, 1998). OmpH is a type of porin, a protein forming a channel in the outer membrane for diffusion of organic molecules into the periplasm (Madigan et al., 2009). This system can also work as a pressure sensing system and it seems to depend on the physical state of the inner membrane (Bartlett, 2002). The basic function of ToxR is to maintain the right membrane structure, cope with starvation and control energy flow under diverse environmental conditions (Bartlett, 2002; Bartlett et al., 2008).

2.1.1.3 Transporter

The cellular process that appears to be most affected by high hydrostatic pressure is membrane transport (Campanaro et al., 2005). Glucose transport is inhibited by a high hydrostatic pressure (Delong and Yayanos, 1987). Transportation of glucose and tryptophan are accompanied by a large

positive volume change (Abe and Horikoshi, 2000). This induces the inhibition of its transportation at high pressure.

The result of this inhibition can be a modification of transporter proteins that transport critical compounds for the cell in piezophiles (Simonato et al., 2006). *Photobacterium profundum* SS9, a bacterium growing at a large range of pressures, have two or more copies for transporters in its genome (Campanaro et al., 2005). These are up-regulated at different pressures and temperatures, hence they might function at different environmental conditions.

2.1.1.4 Other adaptations

Other biological adaptations also exist. Some are associated with cell division and cell morphology. It has been shown that for SS9 RecD is required for cell division and normal cell morphology at high pressure (Bidle and Bartlett, 1999). RecD is a specialised enzyme that takes part in homologous recombination in *E.coli* (Madigan et al., 2009). Piezophilic prokaryotes that are grown at a pressure different from their optimal growth pressure are filamentous, this could be due to a pressure effect on DNA replication or condenstation (Reviewed in Bartlett (2002)). Filamentous growth is also seen for mesophilies incubated at elevated pressure (Zobell and Cobet, 1964; Zobell and Oppenheimer, 1950; Zobell and Cobet, 1962), indicating that for mesophiles cell division is more sensitive to pressure than cell growth (Bartlett, 2002).

Pressure effects on gene expression have also been demonstrated. For gene expression in the piezophilic *Shewanella* a σ^{54} factor and an enhancer-binding pressure-responsive protein is required (Bartlett, 2002). The σ^{54} factor is an alternative sigma factor that is required for nitrogen assimilation (Madigan et al., 2009).

High hydrostatic pressure affects the DNA tertiary structure by leading to a more supercoiled DNA (Tang et al., 1998). The reason for this is the smaller volume required when DNA is compact. Single-stranded DNA binding protein homogeneity is favoured by organisms under high pressure (Bartlett, 2002).

The ribosome in piezophiles is adapted to the high hydrostatic pressure by specific long ribosomal loops (Lauro et al., 2007). The ribosomal 70S particle is formed of the two ribosomal subunits 50S and 30S. As dissociation of ribosome is associated with a volume reduction (Alpas et al., 2003), dissociation/association of the two subunits could also be involved in high pressure adaption (Simonato et al., 2006).

SS9 optimise its energy gain under growth at different pressures by choosing between different metabolic pathways, like amino acid reduction, trimethylamine N-oxide (TMAO) reduction, citrate

fermentation and more (Campanaro et al., 2005). This might be because SS9 is not an obligate piezophile.

The lack of solar radiation in the deep-sea also causes biological adaptations. Since no need for UV repair exist, a light-activated photolyase gene is expected to be absent from the genome of all deep-sea bacteria (Simonato et al., 2006). Hence it is important to protect water samples from the deep-sea from sunlight.

2.1.2 Ecology, diversity and abundance

In the eutrophic zone (<200 m sea depth) and the continental shelf the estimated average prokaryotic cell density is $5 \cdot 10^5$ cells/ml, while at ocean depths greater than 200 m it is one the average $5 \cdot 10^4$ cells/ml (Whitman et al., 1998). While the total abundance decreases, the abundance of chrenarcheota increases with depth (Herndl et al., 2005). Also the relative abundance of γ-Proteobacteria increases in the deep-sea compared to surface waters, while the number of α-Proteobacteria decreases (López-García et al., 2001; Zaballos et al., 2006).

Chloroflexi-related SAR202 bacterioplankton cluster are another bacteria group where abundance increases with depth (Varela et al., 2008). In the Atlantic and the Pacific oceans the percentage of prokaryotic picoplankton identified as SAR202 increased from less than 1 % at 100 m depth, to 10-20 % in the bathypelagic zone (Varela et al., 2008; Morris et al., 2004). Below 1000 m depth the absolute abundance of SAR202 are about constant (Varela et al., 2008). In mesopelagic and epipelagic waters SAR202 accounted for less than 5 % of the total bacterial abundance, while in the bathypelagic zone it accunted for approximately 30 %, and at depths greater than 2500 m SAR202 accounted for up to 40 % of the bacterioplankton (Varela et al., 2008).

At 3000 m depth at the Antarctic Polar Front γ-Proteobacteria were found to be the most abundant and diverse in the bacterial domain, while Euryarchaeota was the most genetic diverse group in the archeal domain in the deep-sea planktonic communities (López-García et al., 2001). Euryarchaeota detected belonged to group II, III and IV.

Psychrophilic piezophiles are likely descendants of psychrophiles today found in the Polar Regions (Lauro et al., 2007). When comparing 16S sequences of psyhropiezophiles with their closest relatives Lauro et al. (2007) found that all piezophiles in their study had a high similarity with non-piezophilic bacteria isolated from Antarctica. The deep-sea has a constantly low temperature, and the effects of high pressure on cells are similar to the effects of low temperature. Thus it might seem more logical that psychrophiles would adapt to living under high pressure, than for shallow-water mesophiles to adapt to both low temperature and high pressure at the same time.

Most piezophilic prokaryotes isolated are psychrophilic facultative anaerobic Gram-negative bacteria species. These bacteria are mainly from the genus *Colwellia* (Lauro et al., 2007), *Moritella* (Nogi and Kato, 1999; Kato et al., 1998), *Photobacterium* (Nogi et al., 1998b; Kato et al., 2008), *Psychromonas* (Nogi et al., 2007), and *Shewanella* (Nogi et al., 1998a; Kato et al., 1998; Nogi and Kato, 1999; Lauro et al., 2007), all within the γ-proteobacteria.

Many piezophiles have never been isolated. Some of these have been identified by 16S rDNA-amplified sequence analysis of microbial communities at different latitudes and see depths. The deep-sea planktonic community at 3000 m depth at the Antarctica Polar Front was analysed by López-García et al. (2001) using this technique. The bacterial groups identified were the SAR 11 group within the α-Proteobacteria, SAR 324 within the δ-Proteobacteria, γ-proteobacteria, Cytophagales, Planctomyces, Gram-positives, and the SAR406 group of environmental sequences. *Colwellia* and *Shewanella* were both identified.

To describe a population of species that is genetically adapted to a certain depth in the water column Lauro and Bartlett (2008) introduced the word bathytype (where bathos is the Greek word for depth). They concluded that because there is closely related microbes that only differ in their bathytype, adaption to deep-sea likely requires relatively few genetic changes. It was shown that the deep bathytypes that are isolated are mostly r-strategist. This means that they are opportunistic and have a high degree of gene regulation (Lauro and Bartlett, 2008). The study further indicated that at intermediate depths both r-strategy and K-strategy might coexist. K-selected species are equilibrium species that usually have a population size close to the carrying capacity of the environment (Lalli and Parsons, 1997).

Research done in the eastern Mediterranean Sea, where temperature is about the same in surface water and deep-water layers, indicate that bacterial diversity in the deep sea is as complex as in surface waters, especially in the free-living community (Moeseneder et al., 2001). Bacteria attached to particles create microenvironments making them less dependent of the trophic situation in the surrounding water. When these particles are transported through the water column bacterial metabolic activity can lead to a depletion of labile particle compounds. The particles thus become more refractory and this causes a decline with depth in complexity of the community of attached bacteria. Further the research performed by Moeseneder et al. (2001) indicated that a smaller subset of the attached bacteria was metabolic active. A distinct deep-water community was found for free-living bacteria. The difference in free-living and attached bacteria communities indicates a lower vertical transport of free-living bacteria than attached bacteria, and limited exchange between these communities (Moeseneder et al., 2001).

In the deep-sea environmental parameters are assumed not to vary a lot at different geographical positions, but surface conditions can vary greatly and thus cause important variations in the nutrient supply and other factors to the deep (López-García et al., 2001). This can cause different bacteria to be detected at the same depth at different latitudes, and different ocean basins.

Bacterial biomass and production in the bathypelagic zone are higher in the subarctic zone than in the subtropical zone of the pacific ocean (Nagata et al., 2000). The biomass was found to be 2-4 times and the production 3-7 times greater in the subarctic than the subtropical zones (Nagata et al., 2000), which is consistent with a high flux of sinking POC in the subarctic and a low flux in the subtropical gyre (Berger and Wefer, 1991). At both latitudes abundance of bacteria decreased with depth (Nagata et al., 2000).

2.1.2.1 DGGE analysis

To study a changing microbial community over time, or how a microbial community changes under different physical and chemical conditions, genetic fingerprinting techniques are useful (Muyzer and Smalla, 1998). These techniques are suitable when comparing a large number of samples and they provide a banding pattern of the genetic diversity in a microbial community (Schäfer and Muyzer, 2001). One of these methods is denaturing gradient gel electrophoresis (DGGE) (Muyzer and Smalla, 1998), which was first used in microbial ecology by Muyzer et al. (1993).

In DGGE, extracted DNA is amplified with primers specific for bacterial 16S rRNA gene fragments (Schäfer and Muyzer, 2001). This gives a mixture of DNA molecules, also called PCR products, which all have similar sizes, but vary in sequences. This sequence variation gives the molecules different melting properties, and thus they can be separated in a polyacrylamide gel containing a gradient of DNA denaturants i.e. a mixture of urea and formamide.

The principle of the separation is that all the different PCR products enter the gel as double-stranded molecules (Schäfer and Muyzer, 2001). They will proceed through the gel at the same time as denaturing conditions become gradually stronger. Since the different molecules have different melting properties they will start to melt at different positions in the gel. When a molecule reach the part of the gel where the denaturing concentrations is strong enough for it to melt, called the melting domain, it changes from a double-stranded molecule to a partially melted molecule. There will be single strands projecting from this partially melted molecule, and this will prevent the molecule from travelling further in the gel. To avoid PCR products from completely dissociate into single stranded molecules, a so called GC-clamp is attached to the 5'-end of the primers used for amplification.

2.1.3 Sampling and cultivation

Bacteria from surface water attach to particles sinking in the water column. In this way they are transported to the deep-sea were they can survive in an inactive state for a long period (Lauro and Bartlett, 2008). These bacteria might become active again when they are isolated and it is thus difficult to know which bacteria isolated from the deep sea are actually piezophiles.

Not many samplers are developed for sampling without decompression and warming. Bianchi et al. (1999) developed a high-pressure serial sampler that can do this. Also JAMSTEC (Japan Agency for Marine-Earth Science and Technology) has developed a deep-sea sampling device (Kato et al., 2008).

To study piezophilic bacteria sampled from the deep-sea, it is important to handle samples quickly after retrieving them when they are still cold (Deming and Colwell, 1985). Warming of deep-sea samples causes severe changes in cell shape (Chastain and Yayanos, 1991) and should be avoided.

Decompression of samples taken from the deep-sea under a stratified-water period will cause a decrease in bacterial activity (Tholosan et al., 1999; Bianchi and Garcin, 1994; Bianchi et al., 1999). At mixed-water periods the opposite effect is shown because more surface water bacteria is transported to the deep-sea by water mixing (Bianchi and Garcin, 1994). To get a more correct picture of the piezophilic community it is thus important to take samples in the stratified water period.

In itself decompression does not lead to immediate morphological changes in a bacterial cell, but when the sample is exposed to atmospheric pressure for an extended period of time the ultrastructure in the cell is changed (Chastain and Yayanos, 1991). These ultrastructural changes are formation of intracellular vesicles, membrane fragments in the culture medium, plasmolysis, cell lysis, formation of extracellular vesicles, and formation of ghost cells.

When a deep-sea sample is decompressed the microbial community can change. Yanagibayashi et al. (1999) cultivated deep-sea sediment samples facultative anaerobically at in situ pressure and atmospheric pressure. *Shewanella* and *Moritella* survived only at in situ pressure were they coexisted in the beginning of the cultivation period. At the end of the experiment *Moritella* was the dominant strain. This shows that when oxygen supply is limited *Moritella* is better adapted than *Shewanella*. Under atmospheric pressure *Pseudomonas* was dominant under the whole cultivation period.

Also when culturing the piezophiles sampled there are difficulties involved. A practical limitation in a closed hydrostatic chamber is sufficient oxygen supply (Abe, 2007). To have an environment close to the deep-sea environment it is also important to keep a constant low temperature and prevent exposure to light.

2.2 Biodegradation

Biodegradation can be looked upon as a biologically catalyzed process leading to a reduction in a chemical's complexity (Alexander, 1999). Ultimate biodegradation, called mineralisation, leads to the products carbondioxide, water and other inorganic substances depending on the structure of the molecule being degraded (Alexander, 1999). The carbon source together with an energy source are also used for growth of new biomass.

2.2.1 Biodegradation pathways

Different chemicals will follow different routes for biodegradation depending on their chemical structure and what enzyme the microorganisms use to initiate degradation. This research focuses on bacterial degradation, and bacteria that can be found in a cold marine environment. Prokaryotes living under different environmental conditions and eukaryotic microorganisms might also have the ability to degrade the chemicals used in this research, but this will not be treated here. The following sub-chapters present biodegradation pathways submitted to the Biocatalysis and Biodegradation Data Base of University of Minnesota (Wackett and Ellis, 1996).

2.2.1.1 Naphthalene

Naphthalene is degraded by *Pseudomonas* (Eaton and Chapman, 1992) starting with dioxygenation by the enzyme naphthalene 1,2-diozygenase (Figure 2-2). This pathway leads to catechol and gentisate. Gentisate is incorporated in metabolism of the amino acid tyrosine (Kanehisa Laboratories, 2011). Catechol is further degraded to *cis*-*cis*-muconate, acetaldehyde and pyruvate (Figure 2-3), which are all part of the intermediary metabolism (McTavish, 2011). The enzyme naphthalene 2,3-dioxygenase is from the thermophilic bacteria *Bacillus thermoleovorans* Hamburg 2 (Annweiler et al., 2000), thus not studied further in this text.

Pseudomonas are a chemoorganotrophic aerobic genra that is part of the γ-proteobacteria phylum and the pseudomonad group (Madigan et al., 2009). The pseudomonad group is an ecological important group found in water and soil, and they are capable of degrading many xenobiotic chemicals (Madigan et al., 2009).

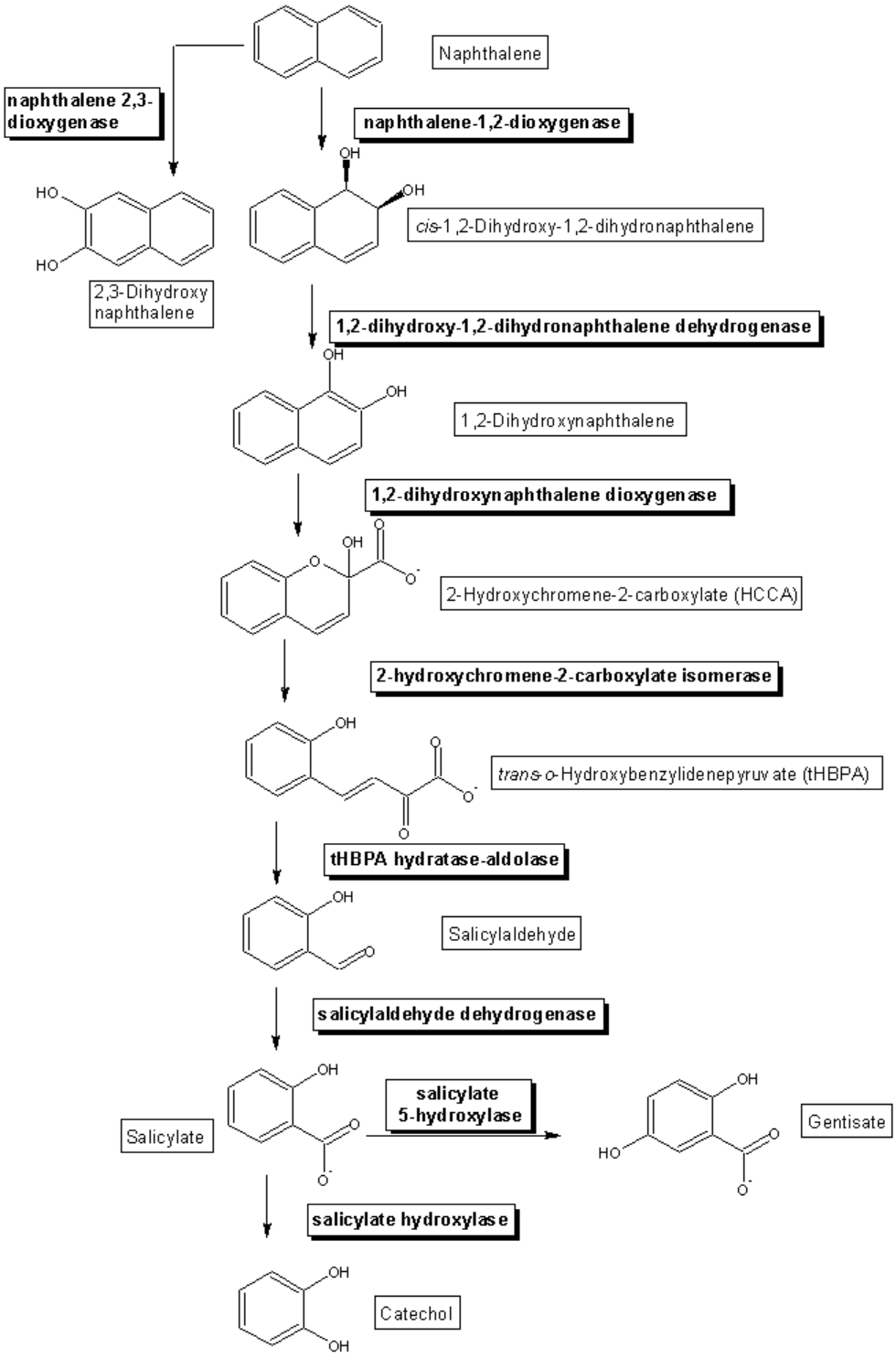

Figure 2-2: Naphthalene biodegradation pathway (Zeng and Essenberg, 2010)

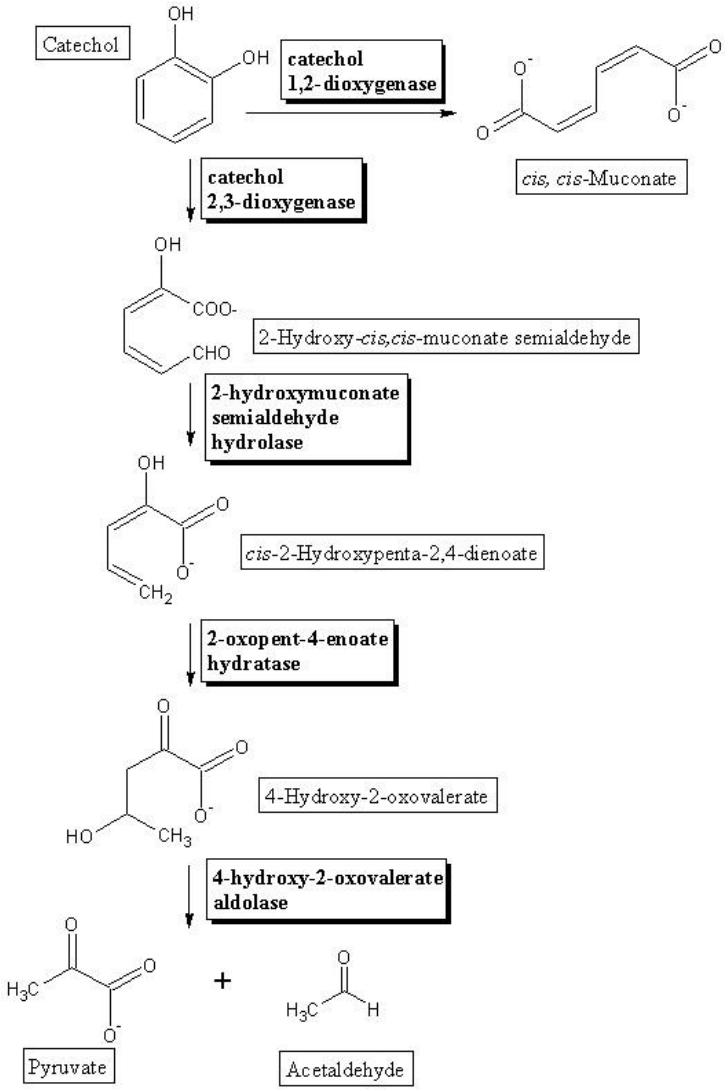

Figure 2-3: Catechol biodegradation pathway (McTavish et al., 2010)

2.2.1.2 Benzene

Benzene is degraded to catechol in two reactions (Figure 2-4). The enzyme benzene 1,2-dioxygenase can be found in *Pseudomonas Putida* (Zamanian and Mason, 1987). Catechol is further degraded to *cis-cis*-muconate, acetaldehyde and pyruvate as described in Figure 2-3. *Cis-cis*-muconate, acetaldehyde and pyruvate are part of the intermediary metabolism (McTavish, 2011).

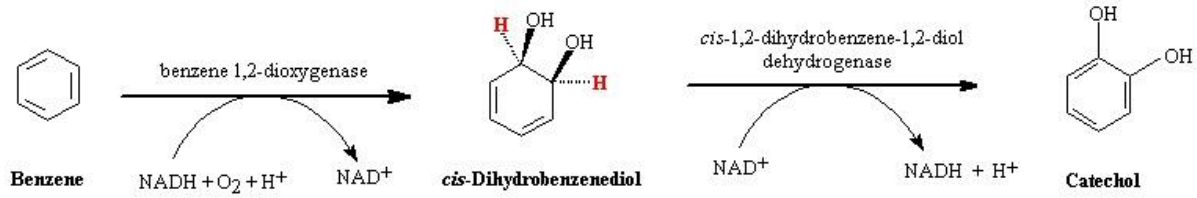

Figure 2-4: Benzene biodegradation pathway (McLeish and Wolfe, 2005; McLeish, 2005)

2.2.1.3 Toluene

Several enzymes and organisms can initiate biodegradation of toluene (Figure 2-5 and Figure 2-6).The enzyme toluene 3-monooxygenase is found in the bacteria *Pseudomonas pickettii* (Olsen et al., 1994). While the toluene dioxygenase is found in *Pseudomonas putida* (Zeng, 2011). *Pseudomonas mendocina* initiate both reactions in Figure 2-6 (Zeng, 2011).

Acetaldehyde and pyruvate are the products in the biodegradataion pathway for toluene displayed in Figure 2-5, these are part of the intermediary metabolism (Zeng, 2011). In the biodegradation pathway initiated by *Pseudomonas mendocina* the products are benzoate and 4-hydroxybenzoate (Figure 2-6).

Benzoate is further degraded to catechol and 4-hydroxybenzoate (Figure 2-7) in reactions initiated by *Pseudomonas* (Feng, 2010). Catechol is further degraded to *cis*-*cis*-muconate, acetaldehyde and pyruvate (Figure 2-3), which are all part of the intermediary metabolism (McTavish, 2011).

4-hydroxybenzoate is degraded to hydroquinone, 3-carboxy-*cis*-*cis*-muconate, 2-hydroxy-4-carboxy-muconate semialdehyde, and catechol (Figure 2-8). The enzyme catalysing the reaction where 4-hydroxybenzoate is degraded to hydroquinone is found in yeast (Eppink et al., 1997), and this pathway is thus not further studied in this text. 3-carboxy-*cis*-*cis*-muconate is part of the intermediary metabolism (Dori et al., 2011), 2-hydroxy-4-carboxy-muconate semialdehyde is further degraded to 4-oxalomesaconate as described in Figure 2-9. 4-oxalomesaconate is part of the intermediary metabolism (Danielson and Mittapalli, 2011).

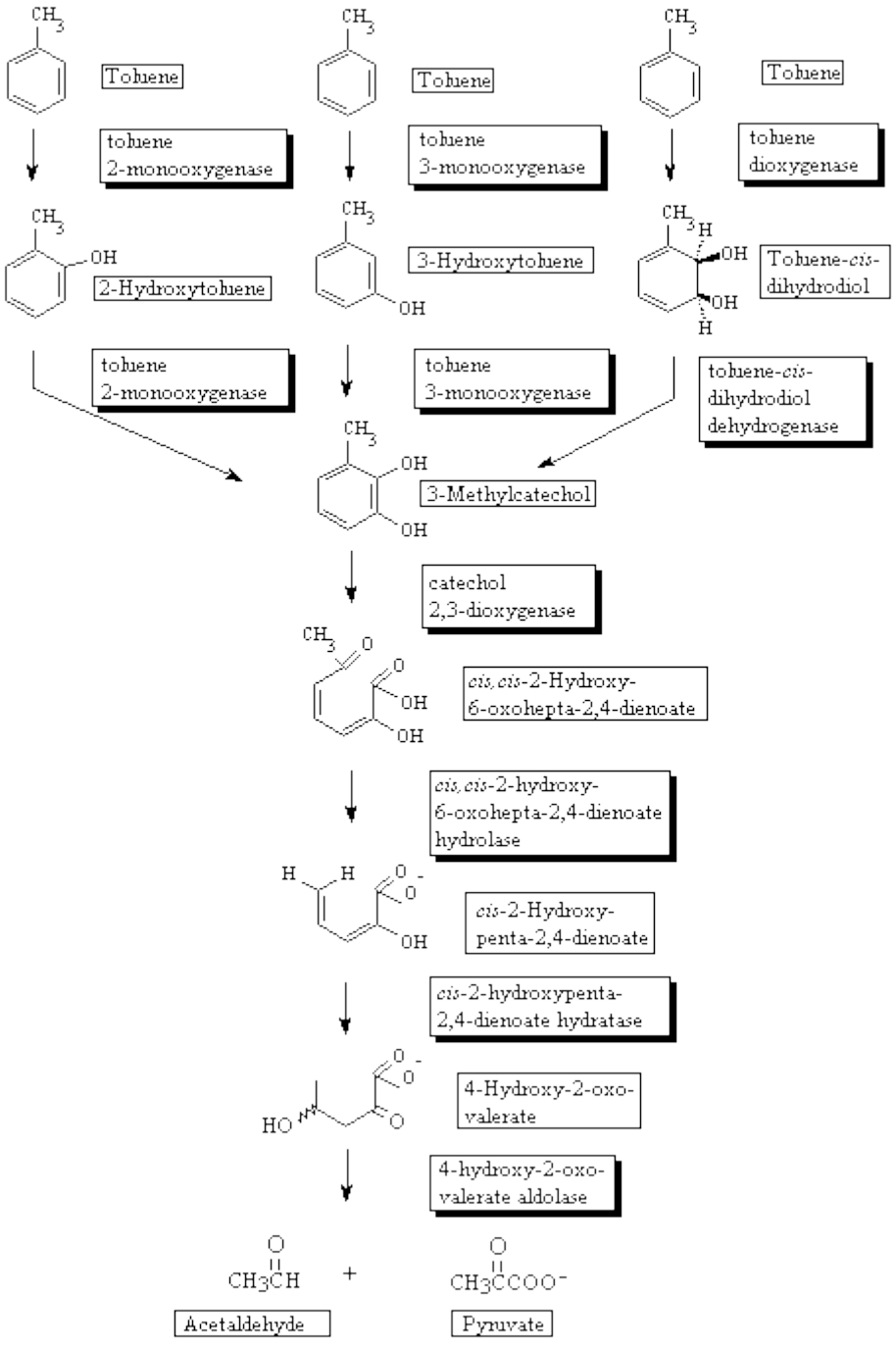

Figure 2-5: Toluene biodegradation pathway map 1 (Oh, 2006)

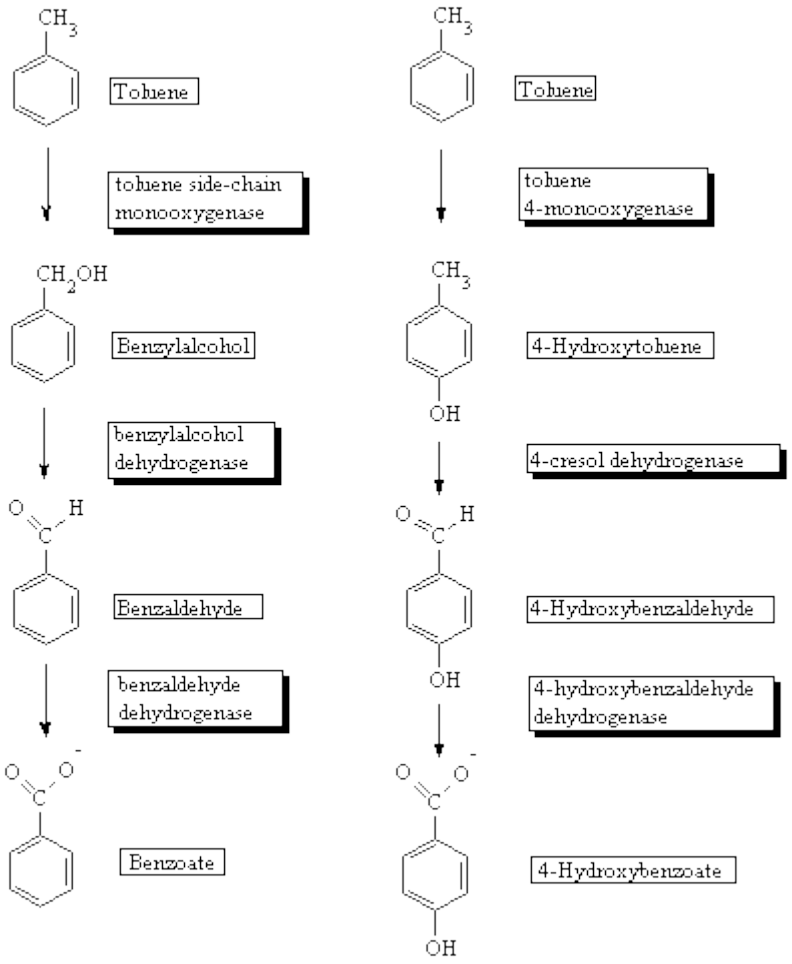

Figure 2-6: Toluene biodegradation pathway map 2 (University of Minnesota, 2006b)

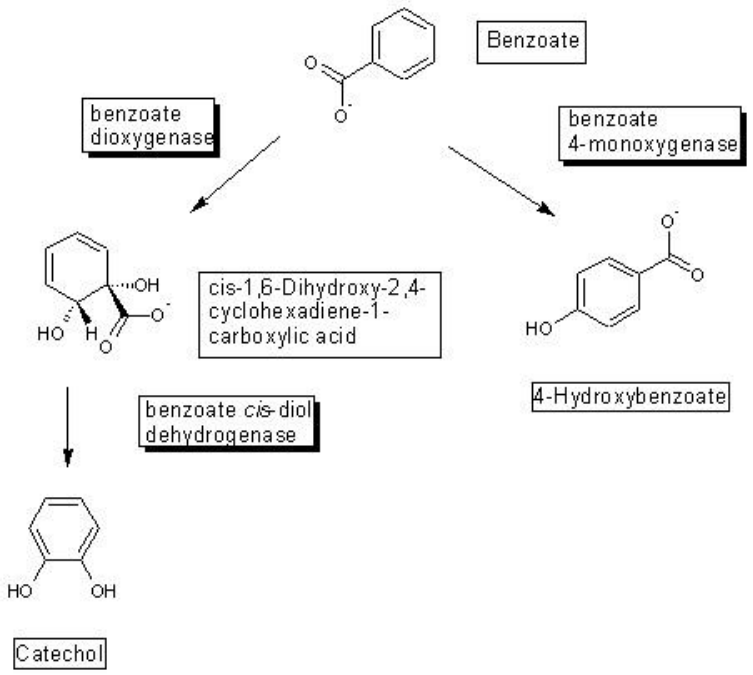

Figure 2-7: Benzoate biodegradation pathway (Feng, 2011)

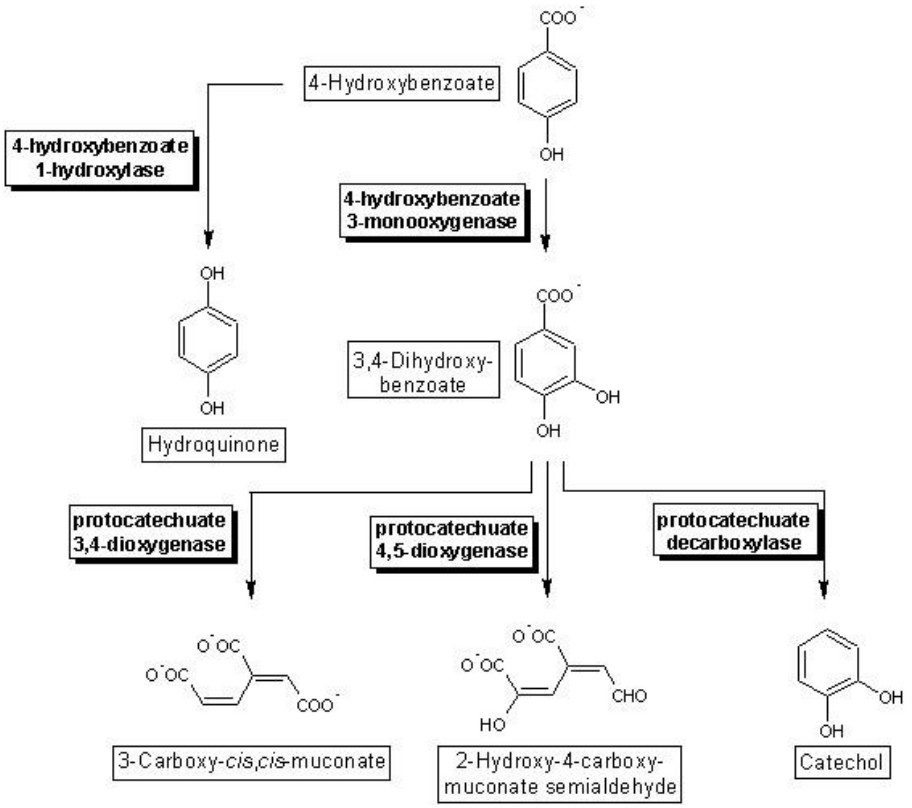

Figure 2-8: 4-hydroxybenoate biodegradation (Oh et al., 2008)

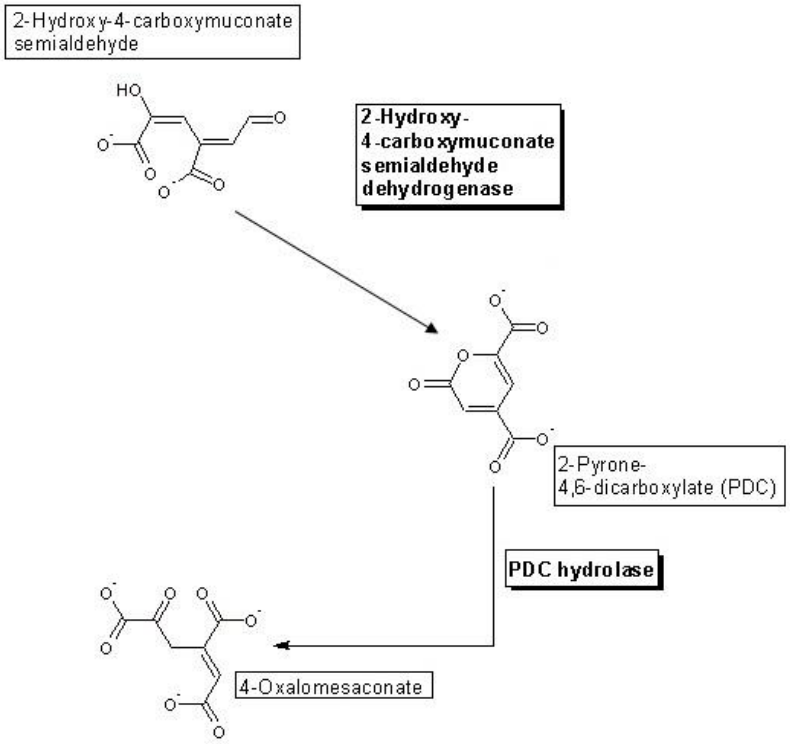

Figure 2-9: 2-hydroxy-4-carboxymuconate semialdehyde degradation pathway (Danielson and Mittapalli, 2010)

2.2.1.4 Ethylbenzene

Ethylbenzene is degraded to propanoate, acetaldehyde and pyruvate after initial dioxygenation by ethylbenzene dioxygenase (Figure 2-10). This enzyme is found in *Pseudomonas* and the products of the resulting reactions, propanoate, acetaldehyde and pyruvate, is part of the intermediary metabolism (McLeish, 2006a). Another enzyme that can initiate degradation of ethylbenzene is naphthalene 1,2-dioxygenase (Figure 2-10), ethylbenzene is then either transformed to styrene in a one step reaction, or to 2-hydroxy-acetophenone in several steps. Both these pathways can be initiated by *Pseudomonas* (McLeish, 2011). 2-hydroxy-aetophenone is not known to be further degraded.

Styrene is then degraded to fumarate and acetoacetate (Figure 2-11) initiated by the enzyme styrene monooxygenase. This enzyme and the following reaction can be found both in the yeast *Exophiala jeanselmei* and in *Pseudomonas putida* (Kraus et al., 2011). Fumarate and acetoacetate are part of the intermediary metabolism (Kraus et al., 2011).

Styrene dioxygenase is another enzyme initiating styrene degradation (Figure 2-12). This reaction can be initiated by the bacteria *Rhodococcus rhodochrous* (Kraus et al., 2011). *Rhodococcus* are soil saprophytes, meaning they live in soil on dead matter, they are also often found in the gut of various insects (Madigan et al., 2009), hence this pathway is not further studied here.

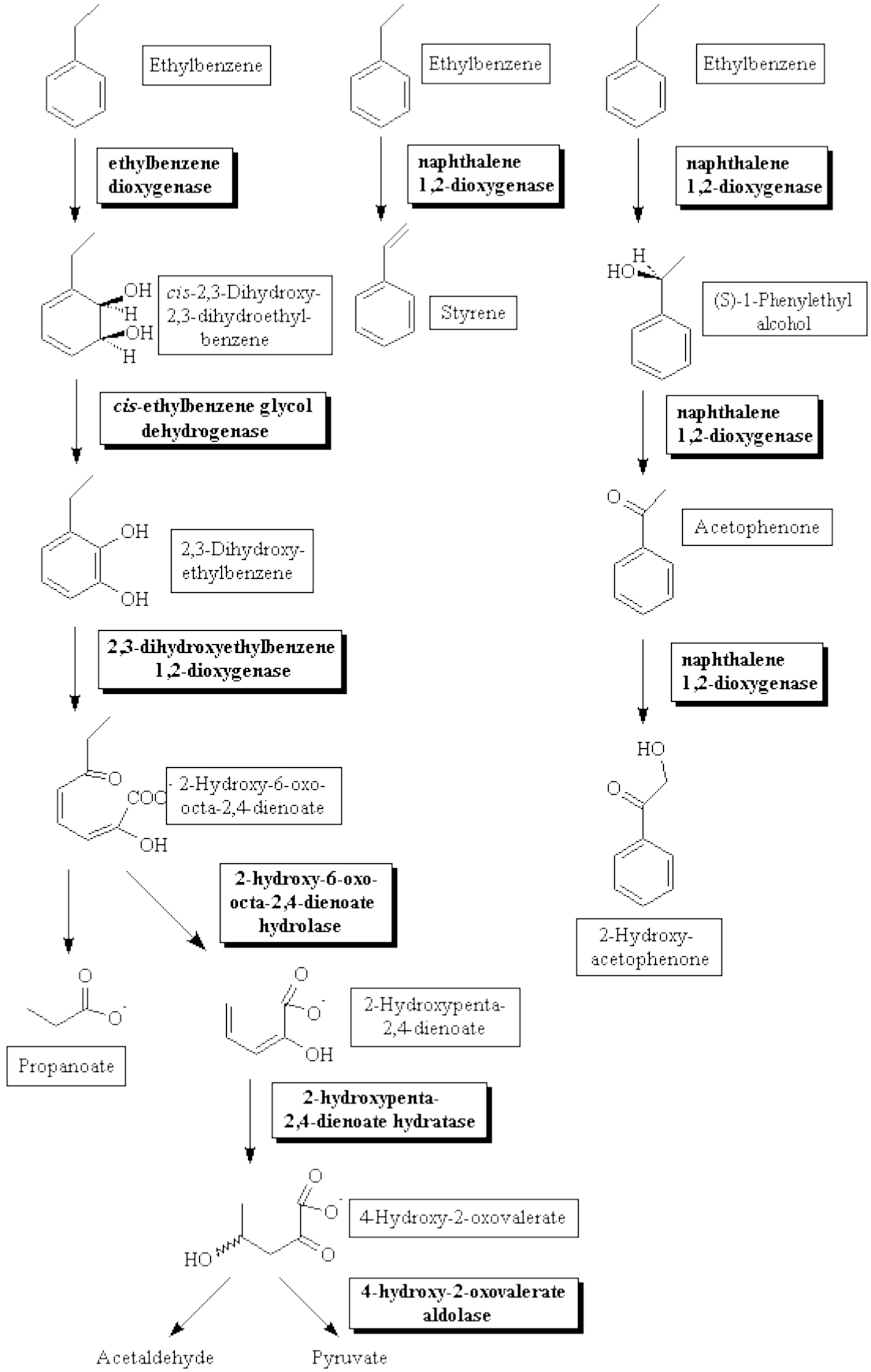

Figure 2-10: Ethylbenzene biodegradation pathway (University of Minnesota, 2006a)

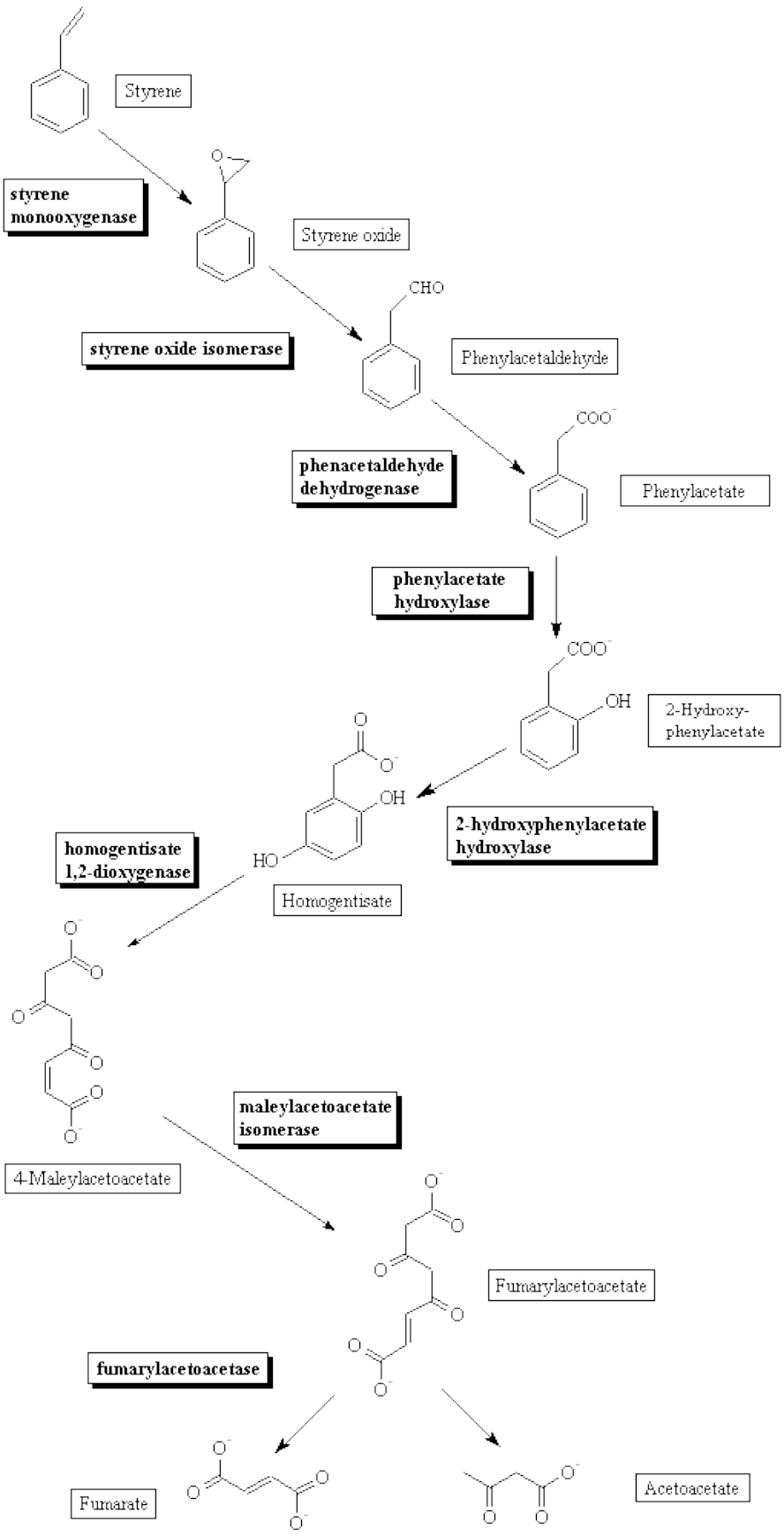

Figure 2-11: Styrene biodegradation pathway map 1 (McLeish, 2006b)

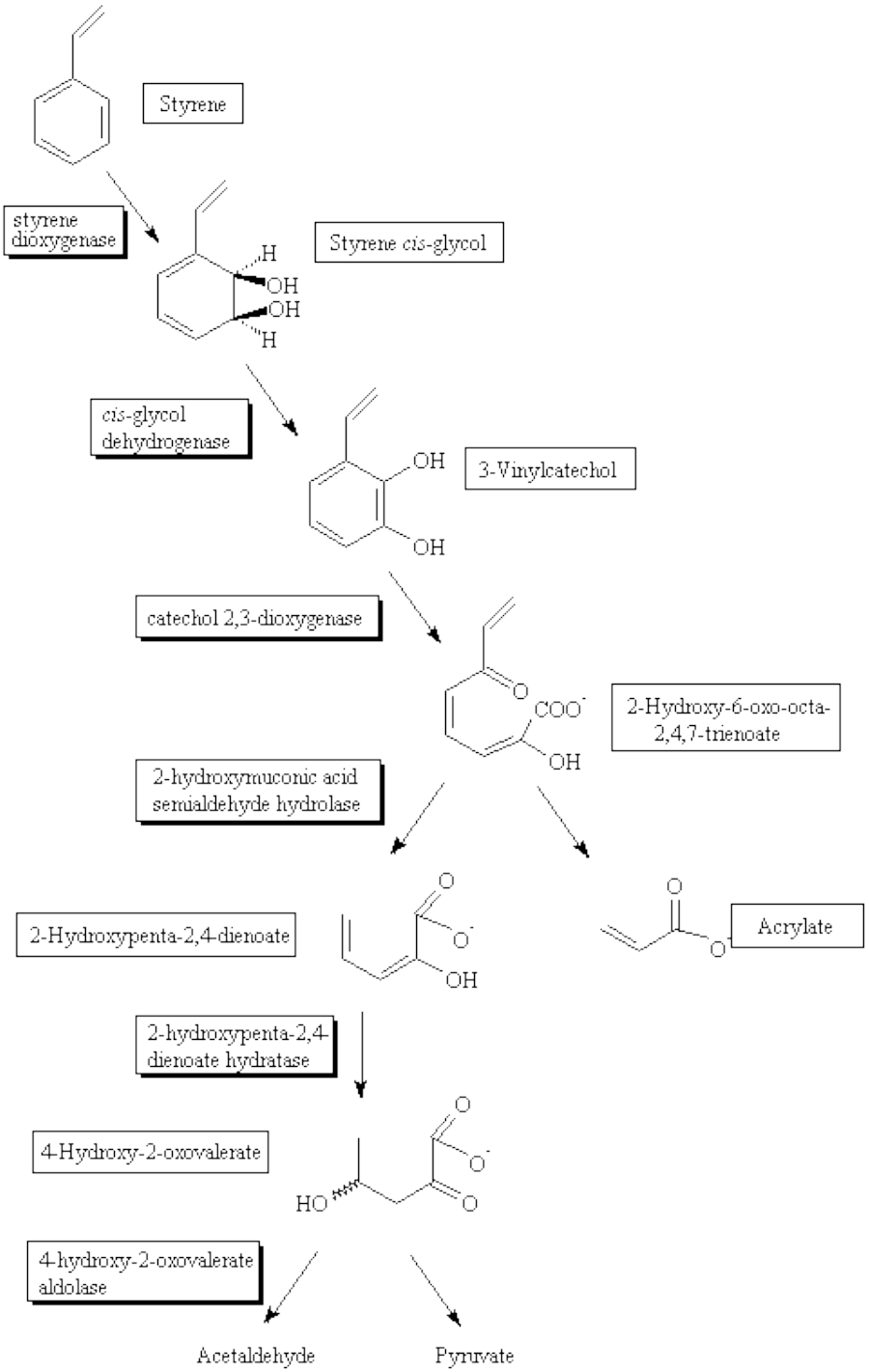

Figure 2-12: Styrene biodegradation pathway map 2 (McLeish, 2006c)

2.2.1.5 o-Xylene

Biological degradation of o-xylene can be initiated by three different enzymes (Figure 2-13). Degradation starting with monooxygenation by xylene monooxygenase, leads to 3-methylcatechol. 3-methylcatechol is also an intermediary compound in degradation of toluene shown in Figure 2-5, and it will be degraded to acetaldehyde and pyruvate which are part of the intermediary metabolism

(Zeng, 2011). The bacteria *Burkholderia cepacia* initialise this biodegradation pathway of o-Xylene. *Burkholderi* are part of the β-proteobacteria and pseudomonad group (Madigan et al., 2009).

Biodegradation of o-xylene with the enzymes o-xylene 3,4-dioxygenase and o-xylene 4,5-dioxygenase (Figure 2-13) is initialised by *Rhodococcus* (Oh and Turnbull, 2009). This pathway is thus not further studied here.

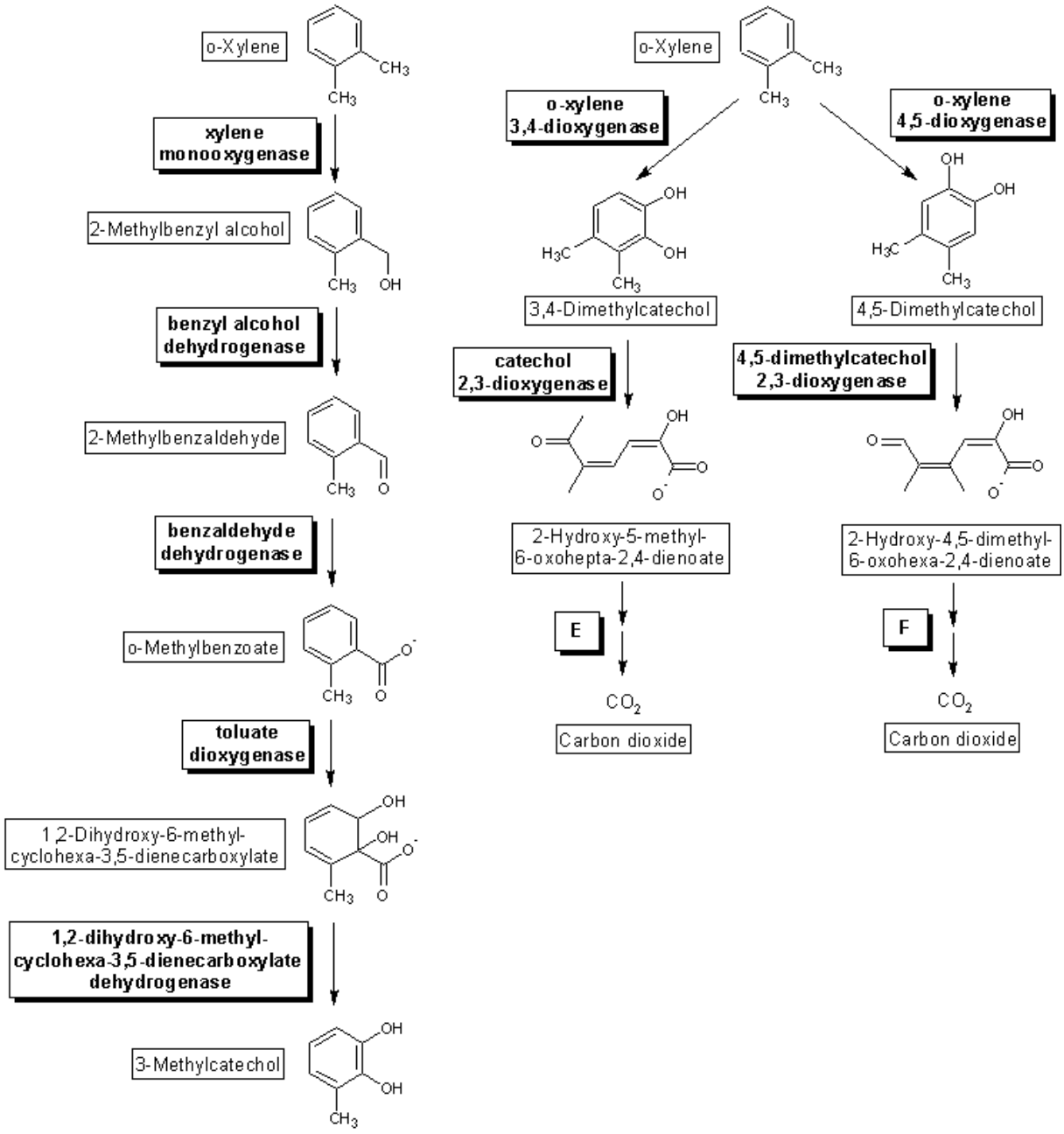

Figure 2-13: o-xylene biodegradation pathway (Oh, 2009)

2.2.2 Biodegradation of hydrocarbons in the deep-sea

In 1974 Schwarz et al. (1974) conducted experiments showing that bacteria from the deep-sea are capable of degrading hydrocarbons under high pressure. The experimental work done had some flaws with for example loss of hydrocarbons through absorption to equipment and evaporation. It was also conducted at 20 °C, while the temperature in the deep-sea is around 2 °C.

Newer research of hydrocarbon degradation by piezophiles was carried out after the Prestige tanker accident (Uad et al., 2010). The research concluded that indigenous bacteria isolated from the deep-sea were capable of degrading hydrocarbons.

The majority of the hydrocarbon degrading strains isolated belonged to the genus *Bacillus* in the Firmicutes branch (Uad et al., 2010). Also some *Brevibacterium* from the Actinobacteria branch, and *Halomonas, Pseudomonas, Marinobacter* and *Pseudoalteromonas* were isolated, these are from the γ-Proteobacteria branch. Most of the isolated bacteria produced exopolymers with emulsifying activity that enhanced biodegradation of hydrocarbons (Uad et al., 2010).

Research done after the Deepwater Horizon oil spill in the Gulf of Mexico indicated that a plume of oil was located at about 1100 m depth for months after the accident (Camilli et al., 2010). The abundance of aromatic hydrocarbons was measured in the water column, and the results indicated a greater abundance in the plume (Camilli et al., 2010).

Hazen et al. (2010) showed that there was an increase in the microbial biomass in the oil plume compared to samples taken outside the plume. Analysis of the bacteria indicated that the diversity of bacteria in the oil plume was lower than in the surrounding ocean. The only bacterial taxa that was significantly enriched inside the plume compared to outside was from the γ-Proteobacteria. Most of these bacteria are related to bacteria that are known hydrocarbon degraders in cold environments. It was also indicated by analysis of individual genes involved in hydrocarbon degradation that the microbial community was going through a fast dynamic adaption in response to the oil spill (Hazen et al., 2010).

Research done by Valentine et al. (2010) indicated that there also existed a plume of the natural gases propane, ethane and methane in the area of the leaking well after the Deepwater Horizon accident. This plume was found at depths greater than 799 m.

Valentine et al. (2010) further investigated the ratios between the gases in different plume areas. It was indicated by the resulting ratios that there was a preferential loss of propane over ethane over methane. This indicates that in the early development and degradation of hydrocarbon plumes in the

deep-sea ethane and propane are the preferred substrates of microorganisms. Butane was identified as a possible third preferred substrate.

The diversity measured by Valentine et al. (2010) in the hydrocarbon plume was also low. Relatives of *Cycloclasticus* and *Colwellia* dominated the majority of the plume locations investigated. The study proposed that one or both of these taxa flourished in the plume because they could consume propane and ethane, and possibly butane. This growth does not eliminate the growth of other bacteria or metabolisms.

The work of Valentine et al. (2010) shows the possibility of a deep hydrocarbon plume microbial community to develop within a short time. In the beginning bacteria consuming propane, ethane and butane grow, followed by bacteria consuming methane and other higher hydrocarbons. A maximum of about two thirds of an ultimate productivity in this plume may arise from the degradation of natural gases (Valentine et al., 2010). But the plume will not be a closed system and a continuous mixing between the plume and the surrounding water will happen. This mixing will most likely have an effect on the bacterial community in the plume.

Kessler et al. (2011) analysed the microbial community present in September 2010 at different stations in the Gulf of Mexico where oxygen anomalies were detected. 5-36 % of the 16S rRNA they cloned and sequenced were methylotrophic bacteria from the genus *Methylocooaceae*, *Methylophaga* and *Methylophilaceae*. At the same time CH_4 concentrations measured were not any higher than normal background levels normally detected in the Gulf of Mexico. The identified community also differed significantly from the community present around the wellhead in June. At that time no methanotrophic bacteria was identified. These findings suggest that a bloom of methanotrophic bacteria occurred in the deep-sea after the Deepwater Horizon blowout, and that the methane released was degraded to CO_2 in about 120 days without any measurable loss to the atmosphere (Kessler et al., 2011).

2.3 Objectives

The goal of this research is to assess whether pressure has an effect on biodegradation of hydrocarbons in seawater. This will be done by performing batch tests with naphthalene and BTEX as carbon source and limiting factor for growth. The tests will be performed in pressure vessels at 80 bar, 170 bar and 340 bar, and at atmospheric pressure. The temperature in the tests will be kept at 2 °C which is typical for the deep-sea environment. At each pressure sampling will be performed five times during the experiment by sacrificing all test tubes in one pressure vessel. To describe the biodegradation process analysis of substrate concentration and cell number will be performed. The microbial community at the different pressures will be analysed at the end of the test.

3 Material and Methods

The following chapter describes the experiments being conducted. It treats preparation of solutions, experimental setup, sampling and sample analysis.

3.1 Solutions and solution preparation

Three modified (N-source) Bushnell-Haas inorganic nutrient solutions of pH 8.2 and a Balch trace element solution were prepared as described in Table 3-1. All solutions were prepared in 1000 ml double distilled water.

Table 3-1: Modified (N-source) Bushnell-Haas inorganic nutrient solutions and Balch trace element solution.

Solution A		Solution B		Solution C		Solution D	
Concentration [g/l]		Concentration [g/l]		Concentration [g/l]		Concentration [g/l]	
K_2HPO_4	16.2	$NaNO_3$	25	$CaCl_2 \cdot 2H_2O$	3.31	EDTA	0.5
KH_2PO_4	0.8	NH_4Cl	0.6	$MgSO_4 \cdot 6H_2O$	2.85	$MnSO_4$	0.4
		$FeCl_3 \cdot 6H_2O$	0.083			$MgSO_4 \cdot 6H_2O$	2.78
		EDTA	0.2			NaCl	1
						$FeSO_4 \cdot 7H_2O$	0.1
						$CoCl_2 \cdot 6H_2O$	0.1
						$CaCl_2 \cdot 2H_2O$	0.1
						$ZnCl_2$	0.1
						$CuSO_4 \cdot 5H_2O$	0.01
						$NiCl_2 \cdot 6H_2O$	0.02
						$AlK(SO_4)_2 \cdot 12H_2O$	0.018
						H_3BO_3	0.01
						$Na_2MoO_4 \cdot 2H_2O$	0.012
						$Na_2WO_4 \cdot 2H_2O$	0.01

An 18 g/l sodium benzoate stock solution was prepared by dissolving 4.50047 g sodium benzoate in 250 ml double distilled water.

A borate buffered formalin solution was prepared according to Sherr et.al (2001), and used for sample preservation in DAPI analysis. A dark 500 ml glass bottle was filled with 450 ml 37 % formalin. A saturated borate buffered solution was made by adding disodium tetraborate decahydrate ($Na_2B_4O_7 \cdot 10H_2O$) until a layer of crystals covered the bottom of the bottle.

Seawater used in the biodegradation experiments was collected from the seawater system at IRIS Aquamiljø (Mekjarvik, Randaberg municipality, Norway). This system has an inlet at 80 m depth in Byfjorden (temperature 7 °C, salinity 32.1 ‰). Seawater was prefiltered in the systems sand filter. It was transferred to 20 l nalgene bottles and transported to the lab (UiS) were it was kept at 2 °C over night for equilibration. It was saturated with oxygen before inoculums were prepared.

3.2 Pressurised biodegradation experiments

To test the pressure effect on biodegradation of hydrocarbons two experiments were performed, one with naphthalene and one with BTEX, o-xylene was chosen from the three xylenes. Preparation of inoculums and test tubes for the two experiments are described in 3.2.1 Naphthalene experiment p. 39 and 3.2.2 BTEX experiment p.40. In the naphthalene experiment five naphthalene test tubes, two negative controls, three positive controls and two blanks were used at each measuring point. In the BTEX experiment five BTEX test tubes, three negative controls, two positive controls and two blanks were used at each measuring point. The total number of 12 test tubes was chosen due to limited space in the high pressure vessels used. Five measuring points were used at each pressure.

Pressure vessels were filled with water allowing safe and fast compression and decompression. Compression was performed by pumping water into the pressure vessels using a Perkin Elmer series 3B HPLC pump. Test tubes were attached to a metal wire as seen in Figure 3-1 A and submerged in the water in the pressure vessels. At atmospheric pressure test tubes were placed in boxes filled with water (Figure 3-1 B). Three different pressure vessels were used (Figure 3-1 C, D and E). Two low pressure vessels and three medium pressure vessels held 80 bar. Five medium pressure vessels held 170 bar, and five high pressure vessels held 340 bar. All the pressure vessels and the boxes used at atmospheric pressure were kept in a cooling cabinet fluctuating at temperatures around 2 °C. Temperature in the water surrounding the test tubes was measured when sampling was performed in the BTEX experiment.

For indication of growth, oxygen demand was measured. In the naphthalene experiment three bottles with 250 ml naphthalene inoculum, three with 250 ml positive control inoculum and one with 250 ml blank inoculum was prepared. Oxygen consumption was measured using a MicroOxymax dynamic respirometer (Columbus Instrument, Ohio USA). In the BTEX experiment three bottles with 400 ml BTEX inoculum and two with 400 ml positive control inoculum was prepared. Biological oxygen demand (BOD) was measured using the Oxitop static respirometry system (WTW, Germany). In both experiments the bottles were kept in the same cooling cabinet as the pressure vessels.

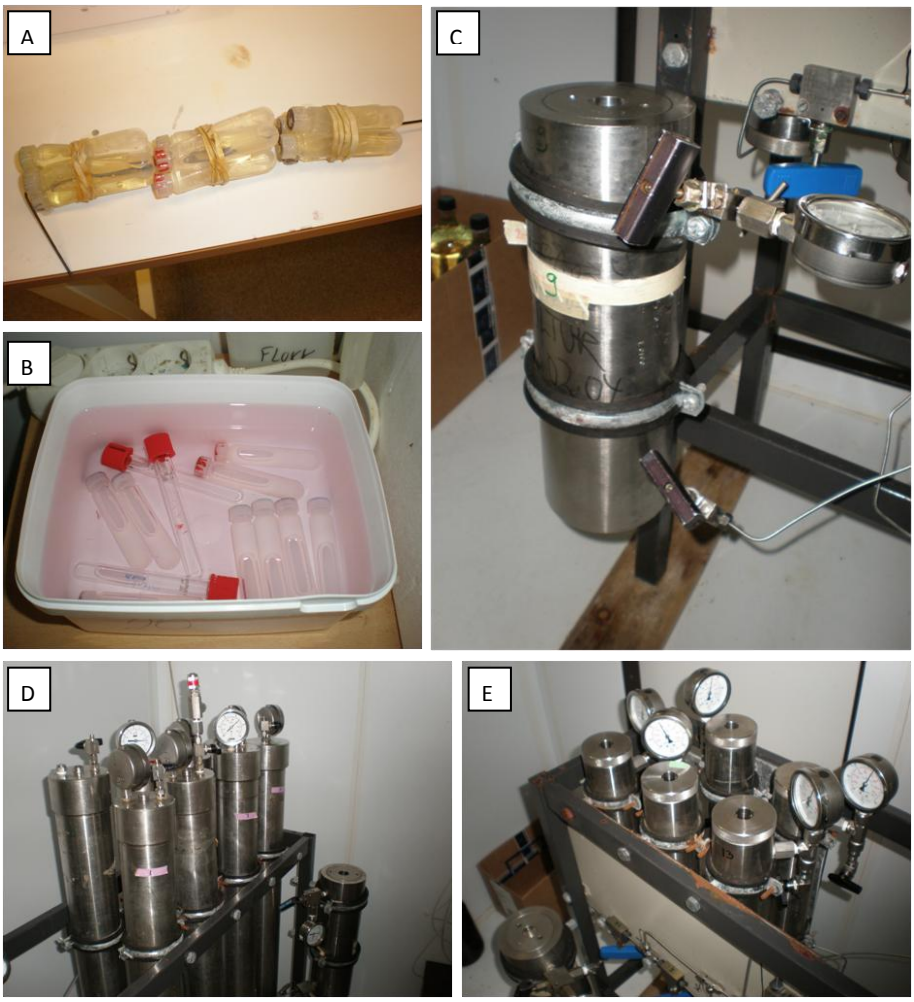

Figure 3-1: A) Teflon FEP tubes B) Test tubes at atmospheric pressure C) Low pressure vessels D) Medium pressure vessels E) High pressure vessels

3.2.1 Naphthalene experiment

A 20.02 mg/l naphthalene stock solution was made by sterile filtering 2 l seawater (refer to 3.1 Solutions and solution preparation p. 37) with a 0.22 µm Sterivex-GV filter, and adding 0.04004 g of naphthalene in an autoclaved bottle. The solution was put on a magnetic stirrer at 50 °C for four days until all naphthalene crystals were dissolved.

A 9.92 mg/l naphthalene inoculum was prepared by mixing seawater and 3 ml of nutrient solution A, B, C and D (Table 3-1 p. 37), 40 µl 34 g/l amino acid solution (R 7131 RPMI-1640 [50X], Sigma-aldrich) and 40 µl vitamin solution (B6891 BME [100X], Sigma-aldrich) in a 2 l autoclaved bottle, to a total mass of 1049.27 g. 700 ml of the 20 mg/l

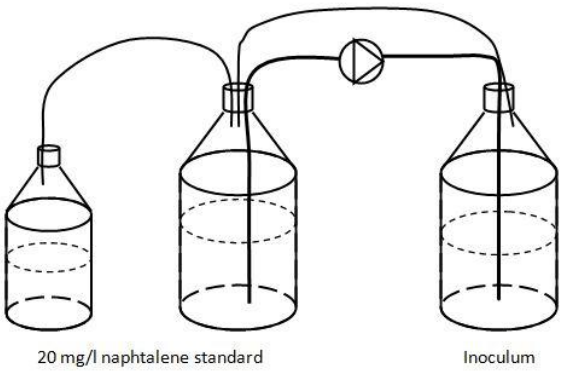

Figure 3-2: Preparation of naphthalene inoculums.

naphthalene standard was transferred to a 1 l bottle, while the rest was kept in the original bottle. The three bottles were then connected as described in Figure 3-2. Headspace of the two bottles containing the naphthalene stock solution was connected, and headspace of the inoculum bottle was connected to the original naphthalene stock solution bottle. 1031.06 g 20 mg/l naphthalene stock solution was then pumped over to the inoculum bottle and mixed with the seawater solution.

Inoculum for blank test tubes was prepared by sterile filtering 256.06 g seawater with a 0.22 µm Sterivex-GV filter. 0.75 ml of nutrient solution A, B, C and D (Table 3-1 p. 37), 10 µl 34 g/l amino acid solution (R 7131 RPMI-1640 [50X], Sigma-aldrich), 10 µl vitamin solution (B6891 BME [100X], Sigma-aldrich) were added, before seawater was added to a total mass of 543.83 g.

Positive control inoculum was prepared by sterile filtering 1021.90 g seawater with a 0.22 µm Sterivex-GV filter. 3 ml of nutrient solution A, B, C and D (Table 3-1 p. 37), 40 µl 34 g/l amino acid solution (R 7131 RPMI-1640 [50X], Sigma-aldrich), 40 µl vitamin solution (B6891 BME [100X], Sigma-aldrich), 2.22 ml 18 g/l sodium benzoate stock solution (3.1 Solutions and solution preparation p. 37) and seawater was added to a total mass of 2083.04 g.

Naphthalene test tubes were prepared by pumping 8.5 ml naphthalene inoculum over in 10 ml Teflon fluorinated ethylene propylene (FEP) tubes (Oak Ridge Centrifuge Tubes, Nalgene Labware). Negative controls were prepared by adding minimum 15 mg sodium azide to tubes containing naphthalene inoculum. Positive control and blank was prepared by pipetting 8.5 ml inoculums over in FEP tubes. Due to lack of Teflon FEP tubes two Duran GL 14 culture tubes with screw-cap (Duran group, Maine, Germany) were used for naphthalene samples, one for negative control and blank, and one or two for positive control at each measuring point at atmospheric pressure. The Duran tubes were made of glass and due to a smaller volume they were filled with 6.5 ml instead of 8.5 ml.

3.2.2 BTEX experiment

A BTEX inoculum, containing 4.37 mg /l benzene, 4.31 mg /l toluene, 4.31 mg/l ethylbenzene and 4.37 mg/l o-xylene, was prepared by mixing seawater (refer to 3.1 Solutions and solution preparation p. 37), 3 ml of nutrient solution A, B, C and D (Table 3-1 p. 37), 40 µl 34 g/l amino acid solution (R 7131 RPMI-1640 [50X], Sigma-aldrich) and 40 µl vitamin solution (B6891 BME [100X], Sigma-aldrich) to a total mass of 2073.64 g. 10 µl benzene, toluene, ethylbenzene and o-xylene was added. Headspace of the inoculum bottle was connected to a BTEX seawater solution of approximately the same concentration as the inoculum.

Positive control inoculum was prepared by mixing 3 ml of nutrient solution A, B, C and D (Table 3-1 p. 37), 40 µl 34 g/l amino acid solution (R 7131 RPMI-1640 [50X], Sigma-aldrich), 40 µl vitamin solution

(B6891 BME [100X], Sigma-aldrich), 2.22 ml 18 g/l sodium benzoate stock solution (refer to 3.1 Solutions and solution preparation p. 37) and seawater to a total mass of 2063.24 g.

Figure 3-3: Preparation of BTEX test tubes.

An inoculum for blank test tubes was prepared by adding 1.5 ml of nutrient solution A, B, C and D (Table 3-1 p. 37), 20 µl 34 g/l amino acid solution (R 7131 RPMI-1640 [50X], Sigma-aldrich), 20 µl vitamin solution (B6891 BME [100X], Sigma-aldrich) and seawater to a total mass of 1032.32 g.

BTEX test tubes was prepared by filling 8.5 ml BTEX inoculum in 10 ml Teflon FEP tubes (Oak Ridge Centrifuge Tubes, Nalgene Labware) using the tap on the bottle shown in Figure 3-3. Negative control tubes was already filled with a minimum of 20 mg sodium azide before BTEX inoculum was added, this to prevent loss of BTEX due to evaporation by opening the tubes an extra time.

Positive control and blank were prepared by pipetting 8.5 ml inoculum over in 10 ml teflon FEP tubes (Oak Ridge Centrifuge Tubes, Nalgene Labware).

At atmospheric pressure Duran GL 14 culture tubes with screw-cap (Duran group, Maine, Germany) were used instead of Teflon FEP tubes for one BTEX sample tube, one negative control and one blank tube. This was due to lack of enough Teflon FEP tubes.

3.3 Sampling and sample processing

Samples for analysis of substrate, cell number and DGGE were taken by sacrificing one pressure vessel at a time. Time for decompression of pressure vessels and sampling was noted. Naphthalene and BTEX test tubes were sampled and analysed for substrate analysis and cell number analysis. Substrate analysis was performed on negative controls, total organic carbon (TOC) and cell number analysis was performed on positive controls. Blank test tubes were sampled for TOC analysis and cell number analysis.

For substrate analysis 2 ml sample was mixed with 200 µl 2 M HCl for conservation. 20 ml clear screw neck vials with 18 mm magnetic screw cap, silicone/PTFE, 35°, 1.3 mm (VWR International) were used. Samples was immediately analysed by GC analysis according to 3.4 Substrate analysis p. 42.

2-20 ml samples were taken for analysis of cell number. 5 % borate buffered formalin (3.1 Solutions and solution preparation p. 37) was added, the sample was shaken and kept in the fridge until further analysed (refer to 3.5 Cell number p. 45).

For TOC analysis 2 ml sample was taken. The sample was filtered with a 0.2 µm GHP Acrodisc 13 filter (PALL), diluted 1:5 with double distilled water through the filter and added 200 µl 2M HCl for conservation. The samples were frozen until further analysed (refer to 3.4.3 TOC p. 45).

Sampling for DGGE analysis was performed for original seawater and at the last measuring point at each pressure in the BTEX experiment. For the original seawater a 2 l sample was taken, at the end of the experiment the five BTEX test tubes were mixed together. The samples were filtered with an autoclaved MF-Millipore 0.22 µm mixed cellulose esters filter. The two first steps of the DNA extraction (refer to 3.6 DNA extraction and DGGE analysis p. 46) were performed before the samples were frozen until further DNA extraction and DGGE analysis were performed.

3.4 Substrate analysis

Static headspace gas chromatography (HS-GC) was used for analysis of naphthalene and BTEX substrate concentrations. For analysis of substrate in positive controls and blanks analysis of total organic carbon (TOC) was performed.

3.4.1 Naphthalene

An Agilent 6890 GC (Matriks) equipped with a FID detector was used for sample analysis. For the calibration and in the beginning of the naphthalene experiment the column used was a 30.0 m x 320.00 µm Agilent 19091J-413 HP-5 5% Phenyl Methyl Siloxane, with a nominal film thickness of 0.25 µm. In the end of the experiment the column used was a 9.7 m x 200.00 µm Supelco Equity 1 fused silica capillary column, with a nominal film thickness of 1.2 µm. The rest of the method stayed the same.

Splitless injection of 250.0 µl at initial temperature 260 °C, purge flow 30.0 mL/in and purge time 1.00 min was applied. A temperature program was used starting at 60 °C hold for 0.20 min before ramping at 50 °C/min to a final temperature of 240 °C. Run time was 3.80 min and equilibration time 0.33 min. Carrier gas was helium at a constant flow of 2.5 ml/min. The FID detector held 250 °C and air flow was 450.0 ml/min. Constant makeup flow at 30.0 ml/min nitrogen was used.

Automatic injections were performed with a Gerstel MPS Headspace Injector. A 2.5 ml headspace syringe was used, it held 85 °C and was flushed for 1.00 min. Sample was prepared for injection by incubation at 65 °C for 5.00 min and a agitator speed of 300 rpm.

3.4.1.1 Calibration

A 10.043 g/l stock solution was made by dissolving 0.50215 g naphthalene in 50 ml Methanol. Working standard was prepared by dilution with autoclaved seawater from the stock solution as described in Table 3-2. Calibration standards were further prepared by dilution of the working standard with a mixture of filtered and autoclaved seawater (Table 3-2). At the lab, seawater was filtered with a 0.45 µm nylon filter from SMI-LabHut for removal of algae growth, and a 0.2 µm GHP membrane filter from PALL Life Sciences to remove bacteria. Filtered seawater was used as the blank standard.

Table 3-2: Preparation of standards for calibration. Working standard was prepared by dilution from stock solution, while the other standards were prepared by dilution from working standard. Autoclaved seawater was used for working standard, while the other standards were prepared with a mixture of filtered and autoclaved seawater.

	Volume diluted [ml]	Total volume [ml]	Concentration [mg/l]
Working standard	1	1000	10.043
2 mg/l standard	20	100	2.009
0.5 mg/l standard	5	100	0.5022
0.05 mg /l standard	0.5	100	0.05022
0.01 mg/l standard	0.1	100	0.01004

Five parallels were prepared for analysis from each standard, the working standard, the calibration standards and the blank. 2 ml of the standard was mixed with 200 µl 2 M HCl for conservation. 20 ml clear screw neck vials with 18 mm magnetic screw cap, silicone/PTFE, 35°, 1.3 mm (VWR International) were used. Loss due to evaporation of naphthalene was at all times minimised by minimising contact between solutions and any gas phase.

3.4.1.2 Matrix interference

In the working standard used for calibration, 1 ml of the methanol stock solution is diluted with autoclaved seawater to 1000 ml. Methanol is thus present as 0.1 % of the matrix in the working standard. In the other calibrations standards, concentration of methanol is even lower as they are further dilutions of the working standard. Kolb and Ettre (2006) state that matrix compounds that is present at a concentration lower than 1 % will not influence solubility of the analyte. The effect of methanol can hence be assumed not to cause a matrix effect. And the calibration is assumed to be representative also for samples that lack methanol in the matrix.

3.4.1.3 Analysis of carryover

Potential carryover was evaluated in the GC instrument by letting one sample of the calibration working standard be analysed, followed by three samples of tap water. Preparation of the samples was the same as for the calibration samples (refer to 3.4.1.1 Calibration p. 43)

3.4.2 BTEX

An Agilent 6890 GC (Matriks) equipped with a FID detector was used. The column used was a 9.7 m x 200.00 µm Supelco Equity 1 fused silica capillary column, with a nominal film thickness of 1.2 µm. Pulsed split injection, with a 10:1 split ratio and 116.1 kPa pressure for 1.00 min was performed. A split flow of 20.0 ml/min and total flow of 25.0 ml/min was used. A 200.0 µl sample was injected at initial temperature 240 °C. A temperature program was used starting at 40°C hold for 1.50 min before ramping at 10 °C/min to 95 °C, 50 °C/min to 180 °C, 120 °C/min to 250°C, hold for 1 min at final temperature. Run time was 10.28 min and equilibration time 0.33 min. Carrier gas was helium at a constant pressure of 116.1 kPa. The FID detector held 280 °C and air flow was 450.0 ml/min. Constant total column and makeup flow at 30.0 ml/min, makeup gas was nitrogen.

Automatic injections were performed with a Gerstel MPS Headspace Injector. A 1.0 ml headspace syringe was used, it held 80 °C and was flushed for 2.00 min. Sample was prepared for injection by incubation at 50 °C for 4.00 min and a agitator speed of 300 rpm.

3.4.2.1 Calibration

A BTEX and naphthalene mixed stock solution was made by mixing 4 ml of benzene, toluene, ethylbenzene and o-xylene, and adding 3.51034 g of naphthalene. Working standard was prepared by dilution with sterile filtered seawater from the stock solution as described in Table 3-3. Calibration standards were further prepared by dilution of the working standard with sterile filtered seawater (Table 3-3). Sterile filtered seawater was used as the blank standard. As naphthalene precipitated when working standard was used, and did not dissolve in seawater after heating and stirring the method was not calibrated for naphthalene analysis.

Table 3-3: Preparation of standards for calibration. Working standard was prepared by dilution from stock solution, while the other standards were prepared by dilution from working standard. Sterile filtered seawater was used for all standards.

	Volume diluted [ml]	Total volume [ml]	Concentration [mg/l]			
			Benzene	Toluene	Ethylbenzene	o-Xylene
Working standard	0.025	1000	5.494	5.419	5.419	5.494
2.7 mg/l standard	50	100	2.747	2.709	2.747	2.709
0.5 mg/l standard	10	100	0.5494	0.5419	0.5494	0.5419
0.05 mg /l standard	1	100	0.05494	0.05419	0.05494	0.05419
0.01 mg/l standard	0.2	100	0.01099	0.01084	0.01099	0.01084

Five parallels were prepared for analysis from each standard, the working standard, the calibration standards and the blank. 2 ml of the standard was mixed with 200 µl 2 M HCl for conservation. 20 ml clear screw neck vials with 18 mm magnetic screw cap, silicone/PTFE, 35°, 1.3 mm (VWR International) was used. Loss due to evaporation of substrates was at all times minimised by minimising contact between solutions and any gas phase.

3.4.3 TOC

TOC analysis was performed using the NPOC (Non-Purgeable Organic Carbon) method on an Analytik-Jena multi N/C 3100 instrument. Calibration was performed using 10 mg C/l, 5 mg C/l, 2.5 mg C/l, 1 mg C/l and 0.5 mg C/l potassium hydrogenphtalate calibration standards. 200 µl 2M HCl was added to the calibration samples in the same way as to all samples from the two experiments. All vials used for TOC analysis was burned for 3 hours at 250 °C to remove carbon from the glassware.

3.5 Cell number

Sampling was performed as described in 3.3 Sampling and sample processing p. 41. Cell number analysis was performed by epifluoresence DAPI (4,6-diamidino-2-phenylidole) direct count according to Sherr et al.(2001). A Sartorius filtering device was used with 0.2 µm black polycarbonate membrane filters (Sigma-aldrich). Samples were frozen until further analysis.

An Olympus BX61 microscope equipped with an EXFO X-Cite 120 PC lamp, Olympus BX-UCB and an Olympus DP72 camera were used. For each samples 10 pictures were taken and the number of cells were counted using adaptive threshold. Cell number X [cells/ml] was calculated using equation 3-1.

Equation 3-1

$$X\left[{}^{cells}/_{ml}\right] = \frac{\frac{\overline{\#\ cells}}{a\,[mm^2]}A[mm^2]}{V_s[ml]}$$

X is cell number [cells/ml], a is 0.02317 mm^2 and it is the area of the pictures taken, A is 309.46 mm^2 and it is the internal area of the cylinder used while filtering the samples. V_s is the sample volume taken [ml].

3.6 DNA extraction and DGGE analysis

DNA extraction was performed using FastDNA spin Kit for Soil (MP Biomedicals) following the manufacturers recommendation (manual). DNA was eluted with 100 µL of molecular grade water and products (5 µL of each) were checked on 2 % agarose gel. Agarose gel was prepared with 50 mL of 1 x TAE (50 x TAE contains Tris base, 2 M, glacial acetic acid, 1 M and EDTA, pH 8.0, 50 mM) (VWR) and 1 g agarose (Merck, electrophoresis grade) and run at 100 V for 45 minutes.

Amplification prior to DGGE was carried out with primers containing a GC clamp. PCR master mix contained a buffer provided with the Taq polymerase kit (5 Prime), 0.1 mM of dNTP's, 10 pM of each primers, 1 µL of community DNA and 0.25 µL of Taq polymerase (5U/µL, 5 Prime). PCR program began with initial activation at 94 °C for 2 minutes followed by 30 cycles of denaturation at 94 °C for 30 sec, annealing at 55 °C for 40 sec and elongation at 72 °C for 1 min. Final elongation at 72 °C for 7 minutes. Products (5 µL of each) were checked on a 2 % agarose gel again and relative amounts of DNA were estimated using ImageLab quantitation tool.

The DGGE was performed with a 6 % acrylamide gel with denaturing gradient of 20 – 70 % (Table 3-4). DGGE run was carried out in Ingeny4U system in 17 L of 1 x TAE buffer at 60 °C, 90 V for 18 hours. Gel was then stained in GelRed (VWR) staining solution (100 µL of 10 000 x GelRed in 1 L of 1 x TAE) for at least 30 minutes after the run. Image was taken in a BioRad GelDocXR imaging system using ImageLab software.

Table 3-4: Composition of 6 % acrylamide gel with denaturing gradient of 20-70 %

	20 % denaturing solution	**70 % denaturing solution**
40 % Acrylamide/Bis [ml]	15	15
50x TAE buffer [ml]	2	2
Formamide (deionized) [ml]	8	28
Urea [g]	8.4	29.4
dH_2O	To 100 ml	To 100 ml

4 Results

This chapter first presents the result of the calibrations performed for naphthalene and BTEX methods on the GC. It then presents the results from the naphthalene biodegradation experiment, including substrate analysis, cell number and respirometric data in the indication bottles. Finally the results of the BTEX biodegradation experiment are shown.

4.1 Naphthalene calibration

The area obtained in the GC analysis was plotted against standard concentration for the calibration plot (Figure 4-1). A simple linear regression line was fitted the data with the method of least squares (Table 8-2 p.90). The p-value for the intercept was 0.5556, which is higher than a normal significance level of 5 %, thus the intercept could not be assumed to be different from zero. A new regression analysis was therefore performed where the intercept coefficient was chosen as zero (Table 8-3 p.90). The R^2 value of 0.979 (Table 8-3 p.90) indicates that the regression line is a good fit to the data.

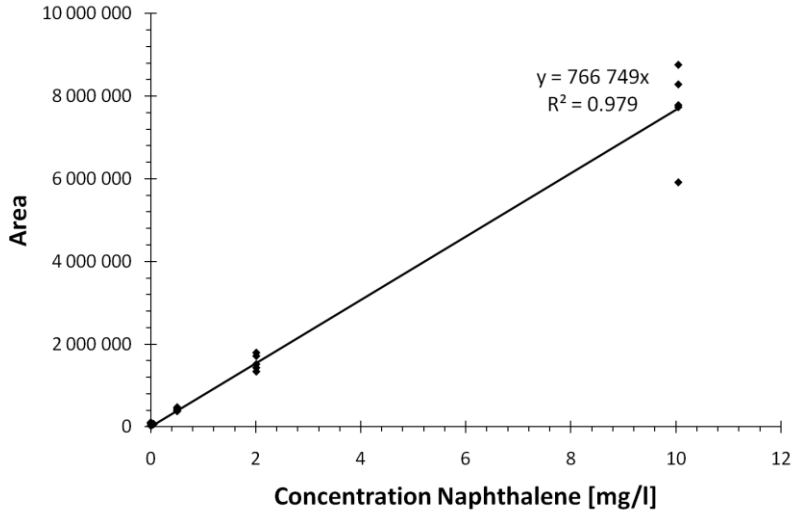

Figure 4-1: Plot of calibration data, with regression line where the constant is assumed to be zero.

From Figure 4-1 one measurement for the 10.043 mg/l naphthalene standard concentration can be identified as a suspected outlier. An outlier analysis of the five areas obtained for the 10.043 mg/l standard concentration was thus performed by calculating a 95 % prediction interval using equation 4-1.

Equation 4-1

$$\left[\bar{X} \pm t_{\alpha/2,n-1}\sqrt{S^2\left(1+\frac{1}{n}\right)}\right]$$

The calculated prediction interval was [4 416 795, 10 969 490]. The area of the suspected outlier measurement was 5 915 535 (Table 8-1 p.89). Hence the suspected outlier was included in the 95 %

prediction interval, and was not significantly different from the other values obtained for the same concentration.

4.1.1 Analysis of residuals

A least square simple linear regression analysis assumes the residuals to be independent and identically distributed variables coming from a $N(0, \sigma^2)$ distribution (Walpole et al., 2007). The residuals are plotted against concentration (Figure 4-2 A), to check if they show random fluctuation around zero and if the variance is constant. In this graph the residuals show an increasing variance with increasing standard concentration. The residuals are also normalised against concentration and plotted (Figure 4-2 B) to see if a constant ratio is seen with increasing concentration. For the three largest standard concentrations the ratio is approximately the same, while for the low standard concentrations calculated ratio is significantly higher.

To ensure that the analysis is not dependent on time, the residuals are plotted against observation number (Figure 4-2 C). No time dependent pattern is seen, but a pattern dependent on the sampling sequence can be seen. Sampling was performed starting with one sample from the lowest concentration, and continuing with one and one sample up to the highest standard concentration, before the sequence was repeated.

The residuals should also be analysed to see if they can be assumed to come from a normal distribution. A normal quantile-quantile plot of the residuals (Figure 4-2 D) where constructed. If the residuals could be assumed to come from a normal distribution, a linear trend would be seen in this graph. This is not the case here, and it can be seen as another consequence caused by the non-homogeneous variance in the calibration analysis.

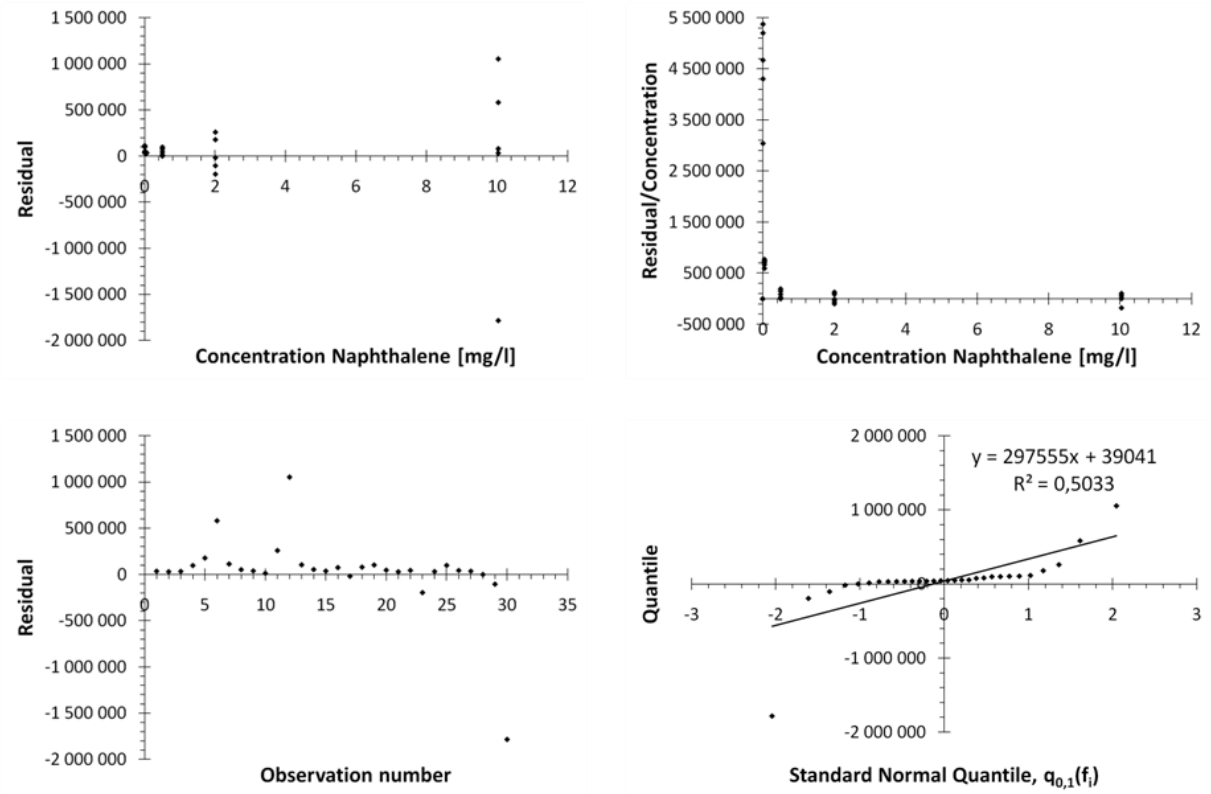

Figure 4-2: A) Residuals plotted against concentration B) Residual divided by concentration plotted against concentration C) Residuals plotted against observation number D) Normal probability plot of residuals

4.1.2 Naphthalene carryover analysis

Analysis of blanks in the calibration run of the GC indicated a certain carryover (Table 8-1 p.89). This was further investigated by analysing one sample of the working standard, followed by three blanks. Figure 8-1 p. 91 show the chromatogram obtained in the carryover analysis run, and Figure 4-3 is the same chromatogram for the three blank solutions zoomed in at the naphthalene peak. These figures show that the peak seen in the blank samples have the same retention time and form as a naphthalene peak, indicating carryover to occur.

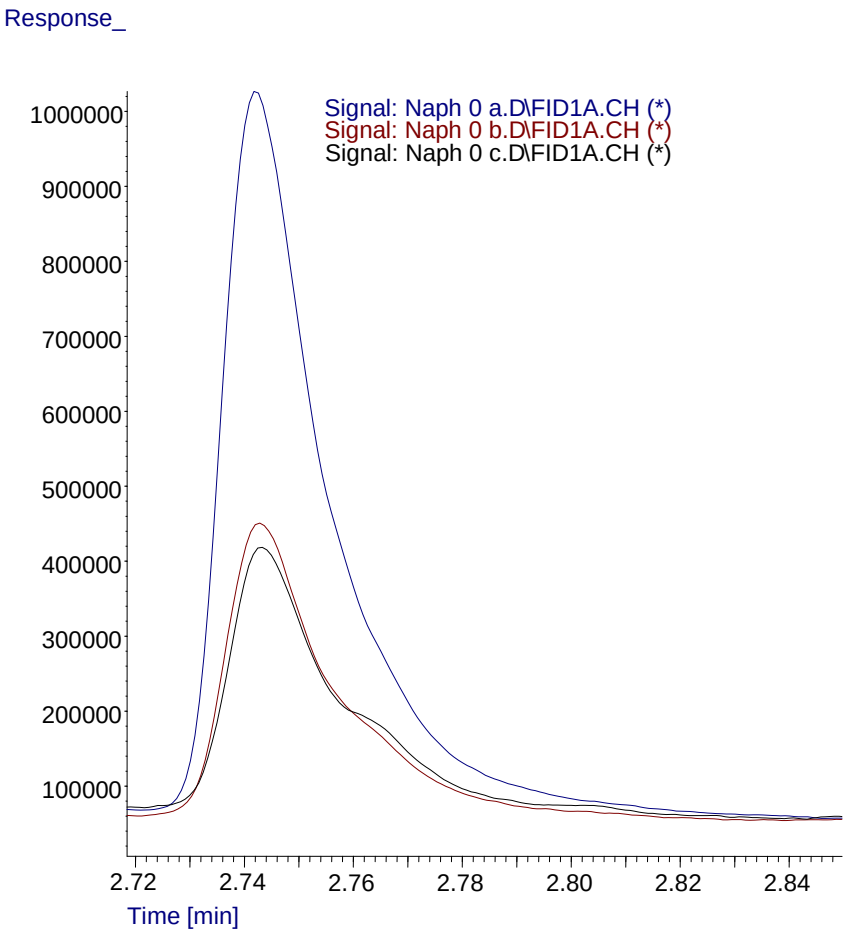

Figure 4-3: Chromatogram zoomed in at the naphthalene peak for the three blank parallels in the carryover analysis. Response on the y-axis is the peak area, the x-axis is retention time in minutes.

The concentration of naphthalene in the blank was calculated based on the calibration performed (Table 4-1). The concentration measured in the first blank indicates carryover of naphthalene in the analysis performed. Standard deviation for the estimated concentration (S_c) was calculated based on equation 4-2 (Skoog et al., 2007).

Equation 4-2

$$S_c = \frac{1}{b}\sqrt{MSE\left(\frac{1}{m}+\frac{1}{n}+\frac{(y_o-\bar{y})^2}{b^2\times S_{xx}}\right)}$$

MSE is mean sum of squared errors around the regression line, b is the slope in the regression model, m is the number of parallels for the new measurement, n is the number of samples analysed in the regression model, y_0 is the new area measured, $\bar{y}$ is average of areas measured in the calibration, and S_{xx} is the sum of squared deviations for the concentrations in the calibration.

Table 4-1: Observation number, area and estimated concentration calculated in the carryover analysis

Observation number	Area	Estimated concentration
1	6 964 881	9.1 ± 0.6
2	88 305	0.1 ±0.5
3	32 015	0.0 ± 0.5
4	18 688	0.0 ± 0.5

4.2 BTEX calibration

The BTEX method was calibrated for benzene, toluene, ethylbenzene and o-xylene. Several linear regressions were performed (refer to appendix 8.2 p.92), before the final linear regression gave the calibration curves shown in Figure 4-4. These regressions all have R squared values greater than 0.99, indicating that almost all variation seen around the regression line is explained by the regression model.

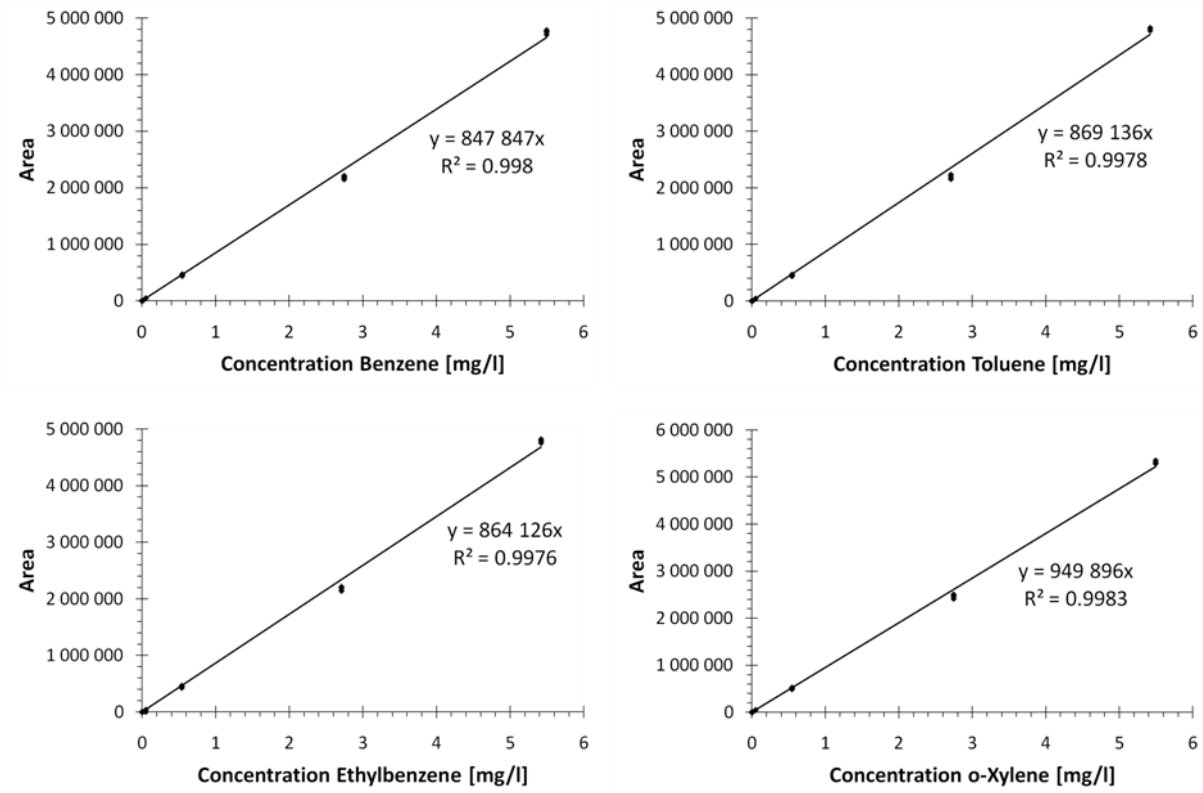

Figure 4-4: Calibration plots for A) Benzene, B) Toluene, C) Ethylbenzene and D) o-Xylene.

4.2.1 Analysis of residuals

Similar to the calibration of naphthalene, residuals are plotted against concentration (Figure 4-5), to check if they show random fluctuation around zero and if the variance is constant. These residual plots are similar for all four compounds and show a pattern indicating that another regression model

than simple linear regression could be more appropriate, i.e. a quadratic regression model. Variance is not constant, but for the two highest concentrations it is approximately the same.

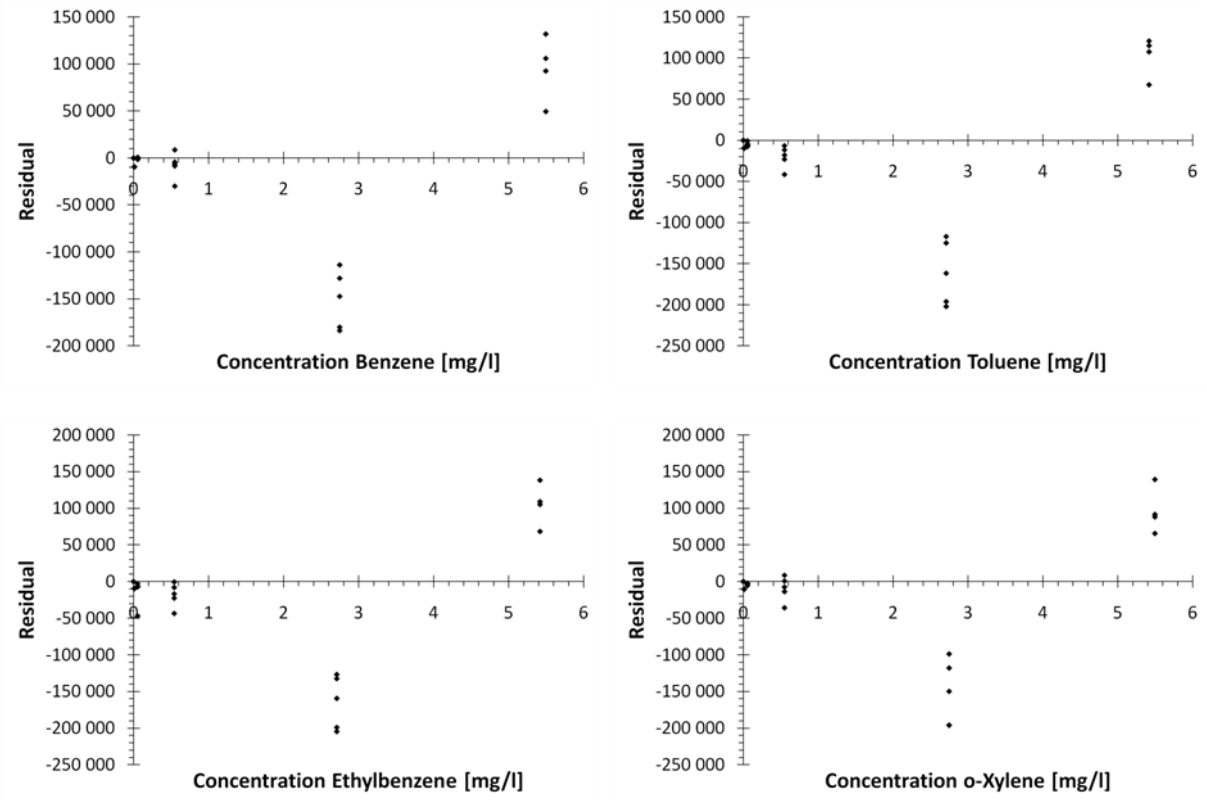

Figure 4-5: Residuals plotted against concentration for BTEX calibrations

To check if residuals are normally distributed a normal quantile-quantile plot can be made. The plot made for the benzene calibration curve is shown in Figure 4-6. Only one example is presented, due to the similarity between calibration curves and residual curves for the different BTEXs. The residuals do not follow a straight line, but a high R squared value indicate that most of the variation can be explained by the regression model.

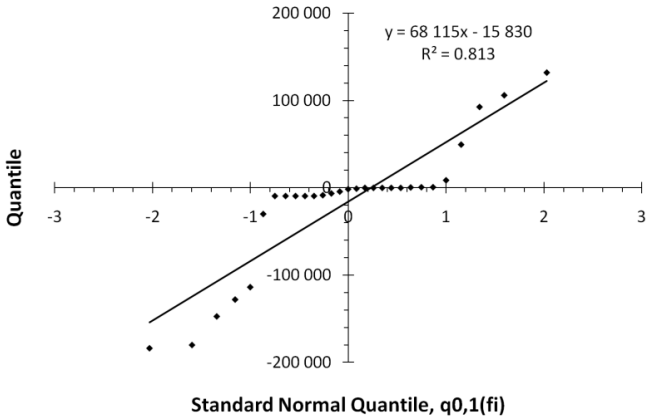

Figure 4-6: Example of a normal quantile-quantile plot, residuals from benzene calibration is used

4.3 Naphthalene experiment

Start concentration in the naphthalene experiment was measured using two different sampling procedures. The first method was to open the inoculum bottle and pipetting a 2 ml sample directly over in a GC vial. In the second sampling method inoculum was pumped over in a vial before 2 ml was transferred to a GC vial using a pipette. Concentrations of naphthalene from samples prepared with both sampling procedures are presented in Table 4-2. A large difference can be seen in measured concentration for the two sampling methods, and start concentration in the test tubes could hence not be determined.

Table 4-2: Concentration measured in samples taken using two different sampling procedures

Sampling method [#]	Naphthalene concentration [mg/l]
1	5.6 ± 0.3
2	1.6 ± 0.3

Nine days into the experiment large pressure drops were discovered in four pressure vessels, two 170 bar vessels and two 340 bar vessels. Water leakage had caused these pressure drops. As these pressure vessels no longer held the appropriate pressure, sampling was performed. The assumption was that no evidence of degradation at the pressure these vessels now where holding, would imply that no degradation would have happened at a higher pressure. At the same time sampling was also performed for samples at 1 bar and 80 bars. In Table 4-3 pressure in the pressure vessels that was decompressed, sampling time and naphthalene concentration measured is given. The large variation in concentration measured in samples taken from the different pressure vessels, indicate that no common start concentration can be found for all the test tubes in the experiment.

Table 4-3: Naphthalene concentration measured and sampling data for the first measuring point.

Pressure vessel [#]	Pressure[1] [bar]	Time [d]	Naphthalene concentration [mg/l]
16	1	9.1	1.7 ± 0.3
10	75 (80)	9.2	2.0 ± 0.3
2	120 (170)	9.8	1.2 ± 0.3
3	105 (170)	9.9	2.2 ± 0.3
11	245 (340)	10.0	2.1 ± 0.3
12	125 (340)	10.1	2.0 ± 0.3

1) Numbers in parentheses are the pressure the pressure vessels were supposed to maintain

To study biodegradation of naphthalene the ratio between average peak area measured in the GC analysis of negative control samples and average peak area measured for naphthalene test samples was calculated (Figure 4-7). Standard deviation for this ratio was calculated using equation 4-3.

Equation 4-3

$$SD(Z) \approx \sqrt{\frac{1}{\bar{Y}^2}\left(S_{\bar{X}}^2 + \frac{\bar{X}^2}{\bar{Y}^2}S_{\bar{Y}}^2\right)}$$

Here Z is used to describe calculated ratio. $\bar{X}$ is average peak area for negative control samples and $\bar{Y}$ is average area measured for naphthalene test samples. Standard error for average peak area measured for negative control samples and naphthalene samples are expressed by $S_{\bar{X}}$ and $S_{\bar{Y}}$ respectively. Figure 4-7 indicates degradation of naphthalene to occur at atmospheric pressure, but not at elevated pressure in this experiment.

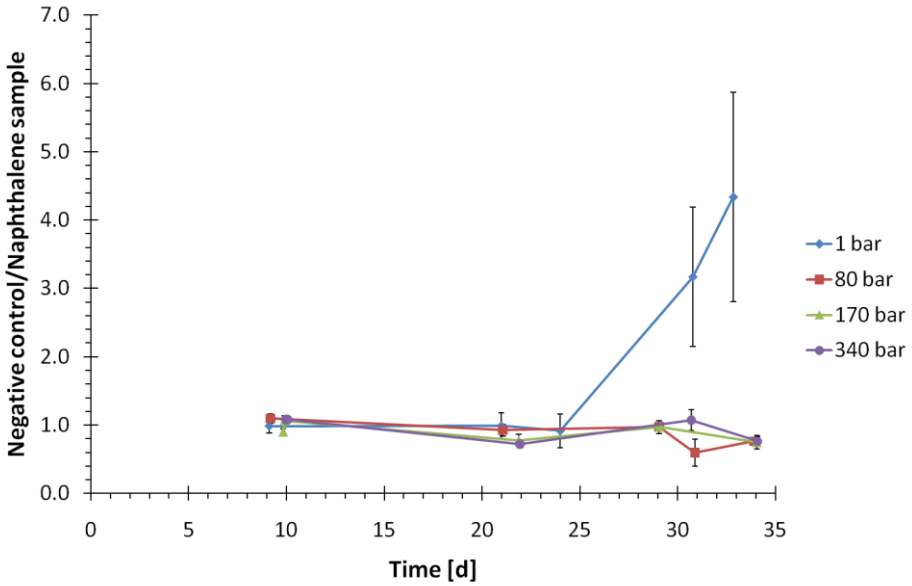

Figure 4-7: Ratio between average peak area measured for negative control and naphthalene samples

A ratio between calculated standard error and average area measured was calculated in percentage (Figure 4-8). This was to show variation in the data obtained, as variance increase under growth, this graph also shows indications of growth at atmospheric pressure and not at elevated pressures.

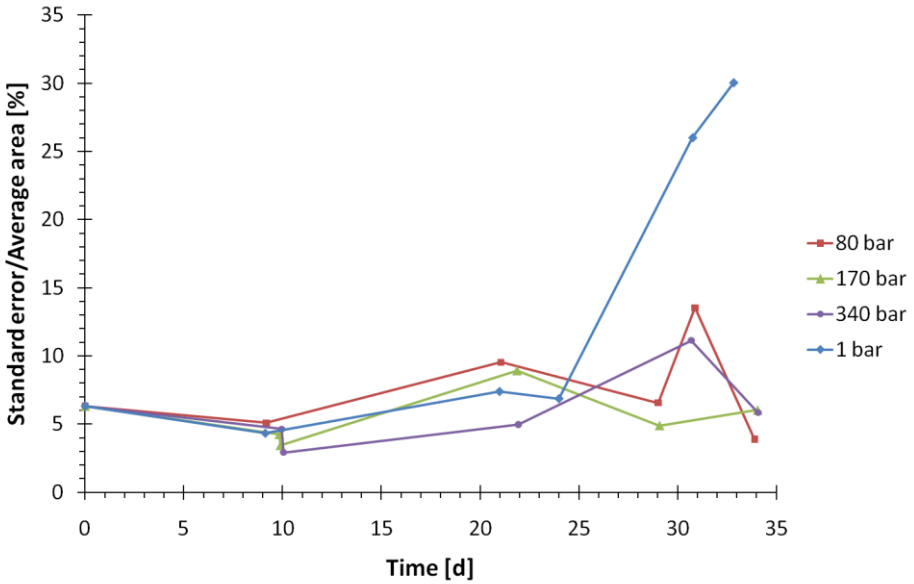

Figure 4-8: Ratio between calculated standard error and average area measured

A substrate plot showing degradation of naphthalene was constructed using relative concentrations (Figure 4-9). Start concentration in the experiment is unknown and considerably lower than the calculated start concentration (3.2.1 Naphthalene experiment p. 39). It also varies for the different test tubes (Table 4-3), thus a common start concentration could not be used in the calculations performed. During the experiment the column used in the GC was also changed, giving different areas for approximately the same naphthalene concentration. The GC method was not calibrated for the second column used, and concentration can thus not be calculated for these data points.

Because of these circumstances, assumptions had to be made when calculating relative concentration at the different measuring points and pressures. The first measuring point was the only one measured with the first GC column used. At this point area measured for negative control were similar to area measured for naphthalene test samples for all pressures (Figure 4-7), hence the batch culture was assumed to still be in the lag phase and degradation assumed to be zero. For 1 and 80 bars samples measured with the second GC column the batch culture was assumed to still be in the lag phase for measuring point two and three, the average area for these two points were thus used as start concentration for the remaining measurements for samples from these pressure. For 170 bar and 340 bar samples the batch culture is assumed to stay in the lag phase throughout the whole experiment, and an average of all measured areas were used as a start concentration for data measured with the second GC column. In Figure 4-9 indications of growth can be seen for samples incubated at 1 bar, a clear pattern indicating growth cannot be seen at 80 bar, 170 bar and 340 bar.

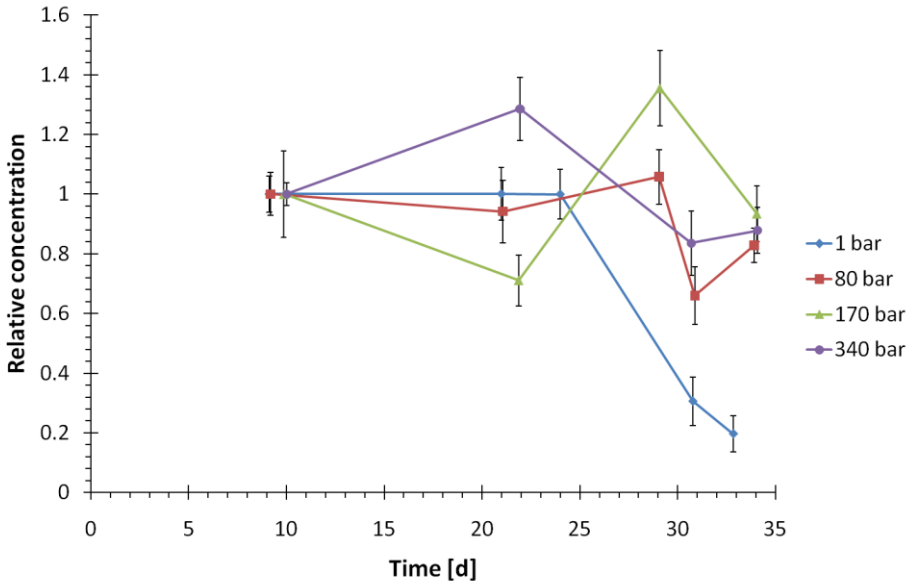

Figure 4-9: Relative concentration calculated for naphthalene.

Cell number was measured using DAPI analysis for samples taken from both naphthalene test tubes (Figure 4-10) and positive control test tubes (Figure 4-11). No clear pattern indicating growth could be detected for naphthalene. Positive control samples show growth at 1 bar and 80 bars, but not at 170 bar and 340 bar. The exponential phase is seen to start earlier at 1 bar than at 80 bars. TOC analysis was also performed on positive control samples, but because of analytical problems this data was not used in this report.

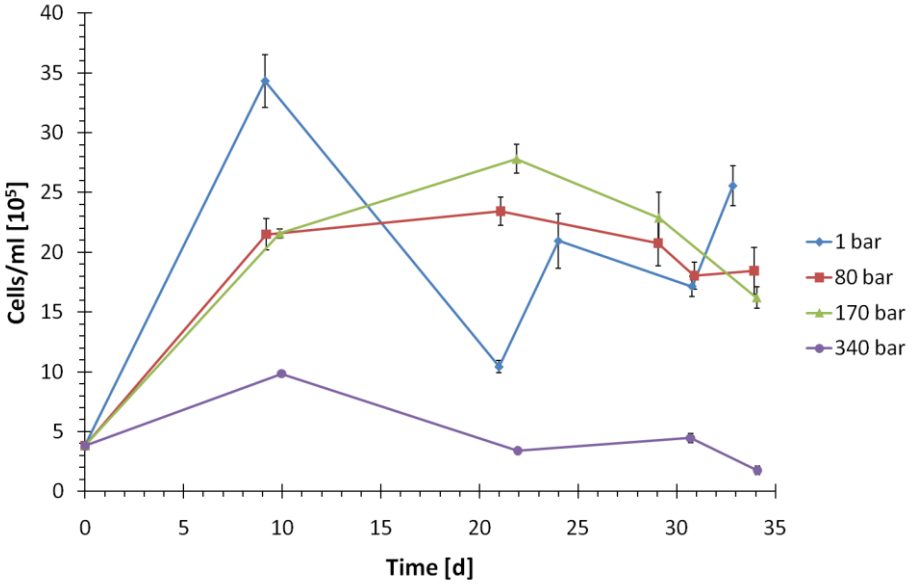

Figure 4-10: Cell number measured for naphthalene samples

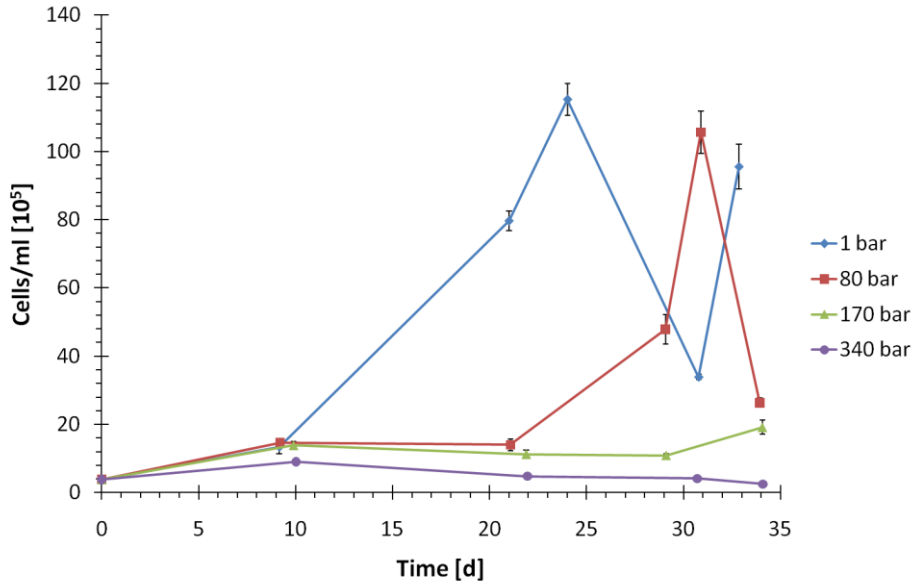

Figure 4-11: Cell number measured for positive control samples

For indicative use under the experiment respirometry was used to follow degradation in three naphthalene tests, three positive control tests and one blank test. Measured accumulated oxygen removed (Figure 4-12) and the rate of oxygen removal (Figure 4-13) are shown. Growth is clearly detected for positive controls, for naphthalene samples indications of growth can be seen in Figure 4-12.

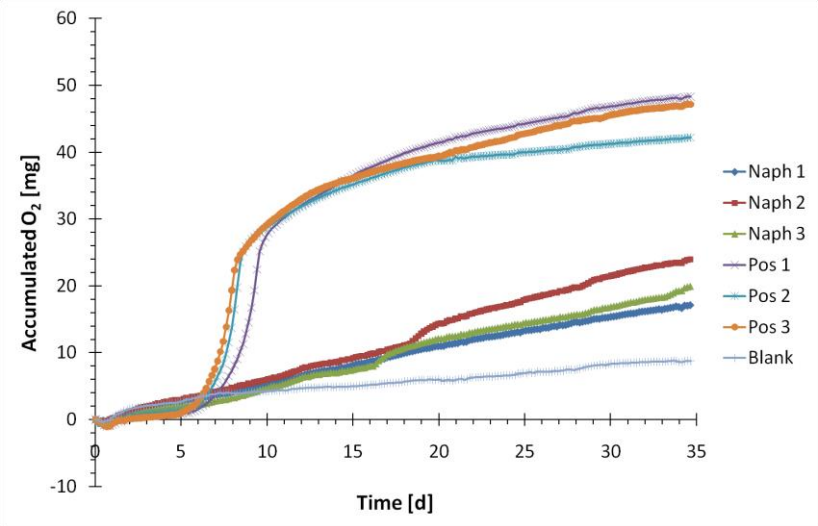

Figure 4-12 Accumulated removal of oxygen [mg] with time

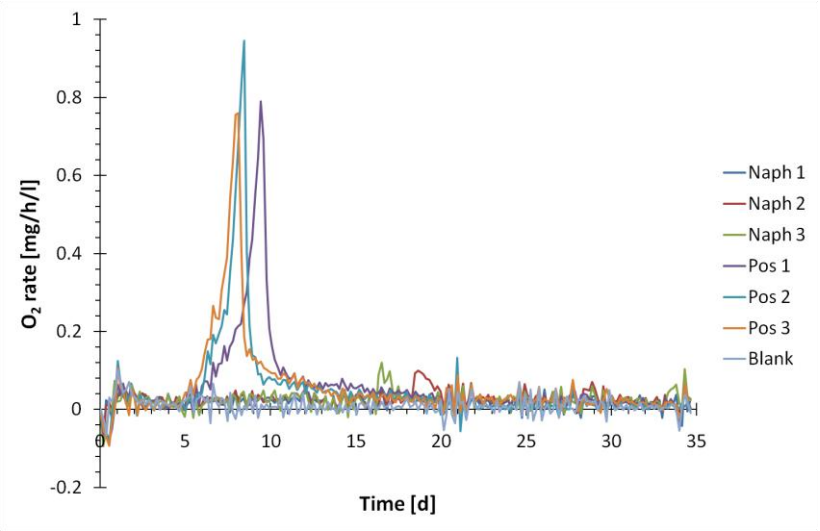

Figure 4-13: Oxygen removal rate [mg/h/l] with time

Temperature was measured in the bottles used for indication of growth (Figure 4-14). For the box and whiskers plot the minimum and maximum levels are the highest value still within 1.5 times interquartile range. At the end of the experiment water temperature was measured in the pressure vessels and boxes at atmospheric pressure while sampling. This temperature was found to be between 2 °C and 3 °C, indicating temperature to be lower in the test tubes, than in the bottles used for indication of growth.

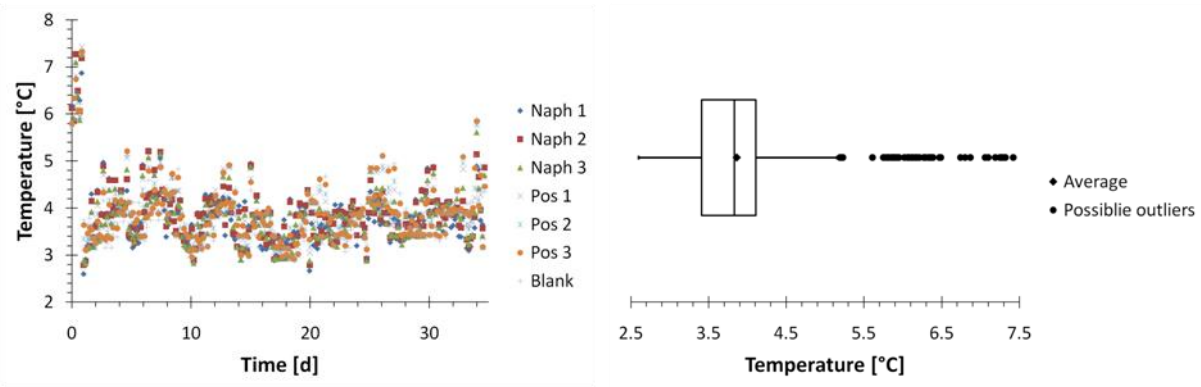

Figure 4-14: Temperature measured in test bottles used for indication of biodegradation

4.4 BTEX experiment

Because of big differences in areas measured in samples from different pressures and times of the experiment, relative concentration of BTEX was calculated. Relative concentration was calculated as the ratio between average area measured for the BTEX samples and average area measured for negative controls at the same measuring point. Standard error for relative concentration was estimated using equation 4-3 p. 54. Graphs showing change in relative concentration with time were made for benzene (Figure 4-15), toluene (Figure 4-16), ethylbenzene (Figure 4-17) and o-xylene (Figure 4-18). Degradation is seen for samples from 1 and 80 bars, and not for samples from 170 and

340 bars. At atmospheric pressures degradation can be seen to start significantly earlier than at 80 bars.

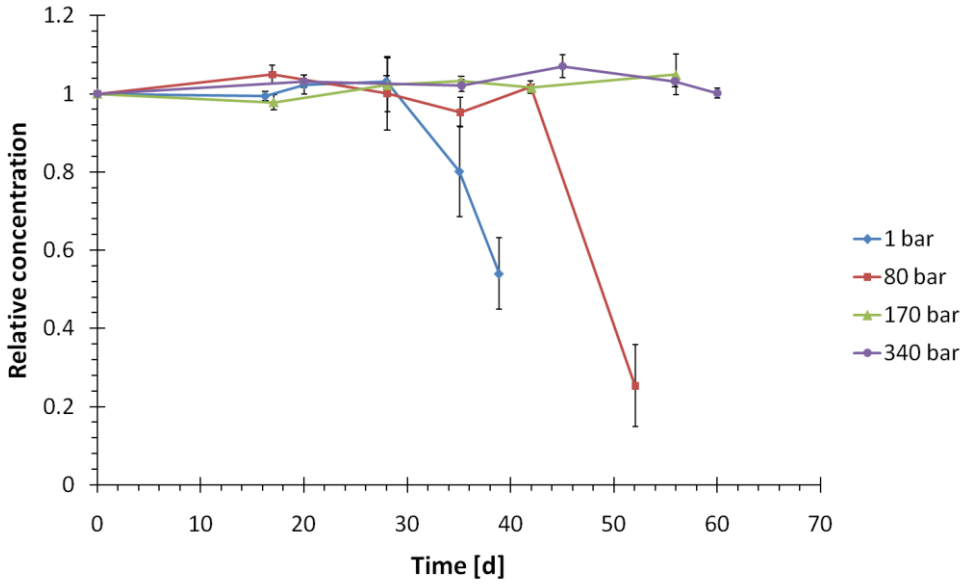

Figure 4-15: Relative concentration calculated for benzene

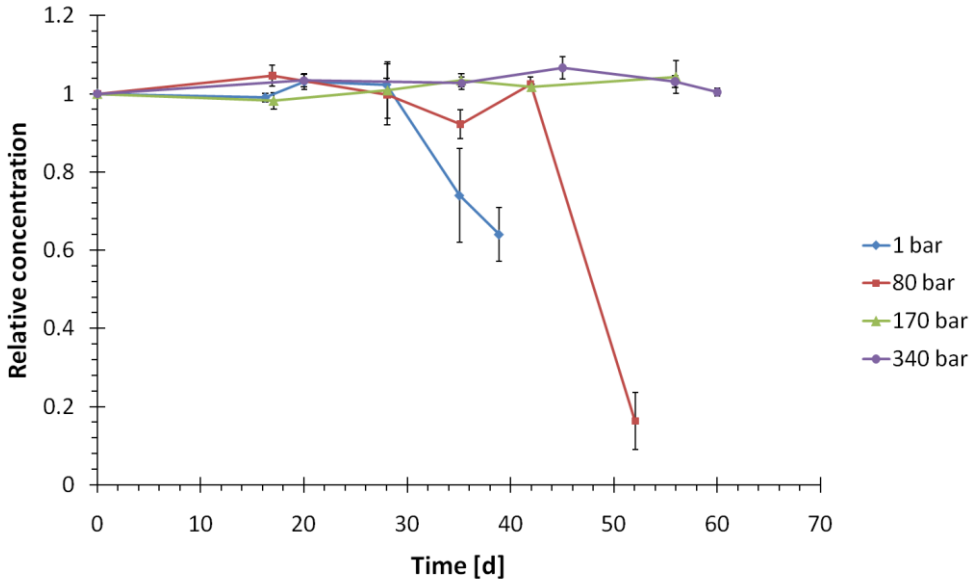

Figure 4-16: Relative concentration calculated for toluene

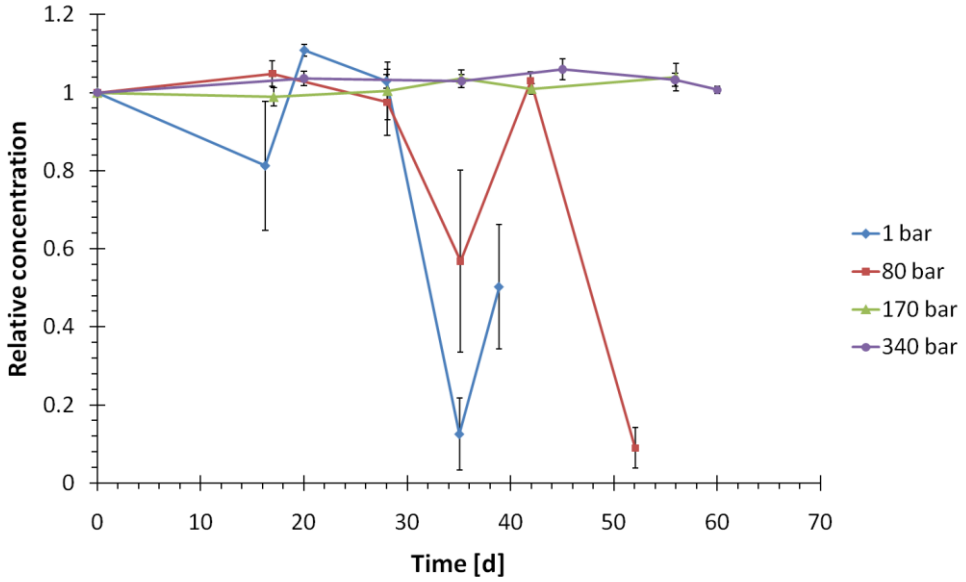

Figure 4-17: Relative concentration calculated for ethylbenzene

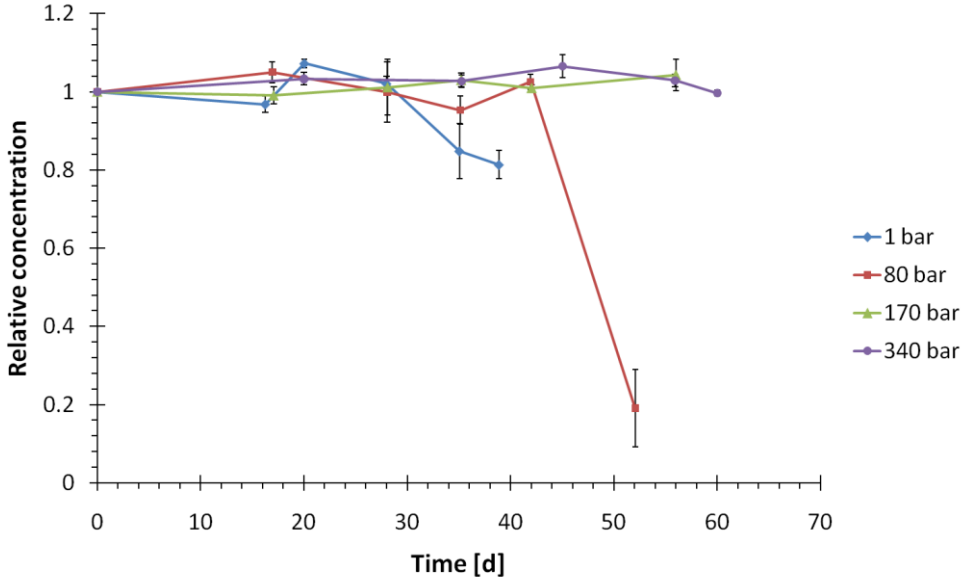

Figure 4-18: Relative concentration calculated for o-xylene

Degradation of BTEX was also calculated in percentage using relative concentrations. Tables showing percentage degraded with time for the different pressures and compounds are shown below. Table 4-4, Table 4-5, Table 4-6 and Table 4-7 show percentage degradation for samples from respectively 1 bar, 80 bar, 170 bar and 340 bar. The same trends are seen in these tables as in the figures above. In the tables, differences in degradation for the different compounds at the same pressure are easier to compare. In samples from both 1 bar and 80 bar ethylbenzene show highest degradation, followed by toluene. At 1 bar degradation of benzene is higher than o-xylene, while o-xylene degradation is higher than benzene degradation in 80 bar samples.

Table 4-4: Percent degradation 1 bar

Time [d]	Benzene [%]	Toluene [%]	Ethylbenzene [%]	o-Xylene [%]
16.3	1 ± 1	1 ± 1	19 ± 17	3 ± 2
20.1	-2 ± 2	-3 ± 2	-11 ± 2	-7 ± 1
28.0	-3 ± 2	-2 ± 2	-3 ± 2	-2 ± 2
35.1	20 ± 12	26 ± 12	87 ± 9	15 ± 7
38.9	35 ± 9	36 ± 7	50 ± 16	19 ± 4

Table 4-5: Percent degradation 80 bar

Time [d]	Benzene [%]	Toluene [%]	Ethylbenzene [%]	o-Xylene [%]
16.9	-5 ± 2	-5 ± 3	-5 ± 3	-5 ± 3
28.1	0 ± 9	0 ± 8	2 ± 9	0 ± 8
35.1	5 ± 4	8 ± 4	43 ± 23	5 ± 4
41.9	-2 ± 2	-3 ± 2	-3 ± 2	-3 ± 2
52.1	75 ± 10	84 ± 7	91 ± 5	81 ± 10

Table 4-6: Percent degradation 170 bar

Time [d]	Benzene [%]	Toluene [%]	Ethylbenzene [%]	o-Xylene [%]
17.1	2 ± 2	2 ± 2	1 ± 2	1 ± 2
28.1	-2 ± 7	-1 ± 7	0 ± 7	-1 ± 7
35.2	-3 ± 1	-3 ± 2	-4 ± 2	-3 ± 2
42.1	-1.5 ± 0.9	-1.8 ± 0.6	-1 ± 1	-1.0 ± 0.8
56.0	-5 ± 5	-4 ± 4	-4 ± 4	-4 ± 4

Table 4-7: Percent degradation 340 bar

Time [d]	Benzene [%]	Toluene [%]	Ethylbenzene [%]	o-Xylene [%]
20.0	-3 ± 2	-3 ± 2	-4 ± 2	-3 ± 2
35.3	-2 ± 1	-3 ± 2	-3 ± 2	-3 ± 2
45.1	-7 ± 3	-7 ± 3	-6 ± 3	-7 ± 3
55.9	-3 ± 1	-3 ± 2	-3 ± 2	-3 ± 2
60.0	0 ± 1	0 ± 1	-1 ± 1	0.4 ± 0.8

Two types of tubes made of different materials were used in the experiment at 1 bar. Measured peak areas differed for samples taken from glass vials and FEP vials, with glass vials having the highest peak areas. Peak area measured for negative control samples in glass tubes was relatively constant (Table 8-9 p.93). Average areas of the different BTEXs measured in negative control samples from glass vials were compared with average area measured in FEP vials, at different times and pressures. This was done by calculating a ratio between average area in FEP vials and average area in glass vials. Graphs showing how this ratio changes with time and pressure are shown in Figure 4-19. The difference between area measured in FEP vials and glass vials was largest for ethylbenzene, and smallest for benzene.

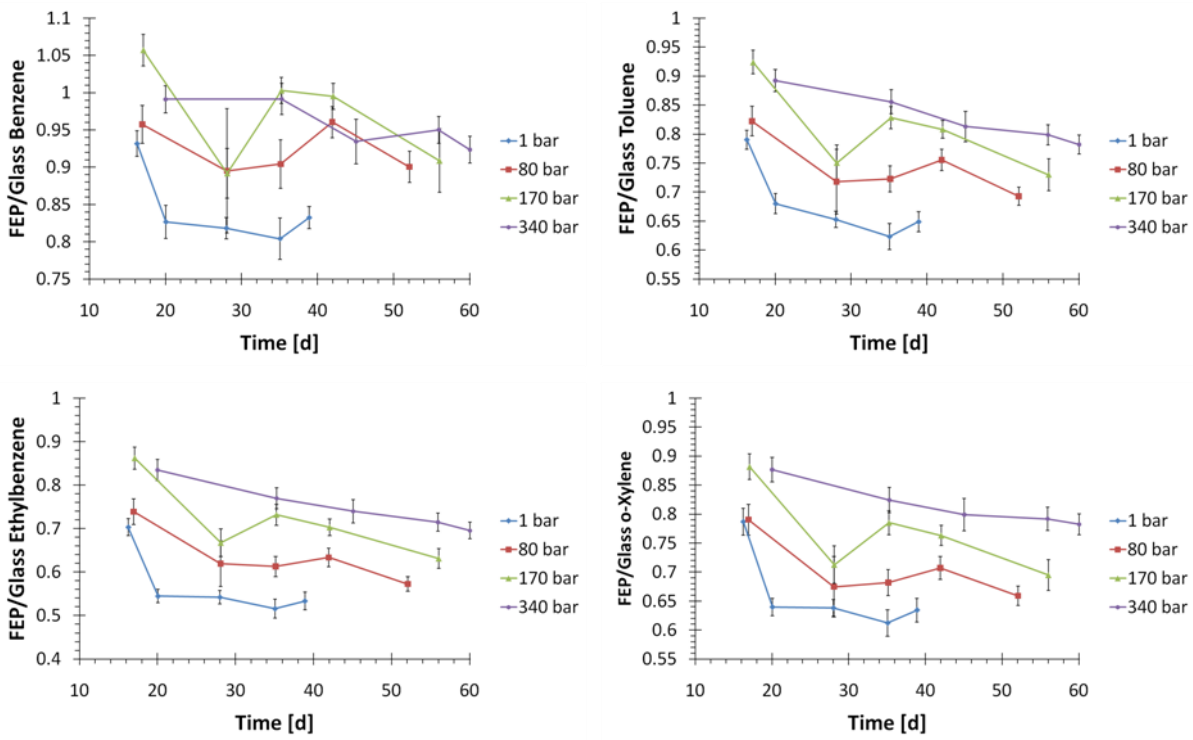

Figure 4-19: Ratio between FEP and glass vial area for A) Benzene, B) Toluene, C) Ethylbenzene and D) o-Xylene

Growth was measured as cell number using DAPI direct count for BTEX (Figure 4-20) and positive control (Figure 4-21) samples. Cell number in BTEX samples do not show the same clear pattern as seen in analysis of substrate. A large increase in cell number caused by growth on BTEX is seen for 80 bar samples, and some growth can also be seen for 1 bar samples. Growth is also seen for the last sampling time at 340 bars, which was not seen in substrate analysis at the same sampling time. In positive controls growth is detected at 80 bars, and no clear growth pattern can be seen at the other pressures (Figure 4-21). TOC analysis was also performed for positive control samples, but because of problems with the analysis this data has not been used.

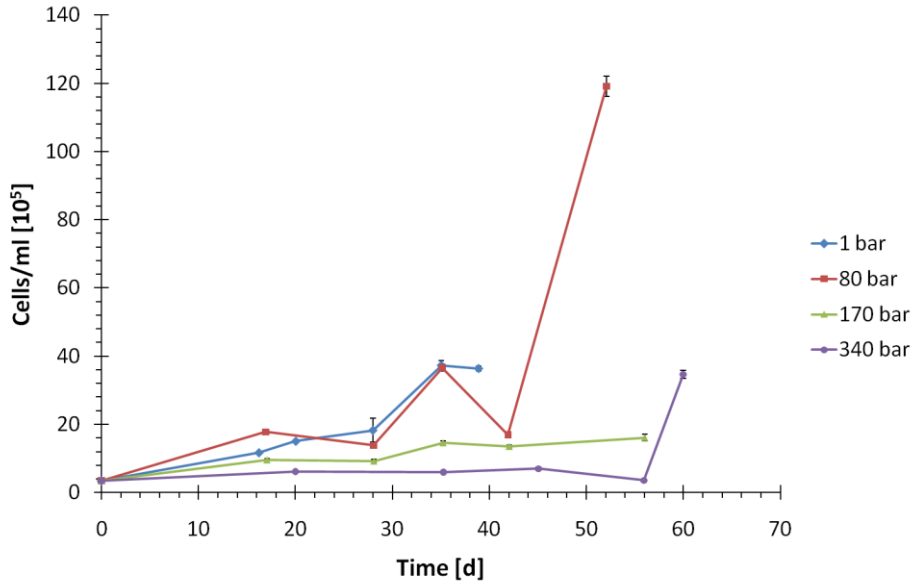

Figure 4-20: Cell number for BTEX samples

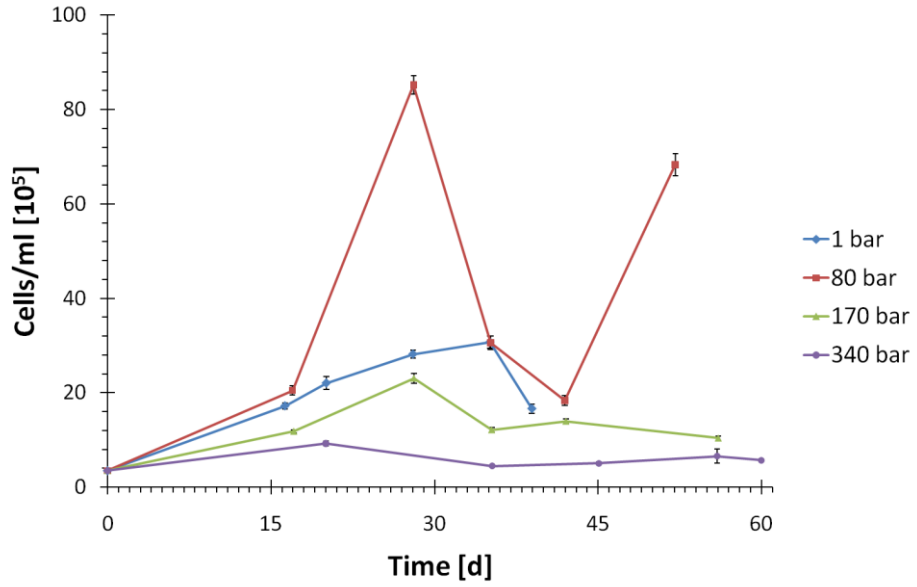

Figure 4-21: Cell number for positive control samples in the BTEX experiment

Bacterial diversity was analysed using DGGE analysis for the original seawater, and at the end of the BTEX experiment at each pressure (Figure 4-22). The samples were analysed in two parallels. Highest diversity is seen in the original sample. Samples from incubation at 1 bar, 80 bar and 170 bar show high similarities to each other, except for two bands only detected at 80 bars. The fingerprint seen for 340 bars is significantly different from the fingerprints found for all the other pressures.

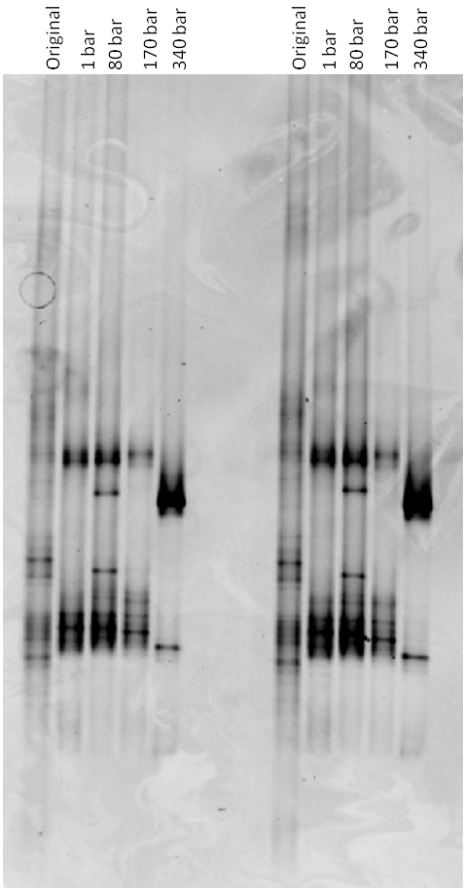

Figure 4-22: DGGE profile of samples taken of original seawater, and at the end of the experiment for 1 bar, 80 bar, 170 bar and 340 bar.

During the experiment temperature was measured in the water in the pressure vessels and boxes used at atmospheric pressure. Figure 4-23 show water temperatures measured. For the box and whiskers plot the minimum and maximum level are the highest value still within 1.5 times interquartile range.

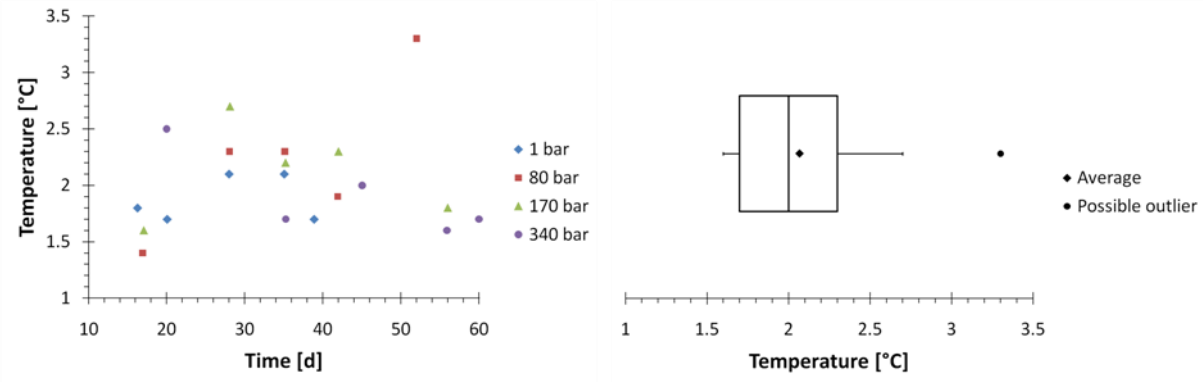

Figure 4-23: A) Temperature varying with time, B) Temperature in BTEX experiment displayed in a box and whiskers plot.

To get an indication of when the exponential phase started in the small test tubes, BOD was measured in three large bottles with BTEX inoculum and two large bottles with positive control inoculum (Figure 4-24). Degradation can be seen both for BTEX samples and positive control samples.

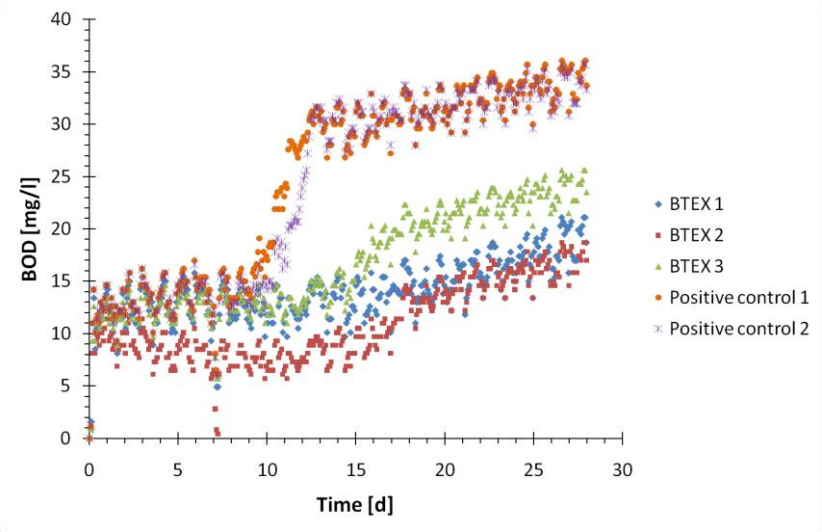

Figure 4-24: BOD measured in bottles used for indication of growth in the BTEX experiment

5 Discussion

This chapter starts with a short discussion of calibrations performed on the GC, and naphthalene and BTEX calibrations are compared. Results from the biodegradation experiments and methodology of these experiments are then treated. It then discusses weaknesses in the experiment and corresponding results, before further research that should be performed is suggested.

5.1 GC calibration

During the GC calibration for naphthalene different methods for preparation of naphthalene standard solutions were performed. Naphthalene was tried dissolved at a 50 mg/l concentration directly in seawater by using ultrasound and heating. This caused naphthalene to form monoclinic prismatic plates by sublimation (O'Neil, 2001). Because of this ultrasound should not be performed on naphthalene solutions when trying to enhance dissolution. Dissolving naphthalene in methanol before diluting it in seawater was chosen for preparation of calibration standards. This method works well for calibration. In biological experiments, were biodegradation of naphthalene is to be studied, methanol cannot be part of the matrix because of diauxic growth (Alexander, 1999).

In the naphthalene calibration, analysis of residuals (Figure 4-2 A p. 49) indicates that the regression model has an increasing variance when the concentration increases. The model assumptions for the simple linear regression model are hence not fulfilled. This is a common condition found in scientific data (Walpole et al., 2007). The dependence of variance on concentration can also be shown by calculating a ratio between residuals and standard concentration, and plot it against standard concentration (Figure 4-2 B p.49). This figure shows that calculated ratio does not vary much with concentration for the three highest concentrations used. For the lower concentration the ratio is bigger, this can be because of carryover giving a bigger measured area.

Residuals were also plotted against observation number (Figure 4-2 C p.49). There is no pattern in this figure to indicate time dependence. A pattern caused by the carryover effect and the sequence used in the analysis can be seen. The different calibration standards were analysed starting with one sample from the lowest concentration, continuing with one sample from each concentration up to the highest concentration, before repeating the sequence. This caused the blank samples to be analysed after the highest concentration giving carryover. If the residuals are approximately normally distributed they should follow a near linear line in Figure 4-2 D p. 49. This is not the case for the residuals from this regression model, something which may be induced by the non-homogeneous variance.

Naphthalene carryover was analysed (Figure 4-3 p. 50 and Table 4-1 p. 51). The chromatogram for the analysis (Figure 8-1 p. 91 and Figure 4-3 p. 50) show that the peaks measured in the blank samples have the same retention time, and are similar to the naphthalene peak in the naphthalene standard analysed. This indicates that there is carryover of naphthalene in the instrument. This carryover can be caused by naphthalene leaking from the septum in the inlet, or leftover naphthalene on the outside of the injection needle. The injection needle is washed inside, but not on the outside. Under injection, the temperature in the inlet increase, which can cause naphthalene absorbed in the septum to leak out.

Calibrations for the BTEX method (Figure 4-5 p. 52) do not show the same increasing variance with concentration as the naphthalene calibration. Scattering of the residuals for the three highest concentrations are approximately the same. The residuals for the three highest concentrations are situated along a curved line, hence indicating a trend in the data. The pattern seen indicate that a non linear regression might be more appropriate, for instance quadratic regression.

The R-squared values for the BTEX regressions are higher than 0.99 for all four substances (Table 8-8 p. 93), indicating that almost all variation are explained by the regression model chosen. R squared for the naphthalene calibration is 0.979 (Table 8-3 p. 90), which is also very high and the model explains almost all of the variation. R squared values are highest for BTEX regressions, indicating a better calibration for the BTEXs than for naphthalene. This is also seen when comparing residuals plot, naphthalene has an increasing variance, while this cannot be concluded about the BTEX calibrations.

Several different factors can explain why variance in the naphthalene calibration is more dependent on concentration than in BTEX calibrations. Naphthalene is a solid being dissolved in methanol and then in distilled water. At higher concentrations naphthalene might precipitate giving slightly different concentrations in the samples analysed at those concentrations. If small crystals are present to a different amount in the samples analysed, and they are dissolved when the sample is heated prior to injection, this can cause a higher variance in areas measured at high concentrations. BTEXs are all liquids being dissolved in water and will thus not precipitate in standard solutions prepared. Preparation of standard solutions was also performed by two distinct methods for the two calibrations, this might cause a different amount of loss due to evaporation. If loss due to evaporation was higher during the naphthalene calibration than in the BTEX calibration this might partly explain the differences seen in the regression analysis performed.

5.2 Biodegradation

In the naphthalene experiments two different columns were used in the GC analysis, giving different responds. Consequently there is no mutual area for start concentration for all the measurements made. There are also variations within the areas measured with the same method. These variations can be caused by how the tubes were prepared and precipitation of naphthalene in the tubes after preparation. When preparing the tubes there was a large loss of naphthalene in the pumping process. For the different tubes this pumping process took variable lengths of time, which give variations in concentration in the test tubes (Table 4-3 p. 53). Pictures taken for DAPI analysis showed crystals in the naphthalene samples (Figure 5-1). Crystals were not detected in positive control and BTEX samples. These crystals were seen in variable amounts in the samples analysed, which indicates precipitation to occur to different extents in the different samples. Naphthalene dissolved in cyclohexane have an emission spectra with a peak at about 375 nm gradually tailing to 500 nm (Prahl and Lindsey, 2011), unless naphthalene crystals show very different emission properties they can be expected to emit some blue light (435-480 nm (Skoog et al., 2007)).

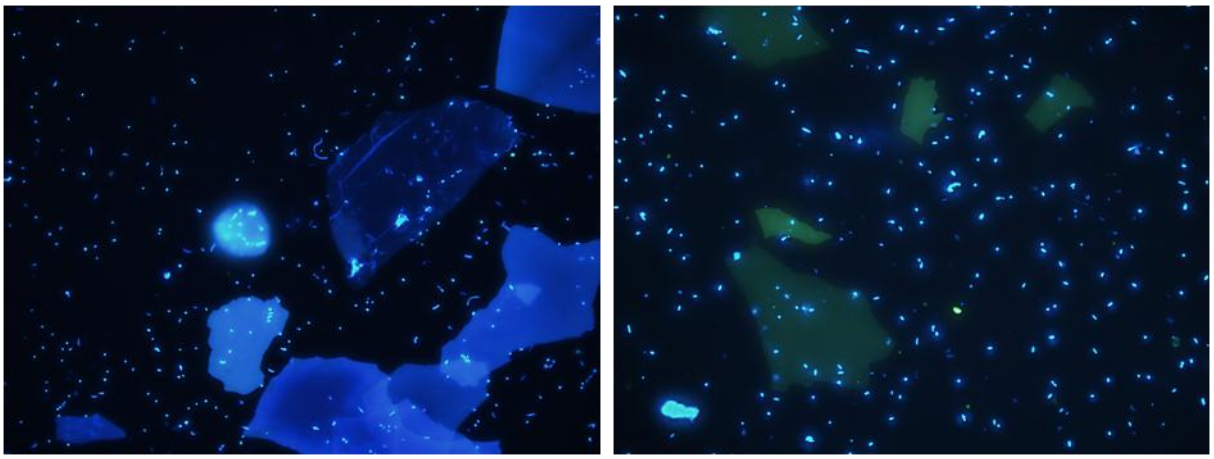

Figure 5-1: DAPI pictures of two different naphthalene samples taken at A) 170 bar day 29, B) 80 bar day 21

Biodegradation of naphthalene was measured for samples incubated at atmospheric pressure after 30.8 days, and not in samples taken after 24.0 days. This can be seen in Figure 4-7 p. 54, and indicates that degradation of naphthalene at atmospheric pressure started somewhere between day 24 and day 31. This graph shows a ratio calculated between area measured in negative control samples and area measured in naphthalene samples. When area measured in negative controls are higher than area measured in naphthalene samples, this indicates degradation of naphthalene. This happens at atmospheric pressure, but not at 80, 170 and 340 bars. This indicates biodegradation of naphthalene to be affected by pressure.

Inherent differences in biological experiment cause a higher standard error in the exponential phase because of degradation starting at slightly different times in the different test tubes. Thus some

samples might be taken in the exponential phase, while others are still in the lag phase or already in stationary phase. Where this is the case, standard errors are higher. Thus in order to get an indication of growth, standard error can be plotted as percentage of average area measured. From Figure 4-8 p. 55 it can be seen that standard error as percentage of average area increase for 1 bar samples from day 24 to day 31. This trend cannot be seen for samples from 80, 170 and 340 bars, indicating degradation of naphthalene at atmospheric pressure, but not at elevated pressure in the experiment.

When a common start concentration cannot be found, relative concentration can be calculated at each measuring point (Figure 4-9 p. 56). The first column was only used at the first sampling time, hence degradation at this point is assumed to be zero. This assumption is valid because the ratio calculated between negative control and naphthalene sample is between 0.9 and 1.1 at this point (Figure 4-7 p. 54). For 80, 170 and 340 bars there are large variations in the relative concentration calculated, but there is no trend indicating degradation. The large variations are caused by different start concentrations in the tubes, hence giving large variations when a common start concentration is assumed. For 1 bar relative concentration calculated follow a substrate degradation curve, indicating degradation to start between day 24 and 31.

In the BTEX experiment there was a difference between peak area measured in the GC analysis for negative control samples incubated in glass tubes and FEP tubes at 1 bar. Area measured in samples from glass tubes was at all times higher than area measured in samples from FEP tubes. Measured area in samples taken from glass tubes was relatively constant with time for all four BTEXs (Table 8-9 p. 93). Hence a ratio between area measured for negative control samples in FEP tubes with area measured in negative control glass tubes was calculated (Figure 4-19 p. 62). Because all negative control test tubes are made using the same inoculum, the difference in concentration measured with GC analysis are possibly and effect of absorption of BTEX into the FEP polymer structure of test tubes. As seen in Figure 4-19 p. 62 absorption is highest for ethylbenzene, followed by o-xylene, toluene and least for benzene. Absorption measured for toluene and o-xylene are almost equal. Apart from 340 bar samples (Table 8-13 p. 94), where absorption of o-xylene are slighty higher than for toluene (Table 8-10, Table 8-11 and Table 8-12 p. 94). This indicates that it is the ethyl and methyl groups that are associated with the polymer, and opens for migration of the substrates into the FEP polymer. Benzene does not have any attached methyl or ethyl groups, and are thus the substrate with least absorption into the polymer.

Another trend detectable in Figure 4-19 p. 62 is that pressure seems to decrease absorption, in other words function as an inhibitor for absorption. Pressure inhibits absorption of BTEXs into the polymer

because absorption causes a volume increase of the polymer. When pressure increases processes causing an increase in volume will be inhibited, this is also seen for piezophilic bacteria (refer to 2.1.1 Biological adaptations p.14). Because the amount of BTEXs present in the samples taken are different for the four pressures used, relative concentration is calculated and used in graphs to give comparable data.

For BTEX samples at 1 bar no degradation is detectable after 28 days for any of the substrates (Table 4-4 p. 61). Over the next week, degradation starts for all four substrates, but to different extents. In samples taken at day 35.1 ethylbenzene shows the fastest degradation with a relative concentration of 0.13 ± 0.09 (Figure 4-17 p. 60), followed by toluene at 0.7 ± 0.1 (Figure 4-16 p. 59), benzene at 0.8 ± 0.1 (Figure 4-15 p. 59), and o-xylene at 0.85 ± 0.07 (Figure 4-18 p. 60). Towards the next, and last, sampling time at day 38.9 benzene, toluene and o-xylene all show a continued degradation, with benzene having the largest drop in relative concentration. For ethylbenzene an increase in relative concentration to 0.5 ± 0.2 is measured.

Samples taken at 80 bars also show degradation of the BTEXs, but at a later time than the samples from atmospheric pressure. At this pressure some degradation is measured for ethylbenzene at day 35.1, followed by no detectable degradation of any of the four substrates at day 41.9 (Table 4-5 p. 61). At day 52.1, degradation is measured for all the BTEXs. Ethylbenzene has the lowest relative concentration at 0.09 ± 0.05 (Figure 4-17 p. 60), followed by toluene at 0.16 ± 0.07 (Figure 4-16 p. 59), o-xylene at 0.2 ±0.1 (Figure 4-18 p. 60) and benzene at 0.3 ± 0.1 (Figure 4-15 p. 59).

Substrate analysis of BTEX samples incubated at 170 and 340 bars show no signs of biodegradation after respectively 56.0 (Table 4-6 p. 61) and 60.0 days (Table 4-7 p. 61). This indicates that pressure has an effect on biodegradation of BTEX in seawater, with degradation starting at 1 bar first, continuing with degradation at 80 bar, and no degradation detectable within two months for samples pressurised to 170 bar and 340 bar. The different BTEXs were also found to biodegrade at different times in a mixture of all four substrates. Bacterial growth starts with ethylbenzene as substrate, followed by toluene. At atmospheric pressure benzene was preferred over o-xylene, while at 80 bar the concentration of o-xylene decreased more than benzene.

For ethylbenzene an increase in relative concentration is measured for samples at 1 bar from day 35.1 to day 38.9 (Figure 4-17 p. 60). For samples from 80 bars degradation is measured at day 35.1, but at day 41.9 the relative concentration calculated is 1.03 ±0.02 (Figure 4-17 p. 60). This indicates that after degradation has started, more ethylbenzene is introduced into the incoulum in some way. When concentration decreases desorption will occur to keep the equilibrium between the two phases. Hence substrate graphs will not follow the trend expected in a normal biodegradation batch

culture test. At atmospheric pressure benzene, which is the substrate with least absorption into the polymere, is the only BTEX where the substrate graph show an increasing rate of degradation from day 35.1 to day 38.9 (Figure 4-15 p. 59). Toluene (Figure 4-16 p. 59) and o-xylene (Figure 4-18 p. 60) at 1 bar show a decreasing concentration from day 35.1 and day 38.9, but at a slower rate than from day 28.0 to day 35.1. Toluene have a slightly higher degradation rate than o-xylene from day 35.1 to day 38.9, which are consistent with absorption of o-xylene being slightly higher than absorption of toluene. Ethylbenzene is the substrate with highest absorption into the FEP polymere, and the only substrate where concentration increased after degradation has started (Figure 4-17 p. 60).

The increase in concentration seen for ethylbenzene cannot be explained only by the absorption/desorption effect. This effect will slow down degradation by slowly releasing more substrate into the water phase as biodegradation proceed, as seen for toluene and o-xylene. For ethylbenzene there is a large increase in concentration. Ethylbenzene is seen to be the first substrate to be degraded, and also the substrate with highest absorption. If rate of degradation is faster than the rate of desorption, ethylbenzene could be fully removed from the water phase, and then an increase in concentration would be seen as more ethylbenzene was released from the polymere. This could explain some of the increase seen for ethylbenzene at atmospheric pressure. Combined with inherent differences in a biological experiment, and the fact that the samples are all taken from different test tubes, this can result in large differences in measured concentrations in the exponential phase. The weakness of this explanation is that if degradation rate is higher than desorption rate, all substrate released into the water phase should be degraded fast, and a large increase in concentration should not be seen.

Cell number was measured using DAPI counting in both the naphthalene experiment and BTEX experiment. Figure 4-10 p. 56 show cell number measured for naphthalene samples. These data are inconclusive since no trends are detectable. At some measuring points more samples were analysed to see if the parallels were similar. The change in cell number was so small, that it was decided not necessary to analyse several parallels to get a good enough picture of the cell number at each sampling time in the experiment.

Cell number measured with DAPI analysis of BTEX samples is shown in Figure 4-20 p. 63. For 80 bar samples there are similarities to the substrate graphs, especially for ethylbenzene (Figure 4-17 p. 60). When substrate concentration decreases, cell number increases. An increase in cell number is seen at the same times as ethylbenzene concentration is seen do decrease in Figure 4-17 p. 60. At day 41.9 when no degradation of ethylbenzene is measurable with GC analysis, cell number is back at a similar level to before growth occurred. For 1 bar, cell numbers also show similarities to the different

substrate graphs (Figure 4-15 p. 59, Figure 4-16 p. 59, Figure 4-17 p. 60 and Figure 4-18 p. 60). When substrate concentration decrease, cell number increase, and from day 35.1 to day 38.9 when ethylbenzene concentration increase, while benzene, toluene and o-xylene concentrations decrease at different rates, there is a small decrease in cell number. Samples from 170 bars are also consistent with substrate data, with no growth detectable.

Cell numbers for samples from 340 bars are consistent with substrate data until the last sampling time. No growth is detectable in samples taken from day 0 to day 55.9, while at day 60 an increase in cell number is seen. While all earlier samples were stored in the fridge for some time before being coloured and counted, the samples taken at day 60 were coloured and counted the same day. This could affect the brightness of the fluorescent cells. Cells will also be more fluorescent when they are growing, because more RNA and DNA are present in growing cells. This could affect the number of cells detected at different times, if several cells in earlier samples were dormant, while at day 60 the cells were slowly starting to grow. At the first sampling times an underestimation of cell number could have happened.

Figure 4-11 p. 57 show cell number measured for positive control samples in the naphthalene experiment. Here growth is detected for samples at atmospheric pressure from day 9 to day 21 and day 24. At 80 bars growth is measured from day 21 to day 29 and day 31. Samples from 170 bars have a small increase from 29 to day 34, which indicate that growth might start around day 31, but the increase is too small to be significant. If more tubes had been available for sampling after this point, it could have shown if cell number continued to increase. Data from 340 bar show that there is no growth on benzoate at this pressure. The measurements taken at day 31 for 1 bar and day 34 for 80 bar have a large decrease in cell number from the previous measurements. For 1 bar cell number increase again when measured at day 33.

Cell number for positive control samples in the BTEX experiment are shown in Figure 4-21 p. 63. Here growth on benzoate is measured for 80 bar samples at two different times. First cell number increase from day 17.0 to day 28.1, before a decrease is seen for the next two sampling times. Cell number increases again from day 42.0 to 52.1. For 1 bar, 170 bars and 340 bars, a large increase in cell number is not observed. The first increase in cell number for 80 bar samples is consistent with data from the naphthalene experiment. A large decrease in cell number was also measured for 80 bar in the naphthalene samples, but the naphthalene experiment ended earlier than the time of the second growth found in the BTEX experiment. Thus this second growth cannot be compared with data from the naphthalene experiment. In the naphthalene experiment a large increase in cell number was also measured for 1 bar samples, this was not found in the BTEX experiment.

The large decrease in cell number after degradation started can partly be an effect of the different batch cultures being at slightly different places in the growth curve. Cell number in a test tube where degradation starts earlier than another tube would have a higher cell number at an earlier time than another tube might have at a later time.

Cell number increases from the original seawater analysed to the first sampling point in both experiments, both for naphthalene (Figure 4-10 p. 56), BTEX (Figure 4-20 p. 63) and positive control samples (Figure 4-11 p. 57 and Figure 4-21 p. 63). In all inoculums inorganic nutrient solutions, amino acid solution and vitamin solution were added in excess to make sure the substrate added would be the single limiting factor for growth. By this method ideal conditions for bacteria to use DOC already available in the seawater as carbon source are rendered possible. The initial increase in cell number can therefore be explained by bacteria utilising the DOC present in seawater

Differences in cell numbers measured can be induced by errors in the DAPI counting performed. Adaptive threshold was used to count bacterial cells with CellSense dimensions. Hence cells with different fluorescence could be counted in the same picture. Cells close together where another problem (Figure 5-2). Here the program could not differentiate between large cells and several small cells placed next to each other. If cells were to close together, they were counted as one cell, hence underestimating the cell number in the exponential growth phase.

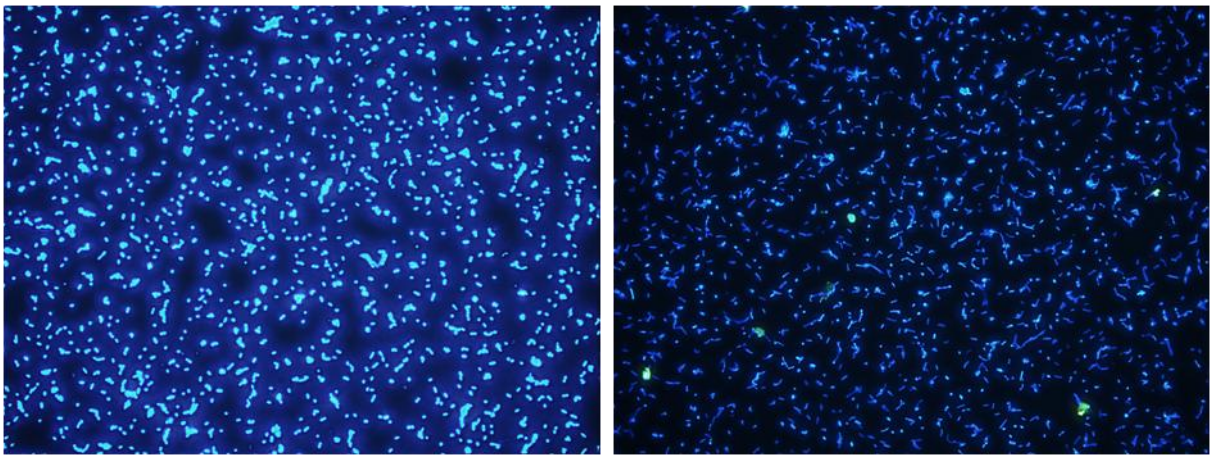

Figure 5-2: A) DAPI picture positive control BTEX experiment 80 bar day 28.1 B) BTEX sample 80 bar day 52.1

Change in bacterial diversity was analysed using the well established DGGE approach (Figure 4-22 p. 64) (Muyzer and Smalla, 1998). The two duplicates are very similar and show the same pattern, this indicates the method to be reliable. In the original sample the highest number of bands is observable, suggesting that the bacterial diversity is highest in the beginning of the experiment. In seawater exposed to BTEX a few specific bands from the original sample became stronger. This is generally assumed to indicate that a few specific species became abundant in the sample, here

probably the BTEX degraders. These species overgrow the other species present in the seawater originally. The 1 bar, 80 bar and 170 bar fingerprints looks very similar, thought at 80 bar two rather strong bands are visible, which are not visible at 1 bar and 170 bars.

The community fingerprint for 340 bars looks significantly different from all others. It has the lowest number of visible bands among all, suggesting low bacterial diversity. This might indicate that fewer bacteria in the original seawater used, tolerate the high pressure of 340 bars. This is also indicated by cell number measured for 340 bars (Figure 4-20 p. 63) being significantly lower than for the other pressures.

Growth was detected in 1 and 80 bar samples, however not in 170 and 340 bar samples. At pressures lower than 100 bar prokaryotes are defined as piezotolerant, while prokaryotes with optimal growth pressure between 100 and 500 bar are piezophilic (Table 2-1 p. 15). The seawater used was collected at 80 meter depth which is equivalent with a pressure of 8 bars. Bacteria present in the beginning of the experiment are hence most likely only piezotolerant. The same species seems to be growing at 1 bar, 80 bars and 170 bars. The dominating band at 340 bars is very weak in the original sample, and it is not seen at the other pressures. This indicate that fewer species available in the seawater used are capable of piezophilic growth, and the abundance in the beginning is very low explaining the low cell numbers measured for 340 bar samples.

The two bands visible for 80 bars that is not seen at atmospheric pressure could be BTEX degraders which grows at elevated pressures. All the bands found in the 1 bar fingerprint are also found in 80 bar samples indicating that the bacteria responsible for BTEX degradation at atmospheric pressure also grow at 80 bars. Growth on BTEX was larger for 80 bar samples, than for 1 bar samples at the end of the experiment when DGGE analysis was performed. This is because the last sampling time at 80 bars was better timed than for 1 bar, the last sampling at atmospheric pressure should have been taken later than what was done. Hence these two bands might also be species becoming dominant later in degradation of BTEX.

The experiments done indicate that increasing pressure slows down degradation of naphthalene and BTEX. These substrates are all commonly found in oil and petroleum products. The oil industry is already concerned with oil spills and their effect on aquatic life. If biodegradation is slower in the deep-sea, this means that the other inhabitants of this part of the ocean will be exposed to the oil released in a possible oil spill for a longer time than what would be the case in surface waters. This makes the deep-sea more vulnerable and sensitive to accidents and exploitation of petroleum resources found below the continental shelves.

The deep-sea includes the largest part of the ocean and is therefore also home to large fish resources. Even the deepest parts of the ocean hold several life forms. For the pelagic fish an oil spill could have devastating consequences. Crude oil is known to contain several xenobiotic compounds such as PAHs (Walker et al., 2006). The PAH benzo(a)pyrene is a known carcinogenic compound (Walker et al., 2006), and a prolonged exposure could have lasting consequences for the deep-sea fish population. Several compounds could also affect the planktonic community, bioaccumulation would then give an increased concentration in fish, and further up the food chain. Humans are even higher in the food chain, and consumption of polluted fish could be a problem.

A hydrocarbon plume was measured after the Deepwater Horizon accident, and it covered a large area of the Gulf of Mexico (refer to 2.2.2 Biodegradation of hydrocarbons in the deep-sea p. 34). This research found an effect indicating a prolonged lag phase in biodegradation of hydrocarbons, which consequently means that oil will be present at a high concentration for a longer time period in the deep-sea than at the sea surface. At the surface other processes, such as evaporation and physical degradation by UV light from the sun would also increase removal of oil from the seawater. In the deep-sea there are no sun light, and no air the compounds can evaporate into.

In the deep-sea the plume can be taken by currents and spread over a large geographical area, similar to volcanic ash being released high into the atmosphere and spread over large geographical areas. When oil is released to the surface waters, preventing the spill to be spread by the wind is hard, but usable equipment exists. If oil released to the deep-sea is taken by large sea currents, it is impossible to prevent it from spreading to large areas. Hence preventing the spill from happening in the first place is most important. When the oil first is released to the deep-sea, one of the most important processes nature has available is to remove it through biodegradation. Hence when pressure is seen to increase the time bacteria need to degrade compounds found in oil, a large oil spill in this region is a potential catastrophe.

5.3 Methodology

In the first biodegradation experiment performed on naphthalene the inoculum solution was made by pumping a standard solution over in a seawater solution, before the inoculum solution was pumped over in test tubes using nalgene tubing. In this process the concentration of naphthalene fell from the expected 9.92 mg/l (refer to 3.2.1 Naphthalene experiment p. 39) to 5.6 mg /l ± 0.3 mg/l (Table 4-2 p. 53) in the naphthalene inoculum used, and to between 1.2 mg /l ± 0.3 mg/l and 2.2 mg/l

± 0.3 mg/l (Table 4-3 p. 53) in naphthalene test tubes. It is hence not advised to use this method for experimental preparation, and it was not used in the BTEX experiment.

Naphthalene concentrations measured using the naphthalene calibrations have approximately the same variance for all concentrations measured (Table 4-2 p. 53 and Table 4-3 p. 53). This is because of a high variance in the calibration (Table 8-3 p. 90) dominating when calculating standard error for measured naphthalene concentration. The high variance from the calibration might be due to the increasing variance found.

Because of the loss of naphthalene in the process of preparing the test tubes the concentration at the start of the naphthalene experiment is unknown. An approximate concentration is known because of measurements done while preparing the test tubes (Table 4-2 p. 53), but these samples were taken in two different ways, and two different averages were found. Substrate test tubes and negative controls were prepared at the same time for every pressure vessel. Hence negative control should give an estimate for naphthalene start concentration, but because negative control tubes were opened an extra time to add sodium azide (negative control inhibitor) there was an additional loss of naphthalene not experienced by the sample tubes. Thus, using negative control as an estimate of start concentration will give an underestimation of the real start concentration of naphthalene in naphthalene test tubes. For BTEX sodium azide was added before the inoculum, so that loss by evaporation would be the same in negative controls and BTEX test tubes.

The naphthalene experiment used two test tubes as negative controls and three as positive controls. In the BTEX experiment this was changed to three negative controls and two positive controls. This was due to negative control serving as a control of BTEX start concentration. If start concentration varies throughout the preparation of test tubes an estimate of the actual start concentration in each pressure vessel can be calculated. By changing the number of negative controls from two to three the standard deviation of measured peak area in negative control samples is improved.

Positive control only serves as a control for growth in the experiment. If there is no growth in positive control, there might be a problem with the seawater used. Thus a lack of growth in the substrate test tubes is not an indication of the substrate not being biodegradable. Since the area found for positive control will not be used to calculate biodegradation, no accuracy is lost by decreasing the number of positive control test tubes from three to two.

The chromatograms obtained for BTEX samples (Figure 8-2 p. 95) and BTEX negative control samples (Figure 8-3 p. 96) show that negative control samples have an extra peak with short retention time. This is most likely an oxidation product caused by sodium azide added in negative control samples,

and it does not affect the data analysis performed for the BTEX experiment. When negative control is used as an assumption of start concentration, a small underestimation of the actual start concentration might happen if some BTEX is oxidized and measured as a separate peak.

Since the experiment was performed under pressure in small pressure vessels, it was performed without any continuous monitoring in the test tubes, and small test tubes were used. To have an indication of when biodegradation started oxygen consumption was measured with respirometry in a few bigger bottles containing the same solution as the small test tubes. In both biodegradation experiments, naphthalene and BTEX degradation was found to start earlier in the big bottles than in the small tubes.

In the big bottles used in the naphthalene experiment, degradation was measured after 6-8 days for positive controls (Figure 4-12 p. 57 and Figure 4-13 p. 58), and indication of growth can be seen after 16.5-19 days for naphthalene samples (Figure 4-12 p. 57). While in the small test tubes degradation for positive control started somewhere between day 10 and day 21 at atmospheric pressure (Figure 4-11 p. 57). Naphthalene degradation at atmospheric pressure started between day 24 and 31 (Figure 4-7 p. 54) in the small tubes.

In the BTEX experiment, degradation in the big bottles was measured in positive control samples after about 10 days (Figure 4-24 p. 65), and for BTEX samples indication of growth can be seen after about 14-16 days (Figure 4-24 p. 65). While for the small test tubes BTEX degradation was first seen in the sample taken out from atmospheric pressure day 35 of the experiment (Table 4-4 p. 61), no degradation was seen day 28. For positive control the data from the DAPI analysis performed are inconclusive for 1 bar samples (Figure 4-21 p. 63), and the TOC data has not been considered due to problems with the method. It is hence not possible to compare data for the big and small bottles for positive control in the BTEX experiment.

This indicates that the length of the lag phase increases for all substrates tested when test volume decreases. Decrease in test volume seems to affect the length of the lag phase most for the BTEXs and least for sodium benzoate used as positive control. This can be explained by the bacterial community available in the seawater at the beginning of the experiment. At both volumes the same community should be present in the original inoculums, since the same inoculums are used, but total number of bacteria available is higher when volume is higher. While benzoate is an easily biodegradable substrate most bacteria should be able to degrade, BTEXs have more complex degradation pathways. The number of bacteria capable of utilising benzoate should thus be higher than the number available to utilise BTEXs. This should be the same for both big and small test tubes, but for the smaller volume fewer bacteria will be available of both types. When a smaller initial

number of bacteria are available for growth, the time it takes for these bacteria to multiply to a number where a visible removal of substrate can be measured will be longer. The lag phase can be seen as the time spent until substrate removal is measurable (Alexander, 1999). Hence benzoate will have a shorter lag phase than naphthalene and BTEX, and the length of the lag phase will increase when the test volume decrease.

Because degradation started earlier in the test bottles used for indication of growth, sampling was performed earlier than needed, and too many times during the lag phase. When the bottles used for indication did not serve as indication of growth, the test tubes at atmospheric pressure was used instead. Sampling was performed at atmospheric pressure first to check for degradation, before continuing with sampling with increasing pressure. This caused too few tubes to be available for sampling when degradation started, and no tubes were available for sampling in stationary and endogenous phase at any of the pressures in neither of the experiments. To solve this problem more measuring points should have been available, especially at atmospheric pressure, seeing as atmospheric pressure was sampled first.

Absorption into the FEP polymer was another challenge not expected in the experiment. Alternatives to FEP vials are glass vials equipped with a septum and a syringe. The syringe would be filled with inoculum, and under compression this inoculum would be injected into the vial. A problem encountered when using glass vials are that glass can shatter under pressure, and leakage around the syringe needle through the septum can occur. Leakage can be minimised by the use of a tick septum making the septum less permeable, but by using a septum, absorption of BTEXs could also be a problem. Because negative control can be used to account for the absorption in FEP tubes, this solution is still safer than using glass vials under pressure.

Naphthalene and BTEX are volatile compounds and at all stages of the experiment where solutions were transferred there is a potential loss by evaporation. This loss was minimised by reducing contact between naphthalene and BTEX solutions and the overlying gas phase. Headspace of inoculums used was also connected to headspace of a solution with a higher concentration during experimental preparation.

5.4 Weaknesses

Continuous monitoring of the test tubes was not possible, thus for the small tubes degradation could not be followed continuously for determination of when sampling should be performed. Because lag phase ended earlier in the bottles monitored with respirometry, compared to the test tubes used in these experiments, these did not function for indication of growth. In the naphthalene experiment,

this resulted in too few tubes for sampling once degradation finally started. During the BTEX experiment sampling was performed approximately once a week for atmospheric pressure after degradation was seen in the indication bottles, and more infrequent for the other pressures. Hence again, especially for 1 bar samples too few tubes were available for sampling when degradation started, and sampling could not be performed in stationary and endogenous phase. Lack of continuous monitoring of the test tubes also makes it difficult to find the exact moment degradation started for different substrates and pressures.

The seawater used in both experiments was collected from 80 meters depth, and held 7 °C. The bacteria present at the beginning of the experiment were thus most likely piezotolerant not piezophilic bacteria. For 170 bars and especially 340 bars this could prolong the lag phase, as fewer bacteria in the original seawater normally would grow at these high pressures.

5.5 Further research

The pressure effect seen on degradation of naphthalene and BTEX in this work should be further documented by performing more experiments. Some experiments should be performed using the same experimental conditions, to verify the data found in this experiment. The methodology used should also be developed to give more sampling points in exponential, stationary and endogenous phase, thus following all the phases of bacterial growth in a batch culture.

Experiments using different substrates or mixtures of substrates should be performed. This should include chemicals typically found in crude oil, and also petroleum products (mixed substrates) such as diesel. Thus a broader picture on what would happen with all substances released in a potential oil spill would be analysed.

Experiments using different experimental conditions should also be performed. The pressures used should be expanded to include more sea depths. The Prestige tanker sank to a depth of 3850 meters (Uad et al., 2010), and pressures around 380 bar to 400 bar would hence be interesting to study. Also expanding within the range of pressure used in this work is important. To more precisely determine at which pressure the pressure effect seen here becomes important, several pressures between 1 bar and 80 bar should be studied.

Experiments should be done using seawater collected from different geographical locations. Use of arctic water could give a better assessment of piezophilic growth because there are many similarities between piezophiles and psychrophiles. Water from the deep-sea should if possible be used. This would give several experimental challenges, because it would be difficult to perform experiments

without decompressing seawater samples taken from the deep sea at any times. Getting seawater samples from the deep sea would also be more expensive.

A way to continuously monitor degradation in the experiments performed should be developed. This makes it easier to know when sampling should be performed for other analytical methods, and give continuous data following the duration of the growth curve. Finding the exact moment degradation started in the experiment would then be possible.

6 Conclusion

This experiment has indicated that the biodegradation process slows down under increased pressure due to a prolonged lag phase. In a 34 day biodegradation experiment degradation of naphthalene was detected for samples at atmospheric pressure, but not for pressurised samples. In another experiment on BTEX degradation started between day 28 and 35 at 1 bar and between day 42 and 52 at 80 bars. No degradation was detected after 56 days for 170 bar and 60 days for 340 bars. Thus degradation in the deep-sea might be slower than in surface water, and weathering of a potential oil spill will take longer. This makes the deep-sea more vulnerable to oil spills and to exploitation of the petroleum resources available in these parts of the oceans.

Other weathering processes such as physical degradation by UV light and evaporation of hydrocarbons to the atmosphere are not part of the weathering process in the deep-sea. There is no sun light in this part of the ocean, and thousands of meters of water lie between the deep-sea and the atmosphere. Hence biodegradation is even more important for removal of oil released to the deep-sea, than for oil spills in surface waters. In the deep parts of the ocean, large sea currents can transport a potential oil spill over a large geographical area. Equipment for hindering oil from spreading at the surface exists, but in the deep-sea this is not easy. If oil first is taken by large ocean currents, large areas of the ocean can be affected.

Oil released in the deep-sea can also have biological effects, as large fish resources are found in the deep-sea. Oil is known to contain several xenobiotics, and by uptake and bioaccumulation these pollutants could affect several levels of the food chain, in the end possibly also humans eating polluted seafood.

Analysis of bacterial diversity using DGGE analysis showed that diversity was highest in the beginning of the experiment. In samples exposed to BTEX diversity went down and a few species became dominant. For samples incubated at 1, 80 and 170 bars the community fingerprints obtained showed high similarity, except for two strong bands only detectable at 80 bars. These two bands can be BTEX degraders present at elevated pressure or species that become dominant at a later stage in the degradation process. At 340 bars the lowest number of bands was seen, and these bands were not seen at the other pressures. This indicates that when compressing a bacterial community found at 8 bars to 340 bars, fewer species tolerate the high pressure.

When inorganic nutrient solutions, amino acid solution and vitamin solution are added in excess to seawater inoculums, an initial increase in cell number is seen. This increase can be explained by

bacteria utilising the DOC pool commonly found in seawater as carbon source when other growth factors become available.

Volume used in the test bottles seems to influence the length of the lag phase, with a smaller volume having a longer lag phase than a test performed on a larger volume. Because the different bottles were filled with the same inoculums, the same bacterial community will be present. The difference between large and small volumes will be that the total amount of bacteria present will increase when volume increases. Hence the time needed for the biomass to multiply to a level where degradation can be seen will be shorter in a larger inoculum volume.

BTEX will absorb into nalgene tubes made of FEP polymers. Absorption is highest for ethylbenzene and lowest for benzene, thus associated with ethyl and methyl groups connected to the aromatic ring structure. When pressure increases, absorption decreases because absorption causes the volume of the polymere to increase. Because of this absorption/desorption process degradation curves seen in an experiment using FEP tubes are slightly different from normal batch culture biodegradation curves. When the substrate concentration becomes low enough, desorption will maintain the equilibrium between the polymer phase and the water phase, and substrate will be released into the water phase.

Weaknesses in the experimental method used in this work include the lack of continuous monitoring. Without continuous monitoring it is impossible to detect the exact moment the exponential phase starts, and sampling at the right moments in the growth curve is difficult. The seawater used in the experiment is collected from 80 meters depth, hence the bacteria used at elevated pressures are not initially piezophilic. Different behaviour can thus not be excluded for an inoculum collected from the deep-sea.

To check for reproducibility in the results from this research more experiments should be done. Further work should also focus on extending the numbers of substrates tested, and to improve the experimental method utilised in this work. Because of similarities between psychrophilic and piezophilic bacteria arctic seawater could be used to get closer to the actual ecology in the deep-sea. The number of pressures analysed should be expanded, and several pressures between 1 bar and 80 bars should be analysed to find the point where pressure becomes a factor affecting biodegradation.

7 References

ABE, F. 2007. Exploration of the effects of high hydrostatic pressure on microbial growth, physiology and survival: Perspectives from piezophysiology. *Bioscience Biotechnology and Biochemistry,* 71**,** 2347-2357.

ABE, F. & HORIKOSHI, K. 2000. Tryptophan permease gene TAT2 confers high-pressure growth in Saccharomyces cerevisiae. *Molecular and Cellular Biology,* 20**,** 8093-8102.

ALEXANDER, M. 1999. *Biodegradation and bioremediation,* San Diego, Academic Press.

ALLEN, E. E., FACCIOTTI, D. & BARTLETT, D. H. 1999. Monounsaturated but not polyunsaturated fatty acids are required for growth of the deep-sea bacterium Photobacterium profundum SS9 at high pressure and low temperature. *Applied and Environmental Microbiology,* 65**,** 1710-1720.

ALPAS, H., LEE, J., BOZOGLU, F. & KALETUNC, G. 2003. Evaluation of high hydrostatic pressure sensitivity of Staphylococcus aureus and Escherichia coli O157 : H7 by differential scanning calorimetry. *International Journal of Food Microbiology,* 87**,** 229-237.

ANNWEILER, E., RICHNOW, H. H., ANTRANIKIAN, G., HEBENBROCK, S., GARMS, C., FRANKE, S., FRANCKE, W. & MICHAELIS, W. 2000. Naphthalene degradation and incorporation of naphthalene-derived carbon into biomass by the thermophile Bacillus thermoleovorans. *Applied and Environmental Microbiology,* 66**,** 518-523.

ARÍSTEGUI, J., GASOL, J. M., DUARTE, C. M. & HERNDL, G. J. 2009. Microbial oceanography of the dark ocean's pelagic realm. *Limnology and Oceanography,* 54**,** 1501-1529.

BARTLETT, D. H. 2002. Pressure effects on in vivo microbial processes. *Biochimica Et Biophysica Acta-Protein Structure and Molecular Enzymology,* 1595**,** 367-381.

BARTLETT, D. H., FERGUSON, G. & VALLE, G. 2008. Adaptions of the psychrotolerant piezophile *Photobacterium profundum* strain SS9. *In:* MICHIELS, C., BARTLETT, D. H. & AERTSEN, A. (eds.) *High-pressure microbiology.* Washington, DC: ASM Press.

BERGER, W. & WEFER, G. 1991. Productivity of the glacial ocean: Discussion of the iron hypothesis. *Limnology and Oceanography,* 36**,** 1899-1918.

BIANCHI, A. & GARCIN, J. 1994. Bacterial response to hydrostatic-pressure in seawater samples collected in mixed-water and stratified-water conditions. *Marine Ecology-Progress Series,* 111**,** 137-141.

BIANCHI, A., GARCIN, J. & THOLOSAN, O. 1999. A high-pressure serial sampler to measure microbial activity in the deep sea. *Deep-Sea Research Part I-Oceanographic Research Papers,* 46**,** 2129-2142.

BIDLE, K. A. & BARTLETT, D. H. 1999. RecD function is required for high-pressure growth of a deep-sea bacterium. *Journal of Bacteriology,* 181**,** 2330-2337.

CAMILLI, R., REDDY, C. M., YOERGER, D. R., VAN MOOY, B. A. S., JAKUBA, M. V., KINSEY, J. C., MCINTYRE, C. P., SYLVA, S. P. & MALONEY, J. V. 2010. Tracking Hydrocarbon Plume Transport and Biodegradation at Deepwater Horizon. *Science,* 330**,** 201-204.

CAMPANARO, S., VEZZI, A., VITULO, N., LAURO, F. M., D'ANGELO, M., SIMONATO, F., CESTARO, A., MALACRIDA, G., BERTOLONI, G., VALLE, G. & BARTLETT, D. H. 2005. Laterally transferred elements and high pressure adaptation in Photobacterium profundum strains. *Bmc Genomics,* 6.

CHASTAIN, R. A. & YAYANOS, A. A. 1991. Ultrastructural changes in an obligately barophilic marine bacterium after decompression. *Applied and Environmental Microbiology,* 57**,** 1489-1497.

DANIELSON, J. & MITTAPALLI, S. 2010. *Syringate Graphical Pathway Map* [Online]. University of Minesota - Biocatalysis/Biodegradation Database. Available: http://umbbd.msi.umn.edu/syr/syr_image_map.html [Accessed 27.04. 2011].

DANIELSON, J. & MITTAPALLI, S. 2011. *Syringate Pathway Map* [Online]. University of Minesota - Biocatalysis/Biodegradation Database. Available: http://umbbd.msi.umn.edu/syr/syr_map.html [Accessed 27.04. 2011].

DELONG, E. F. & YAYANOS, A. A. 1986. Biochemical function and ecological significance of novel bacterial lipids in deep-sea procaryotes. *Applied and Environmental Microbiology,* 51**,** 730-737.

DELONG, E. F. & YAYANOS, A. A. 1987. Properties of the glucose transport system in some deep-sea bacteria. *Applied and Environmental Microbiology,* 53**,** 527-532.

DEMING, J. W. & COLWELL, R. R. 1985. Observations of barophilic microbial activity in samples of sediment and intercepted particulates from the Demerara abyssal plain. *Applied and Environmental Microbiology,* 50**,** 1002-1006.

DORI, Y., OH, D. J., STEPHENS, S. & TURNBULL, M. 2011. *Vanillin Pathway Map* [Online]. University of Minesota - Biocatalysis/Biodegradation Database. Available: http://umbbd.msi.umn.edu/van/van_map.html [Accessed 27.04 2011].

EATON, R. W. & CHAPMAN, P. J. 1992. Bacterial metabolism of naphthalene: construction and use of recombinant bacteria to study ring cleavage of 1,2-dihydroxynaphthalene and subsequent reactions. *Journal of Bacteriology,* 174**,** 7542-7554.

ELVERT, M., SUESS, E., GREINERT, J. & WHITICAR, M. J. 2000. Archaea mediating anaerobic methane oxidation in deep-sea sediments at cold seeps of the eastern Aleutian subduction zone. *Organic Geochemistry,* 31**,** 1175-1187.

EPPINK, M. H. M., BOEREN, S. A., VERVOORT, J. & VANBERKEL, W. J. H. 1997. Purification and properties of 4-hydroxybenzoate 1-hydroxylase (decarboxylating), a novel flavin adenine dinculeotide-dependent monooxygenase from Candida parapsilosis CBS604. *Journal of Bacteriology,* 179**,** 6680-6687.

FANG, J., ZHANG, L. & BAZYLINSKI, D. A. 2010. Deep-sea piezosphere and piezophiles: geomicrobiology and biogeochemistry. *Trends in Microbiology,* 18**,** 413-422.

FENG, J. 2010. *Benzoate Pathway* [Online]. University of Minnesota - Biocatalysis/Biodegradation database. Available: http://umbbd.msi.umn.edu/benz2/benz2_map.html [Accessed 27.04. 2011].

FENG, J. 2011. *Benzoate Graphical Pathway Map* [Online]. University of Minnesota - Biocatalysis/Biodegradation database. Available: http://umbbd.msi.umn.edu/benz2/benz2_image_map.html [Accessed 27.04. 2011].

FUKUDA, H., SOHRIN, R., NAGATA, T. & KOIKE, I. 2007. Size distribution and biomass of nanoflagellates in meso- and bathypelagic layers of the subarctic Pacific. *Aquatic Microbial Ecology,* 46**,** 203-207.

HAZEN, T. C., DUBINSKY, E. A., DESANTIS, T. Z., ANDERSEN, G. L., PICENO, Y. M., SINGH, N., JANSSON, J. K., PROBST, A., BORGLIN, S. E., FORTNEY, J. L., STRINGFELLOW, W. T., BILL, M., CONRAD, M. E., TOM, L. M., CHAVARRIA, K. L., ALUSI, T. R., LAMENDELLA, R., JOYNER, D. C., SPIER, C., BAELUM, J., AUER, M., ZEMLA, M. L., CHAKRABORTY, R., SONNENTHAL, E. L., D'HAESELEER, P., HOLMAN, H.-Y. N., OSMAN, S., LU, Z., VAN NOSTRAND, J. D., DENG, Y., ZHOU, J. & MASON, O. U. 2010. Deep-Sea Oil Plume Enriches Indigenous Oil-Degrading Bacteria. *Science,* 330**,** 204-208.

HERNDL, G. J., REINTHALER, T., TEIRA, E., VAN AKEN, H., VETH, C., PERNTHALER, A. & PERNTHALER, J. 2005. Contribution of Archaea to total prokaryotic production in the deep Atlantic Ocean. *Applied and Environmental Microbiology,* 71**,** 2303-2309.

HEWSON, I., STEELE, J. A., CAPONE, D. G. & FUHRMAN, J. A. 2006. Remarkable heterogeneity in meso- and bathypelagic bacterioplankton assemblage composition. *Limnology and Oceanography,* 51**,** 1274-1283.

KANEHISA LABORATORIES. 2011. *Tyrosine metabolism - Reference pathway* [Online]. Kyoto Encyclopedia of Genes and Genomes. Available: http://www.genome.jp/kegg-bin/show_pathway?map00350 [Accessed 20.04 2011].

KANEKO, H., TAKAMI, H., INOUE, A. & HORIKOSHI, K. 2000. Effects of hydrostatic pressure and temperature on growth and lipid composition of the inner membrane of barotolerant Pseudomonas sp BT1 isolated from the deep-sea. *Bioscience Biotechnology and Biochemistry,* 64**,** 72-79.

KATO, C., LI, L., NOGI, Y., NAKAMURA, Y., TAMAOKA, J. & HORIKOSHI, K. 1998. Extremely barophilic bacteria isolated from the Mariana Trench, Challenger Deep, at a depth of 11,000 meters. *Applied and Environmental Microbiology,* 64**,** 1510-1513.

KATO, C., NOGI, Y. & ARAKAWA, S. 2008. Isolation, cultivation, and diversity of deep-sea piezophiles. *In:* MICHIELS, C., BARTLETT, D. H. & AERTSEN, A. (eds.) *High-pressure microbiology.* Washington, DC: ASM Press.

KESSLER, J. D., VALENTINE, D. L., REDMOND, M. C., DU, M. R., CHAN, E. W., MENDES, S. D., QUIROZ, E. W., VILLANUEVA, C. J., SHUSTA, S. S., WERRA, L. M., YVON-LEWIS, S. A. & WEBER, T. C. 2011. A Persistent Oxygen Anomaly Reveals the Fate of Spilled Methane in the Deep Gulf of Mexico. *Science,* 331**,** 312-315.

KOLB, B. & ETTRE, L. S. 2006. *Static headspace-gas chromatography: theory and practice,* Hoboken, Wiley-Interscience.

KRAUS, D., MARCONI, A., LIND, K. E. & MCLEISH, R. 2011. *Styrene pathway map* [Online]. University of Minesota - Biocatalysis/Biodegradation Database. Available: http://umbbd.msi.umn.edu/sty/sty_map.html [Accessed 08.03. 2011].

LALLI, C. M. & PARSONS, T. R. 1997. *Biological oceanography: an introduction,* Oxford, Butterworth-Heinemann.

LAMPITT, R. S. 2001. Marine Snow. *In:* JOHN, H. S. (ed.) *Encyclopedia of Ocean Sciences.* Oxford: Academic Press.

LAURO, F. M. & BARTLETT, D. H. 2008. Prokaryotic lifestyles in deep sea habitats. *Extremophiles,* 12**,** 15-25.

LAURO, F. M., CHASTAIN, R. A., BLANKENSHIP, L. E., YAYANOS, A. A. & BARTLETT, D. H. 2007. The unique 16S rRNA genes of piezophiles reflect both phylogeny and adaptation. *Applied and Environmental Microbiology,* 73**,** 838-845.

LÓPEZ-GARCÍA, P., LÓPEZ-LÓPEZ, A., MOREIRA, D. & RODRÍGUEZ-VALERA, F. 2001. Diversity of free-living prokaryotes from a deep-sea site at the Antarctic Polar Front. *Fems Microbiology Ecology,* 36**,** 193-202.

LUNDSTEN, L., PAULL, C. K., SCHLINING, K. L., MCGANN, M. & USSLER, W. 2010. Biological characterization of a whale-fall near Vancouver Island, British Columbia, Canada. *Deep-Sea Research Part I-Oceanographic Research Papers,* 57**,** 918-922.

MADIGAN, M. T., MARTINKO, J. M., DUNLAP, P. V. & CLARK, D. P. 2009. *Brock Biology of microorganisms,* San Francisco, Pearson Benjamin Cummings.

MCLEISH, R. 2005. *From cis-Dihydrobenzenediol to Catechol* [Online]. University of Minesota - Biocatalysis/Biodegradation Database. Available: http://umbbd.msi.umn.edu/servlets/pageservlet?ptype=r&reacID=r0080 [Accessed 20.04 2011].

MCLEISH, R. 2006a. *Ethylbenzene pathway map* [Online]. University of Minesota - Biocatalysis/Biodegradation Database. Available: http://umbbd.msi.umn.edu/ethb2/ethb2_map.html [Accessed 08.03. 2011].

MCLEISH, R. 2006b. *Styrene Graphical Pathway Map (1)* [Online]. University of Minesota - Biocatalysis/Biodegradation Database. Available: http://umbbd.msi.umn.edu/sty/sty_image_map.html [Accessed 27.04. 2011].

MCLEISH, R. 2006c. *Styrene Graphical Pathway Map (2)* [Online]. University of Minesota - Biocatalysis/Biodegradation Database. Available: http://umbbd.msi.umn.edu/sty/sty_image_map2.html [Accessed 27.04. 2011].

MCLEISH, R. 2011. *Ethylbenzene pathway map* [Online]. University of Minesota - Biocatalysis/Biodegradation Database. Available: http://umbbd.msi.umn.edu/ethb2/ethb2_map.html [Accessed 08.03. 2011].

MCLEISH, R. & WOLFE, M. 2005. *From Benzene to cis-Dihydrobenzenediol* [Online]. University of Minnesota - Biocatalysis/Biodegradation Database. Available: http://umbbd.msi.umn.edu/servlets/pageservlet?ptype=r&reacID=r0079 [Accessed 20.04 2011].

MCTAVISH, H. 2011. *Nitrobenzene Pathway Map* [Online]. University of Minesota - Biocatalysis/Biodegradation Database. Available: http://umbbd.msi.umn.edu/nb/nb_map.html [Accessed 27.04. 2011].

MCTAVISH, H., ROE, D. & ESSENBERG, C. 2010. *Nitrobenzene graphical pathway map* [Online]. University of Minesota - Biocatalysis/Biodegradation Database. Available: http://umbbd.msi.umn.edu/nb/nb_image_map.html [Accessed 20.04 2011].

MOESENEDER, M. M., WINTER, C. & HERNDL, G. J. 2001. Horizontal and vertical complexity of attached and free-living bacteria of the eastern Mediterranean Sea, determined by 16S rDNA and 16S rRNA fingerprints. *Limnology and Oceanography,* 46**,** 95-107.

MORRIS, R. M., RAPPE, M. S., URBACH, E., CONNON, S. A. & GIOVANNONI, S. J. 2004. Prevalence of the Chloroflexi-related SAR202 bacterioplankton cluster throughout the mesopelagic zone and deep ocean. *Applied and Environmental Microbiology,* 70**,** 2836-2842.

MUYZER, G., DE WAAL, E. C. & UITTERLINDEN, A. G. 1993. Profiling of complex microbial populations by denaturing gradient gel electrophoresis analysis of polymerase chain reaction-amplified genes coding for 16S rRNA. *Applied and Environmental Microbiology,* 59**,** 695-700.

MUYZER, G. & SMALLA, K. 1998. Application of denaturing gradient gel electrophoresis (DGGE) and temperature gradient gel electrophoresis (TGGE) in microbial ecology. *Antonie van Leeuwenhoek,* 73**,** 127-141.

NAGATA, T., FUKUDA, H., FUKUDA, R. & KOIKE, I. 2000. Bacterioplankton distribution and production in deep Pacific waters: Large-scale geographic variations and possible coupling with sinking particle fluxes. *Limnology and Oceanography,* 45**,** 426-435.

NAGATA, T., TAMBURINI, C., ARÍSTEGUI, J., BALTAR, F., BOCHDANSKY, A. B., FONDA-UMANI, S., FUKUDA, H., GOGOU, A., HANSELL, D. A., HANSMAN, R. L., HERNDL, G. J., PANAGIOTOPOULOS, C., REINTHALER, T., SOHRIN, R., VERDUGO, P., YAMADA, N., YAMASHITA, Y., YOKOKAWA, T. & BARTLETT, D. H. 2010. Emerging concepts on microbial processes in the bathypelagic ocean - ecology, biogeochemistry, and genomics. *Deep-Sea Research Part Ii-Topical Studies in Oceanography,* 57**,** 1519-1536.

NOGI, Y., HOSOYA, S., KATO, C. & HORIKOSHI, K. 2007. Psychromonas hadalis sp nov., a novel plezophilic bacterium isolated from the bottom of the Japan Trench. *International Journal of Systematic and Evolutionary Microbiology,* 57**,** 1360-1364.

NOGI, Y. & KATO, C. 1999. Taxonomic studies of extremely barophilic bacteria isolated from the Mariana Trench and description of Moritella yayanosii sp. nov., a new barophilic bacterial isolate. *Extremophiles,* 3**,** 71-77.

NOGI, Y., KATO, C. & HORIKOSHI, K. 1998a. Taxonomic studies of deep-sea barophilic Shewanella strains and description of Shewanella violacea sp. nov. *Archives of Microbiology,* 170**,** 331-338.

NOGI, Y., MASUI, N. & KATO, C. 1998b. Photobacterium profundum sp. nov., a new, moderately barophilic bacterial species isolated from a deep-sea sediment. *Extremophiles,* 2**,** 1-7.

O'NEIL, M. J. 2001. *The Merck index: an encyclopedia of chemicals, drugs, and biologicals,* Whitehouse Station, N.J., Merck & Co.

OH, D. J. 2006. *Toluene Graphical Pathway Map (2)* [Online]. University of Minesota - Biocatalysis/Biodegradation Database. Available: http://umbbd.msi.umn.edu/tol/tol_image_map2.html [Accessed 20.04 2011].

OH, D. J. 2009. *o-Xylene Graphical Pathway Map* [Online]. University of Minesota - Biocatalysis/Biodegradation Database. Available: http://umbbd.msi.umn.edu/oxy/oxy_image_map.html [Accessed 29.04. 2011].

OH, D. J., STEPHENS, S. & TURNBULL, M. 2008. *Vanillin Graphical Pathway Map* [Online]. University of Minesota - Biocatalysis/Biodegradation Database. Available: http://umbbd.msi.umn.edu/van/van_image_map.html [Accessed 27.04. 2011].

OH, D. J. & TURNBULL, M. 2009. *o-Xylene Pathway Map* [Online]. University of Minesota - Biocatalysis/Biodegradation Database. Available: http://umbbd.msi.umn.edu/oxy/oxy_map.html [Accessed 29.04. 2011].

OLSEN, R. H., KUKOR, J. J. & KAPHAMMER, B. 1994. A novel toluene-3-monooxygenase pathway cloned from Pseudomonas pickettii PKO1. *Journal of Bacteriology,* 176**,** 3749-3756.

PRAHL, S. & LINDSEY, J. 2011. *Naphthalene* [Online]. Oregon Medical Laser Center. Available: http://omlc.ogi.edu/spectra/PhotochemCAD/html/naphthalene.html [Accessed 28.06. 2011].

PRIEUR, D., ERAUSO, G. & JEANTHON, C. 1995. Hyperthermophilic life at deep-sea hydrothermal vents. *Planetary and Space Science,* 43**,** 115-122.

SCHWARTZ, J. R., WALKER, J. D. & COLWELL, R. R. 1974. Deep-sea bacteria: growth and utilization of hydrocarbons at ambient and in situ pressure. *Applied Microbiology,* 28**,** 982-986.

SCHÄFER, H. & MUYZER, G. 2001. Denaturing gradient gel electrophoresis in marine microbial ecology. *In:* PAUL, J. H. (ed.) *Marine microbiology.* San Diego: Academic Press.

SHERR, B., SHERR, E. & DEL GIORGION, P. 2001. Enumeration of total and highly active bacteria. *In:* PAUL, J. H. (ed.) *Marine microbiology.* San Diego: Academic Press.

SIMONATO, F., CAMPANARO, S., LAURO, F. M., VEZZI, A., D'ANGELO, M., VITULO, N., VALLE, G. & BARTLETT, D. H. 2006. Piezophilic adaptation: a genomic point of view. *Journal of Biotechnology,* 126**,** 11-25.

SKOOG, D. A., HOLLER, F. J. & CROUCH, S. R. 2007. *Principles of instrumental analysis,* Belmont, Thomson Brooks/Cole.

TANG, G. Q., TANAKA, N. & KUNUGI, S. 1998. In vitro increases in plasmid DNA supercoiling by hydrostatic pressure. *Biochimica Et Biophysica Acta-Gene Structure and Expression,* 1443**,** 364-368.

THOLOSAN, O., GARCIN, J. & BIANCHI, A. 1999. Effects of hydrostatic pressure on microbial activity through a 2000 m deep water column in the NW Mediterranean Sea. *Marine Ecology-Progress Series,* 183**,** 49-57.

UAD, I., SILVA-CASTRO, G. A., POZO, C., GONZÁLEZ-LÓPEZ, J. & CALVO, C. 2010. Biodegradative potential and characterization of bioemulsifiers of marine bacteria isolated from samples of seawater, sediment and fuel extracted at 4000 m of depth (Prestige wreck). *International Biodeterioration & Biodegradation,* 64**,** 511-518.

UNIVERSITY OF MINNESOTA. 2006a. *Ethylbenzene Graphical Pathway Map* [Online]. University of Minesota - Biocatalysis/Biodegradation Database. Available: http://umbbd.msi.umn.edu/ethb2/ethb2_image_map.html [Accessed 27.04. 2011].

UNIVERSITY OF MINNESOTA. 2006b. *Toluene Graphical Pathway Map (1)* [Online]. University of Minesota - Biocatalysis/Biodegradation Database. Available: http://umbbd.msi.umn.edu/tol/tol_image_map1.html [Accessed 20.04 2011].

VALENTINE, D. L., KESSLER, J. D., REDMOND, M. C., MENDES, S. D., HEINTZ, M. B., FARWELL, C., HU, L., KINNAMAN, F. S., YVON-LEWIS, S., DU, M., CHAN, E. W., TIGREROS, F. G. & VILLANUEVA, C. J. 2010. Propane Respiration Jump-Starts Microbial Response to a Deep Oil Spill. *Science,* 330**,** 208-211.

VARELA, M. M., VAN AKEN, H. M. & HERNDL, G. J. 2008. Abundance and activity of Chloroflexi-type SAR202 bacterioplankton in the meso- and bathypelagic waters of the (sub)tropical Atlantic. *Environmental Microbiology,* 10**,** 1903-1911.

WACKETT, L. P. & ELLIS, L. B. M. 1996. The University of Minnesota Biocatalysis/Biodegradation Database: A novel microbiological method on the World Wide Web. *Journal of Microbiological Methods,* 25**,** 91-93.

WALKER, C. H., HOPKIN, S. P., SIBLY, R. M. & PEAKALL, D. B. 2006. *Principles of ecotoxicology,* Boca Raton, Fla., CRC Taylor & Francis.

WALPOLE, R. E., MYERS, R. H., MYERS, S. L. & YE, K. 2007. *Probability & statistics for engineers & scientists,* London, Pearson Education International.

WELCH, T. J. & BARTLETT, D. H. 1998. Identification of a regulatory protein required for pressure-responsive gene expression in the deep-sea bacterium Photobacterium species strain SS9. *Molecular Microbiology,* 27**,** 977-985.

WHITMAN, W. B., COLEMAN, D. C. & WIEBE, W. J. 1998. Prokaryotes: The unseen majority. *Proceedings of the National Academy of Sciences of the United States of America,* 95**,** 6578-6583.

YANAGIBAYASHI, M., NOGI, Y., LI, L. & KATO, C. 1999. Changes in the microbial community in Japan Trench sediment from a depth of 6292 m during cultivation without decompression. *Fems Microbiology Letters,* 170**,** 271-279.

YANO, Y., NAKAYAMA, A., ISHIHARA, K. & SAITO, H. 1998. Adaptive changes in membrane lipids of barophilic bacteria in response to changes in growth pressure. *Applied and Environmental Microbiology,* 64**,** 479-485.

YAYANOS, A. A. 1995. Microbiology to 10,500 meters in the deep-sea. *Annual Review of Microbiology,* 49**,** 777-805.

ZABALLOS, M., LOPEZ-LOPEZ, A., OVREAS, L., BARTUAL, S. G., D'AURIA, G., ALBA, J. C., LEGAULT, B., PUSHKER, R., DAAE, F. L. & RODRIGUEZ-VALERA, F. 2006. Comparison of prokaryotic diversity at offshore oceanic locations reveals a different microbiota in the Mediterranean Sea. *Fems Microbiology Ecology,* 56**,** 389-405.

ZAMANIAN, M. & MASON, J. R. 1987. Benzene dioxygenase in Pseudomonas putida: Subunit composition and immuno-cross-reactivity with other aromatic dioxygenases. *Biochemical Journal,* 244**,** 611-616.

ZENG, Y. 2011. *Toluene Pathway Map* [Online]. University of Minesota - Biocatalysis/Biodegradation Database. Available: http://umbbd.msi.umn.edu/tol/tol_map.html [Accessed 20.04 2011].

ZENG, Y. & ESSENBERG, C. 2010. *Naphthalene graphical pathway map* [Online]. University of Minesota - Biocatalysis/Biodegradation Database. Available: http://umbbd.msi.umn.edu/naph/naph_map.html [Accessed 08.03. 2011].

ZOBELL, C. & JOHNSON, F. 1949. The influence of hydrostatic pressure on the growth and viability of terrestrial and marine bacteria. *Journal of Bacteriology,* 57**,** 179.

ZOBELL, C. E. & COBET, A. B. 1962. Growth, reproduction, and death rates of Escherichia coli at increased hydrostatic pressures. *Journal of Bacteriology,* 84**,** 1228.

ZOBELL, C. E. & COBET, A. B. 1964. Filament formation by Escherichia coli at increased hydrostatic pressures. *Journal of Bacteriology,* 87**,** 710.

ZOBELL, C. E. & OPPENHEIMER, C. H. 1950. Some effects of hydrostatic pressure on the multiplication and morphology of marine bacteria. *Journal of Bacteriology,* 60**,** 771.

8 Appendix

The following chapter contains figures, tables and data used in results and discussion.

8.1 Naphthalene calibration

Table 8-1 show the data obtained in the calibration experiment and the calculated residuals from the regression model. Table 8-2 show the regression model in the calibration when the intercept is not assumed to be 0. Table 8-3 show the regression model in the calibration experiment when the intercept is assumed to be zero. Chromatogram obtained in carryover analysis is shown in Figure 8-1.

Table 8-1: Concentration, area obtained, observation number and calculated residual from regression analysis were intercept coefficient is zero for calibration analysis.

Concentration [mg/l]	Area	Observation number	Residual
0.00000	35 634	1	35 634
0.00000	113 833	7	113 833
0.00000	104 944	13	104 944
0.00000	102 831	19	102 831
0.00000	98 549	25	98 549
0.01004	38 252	2	30 552
0.01004	59 950	8	52 250
0.01004	61 700	14	54 000
0.01004	54 618	20	46 918
0.01004	50 938	26	43 238
0.05022	72 145	3	33 643
0.05022	77 232	9	38 730
0.05022	75 724	15	37 222
0.05022	68 408	21	29 906
0.05022	74 498	27	35 996
0.5022	482 172	4	97 149
0.5022	398 301	10	13 278
0.5022	460 303	16	75 280
0.5022	428 853	22	43 830
0.5022	385 160	28	137
2.009	1 718 562	5	178 471
2.009	1 799 649	11	259 558
2.009	1 522 205	17	-17 886
2.009	1 344 112	23	-195 979
2.009	1 435 806	29	-104 285
10.04	8 282 247	6	581 792
10.04	8 754 786	12	1 054 331
10.04	7 780 644	18	80 189
10.04	7 732 500	24	32 045
10.04	5 915 535	30	-1 784 920

Table 8-2: Data from regression analysis of calibration data

Regression statistics	
Multiple R	0.9896
R-squared	0.9793
Adjusted R-squared	0.9785
Standard error	414503
Observation	30

Variance analysis

	df	*SS*	*MS*	*F*	*Signifkans-F*
Regression (R)	1	2.27E+14	2.27E+14	1323.42	4.05E-25
Residuals (E)	28	4.81E+12	1.72E+11		
Total (T)	29	2.32E+14			

	Coefficient	*Standard error*	*t-Stat*	*P-value*	*Lower 95%*	*Upper 95%*
Intercept	52208	87513	0.5966	0.5556	-127055	231470
Concentration	760486	20905	36.38	4.05E-25	717664	803307

Table 8-3: Data from regression analysis of calibration data when intercept coefficient is 0

Regression statistics	
Multiple R	0.9922
R-squared	0.9845
Adjusted R-squared	0.9500
Standard error	409874
Observations	30

Variance analysis

	Df	*SS*	*MS*	*F*	*Signifkans-F*
Regression (R)	1	3.09E+14	3.09E+14	1839.88	4.35E-27
Residuals (E)	29	4.87E+12	1.68E+11		
Total (T)	30	3.14E+14			

	Coefficients	*Standard error*	*t-Stat*	*P-value*	*Lower 95%*	*Upper 95%*
Intercept	0	#I/T	#I/T	#I/T	#I/T	#I/T
Concentration	766749	17876	42.89	8.65E-28	730189	803308

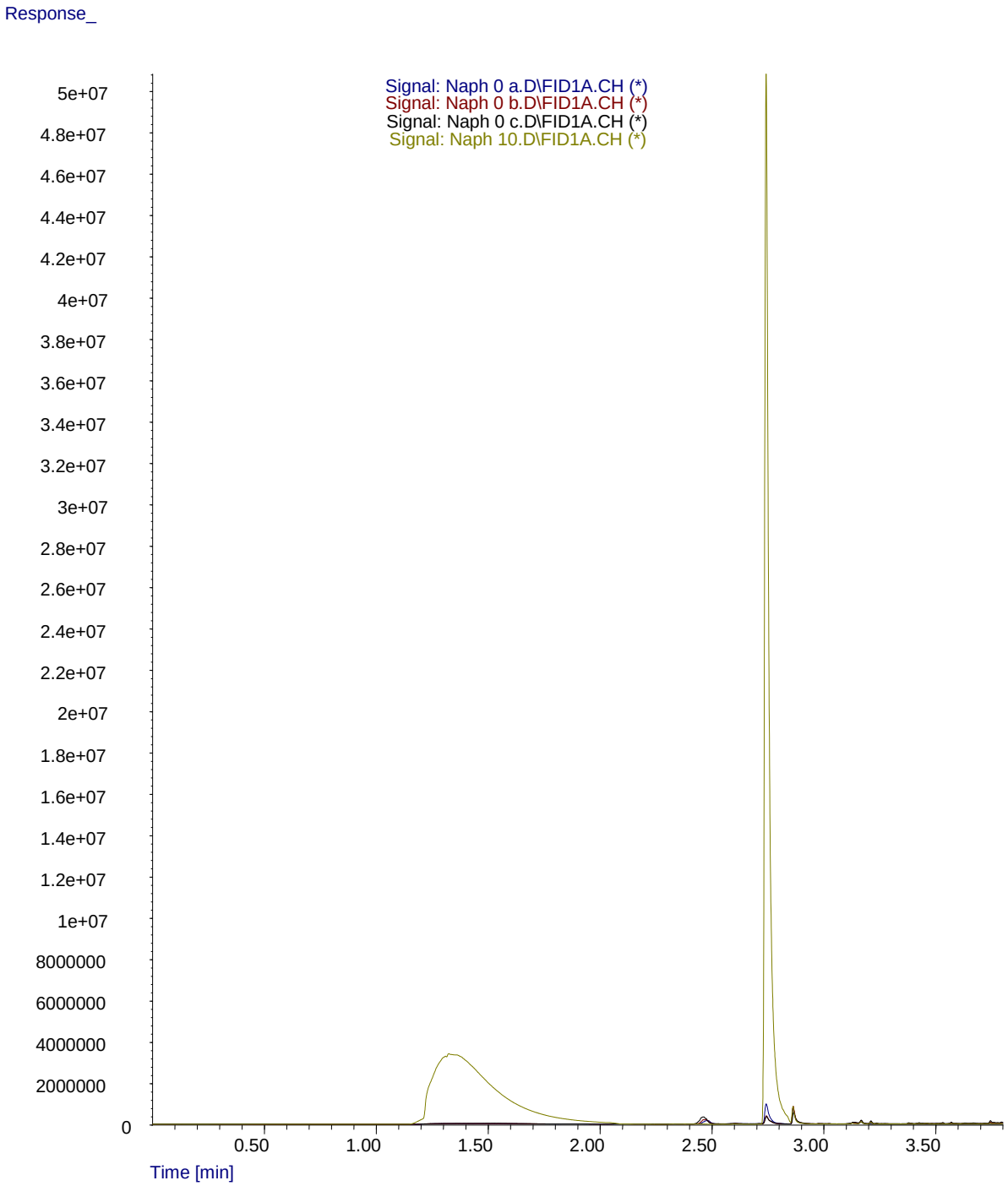

Figure 8-1: Chromatogram for the naphthalene calibration working standard (Naph 10) and three blank samples in the carryover analysis. Response on the y-axis is the peak area, the x-axis is retention time in minutes

8.2 BTEX calibration

The regression analysis tool in excel was used to analyse the data from the BTEX calibration run. First a simple linear regression was used for all 30 data point (Table 8-4). Here p-values for the intercepts are larger than 0.05, the normal significance level used, thus intercepts cannot be assumed to be different from 0. A new regression was hence performed forcing the line through zero (Table 8-5).

Table 8-4: Linear regression for all 30 data points

	Benzene	Toluene	Ethylbenzene	o-Xylene
Intercept	-3 182	-8 849	-12 769	-5 525
p-value intercept	0.9566	0.8778	0.8128	0.9223
Slope	807 576	830 686	829 583	911 666
p-value slope	0.0000	0.0000	0.0000	0.0000

Table 8-5: Linear regression for all 30 data points forced through zero.

	Benzene	Toluene	Ethylbenzene	o-Xylene
Slope	806 835	828 595	826 569	910 380
p-value slope	0.0000	0.0000	0.0000	0.0000

Outlier analysis was performed on the residuals calculated in this regression (Table 8-6). One suspected outlier was identified. For all four substrates this data point was found not to be included in a prediction interval calculated, thus a new regression analysis without this data point was performed (Table 8-7). The intercept was also this time found not to be different from zero, and a last regression analysis forcing the regression line through zero was performed (Table 8-8).

Table 8-6: Outlier analysis on residuals

	Benzene	Toluene	Ethylbenzene	o-Xylene
Suspected outlier	-1 194 273	-1 164 734	-1 078 738	-1 150 684
Prediction interval	[-527 629, 523 452]	[-522 748, 511 143]	[-492 608, 475 847]	[-512 617, 505 365]

Table 8-7: Linear regression without outlier

	Benzene	Toluene	Ethylbenzene	o-Xylene
Intercept	-23 427	-28 703	-31 103	-25 042
p-value intercept	0.1719	0.1166	0.0973	0.1521
Slope	853 527	876 197	871 771	955 967
p-value slope	0.0000	0.0000	0.0000	0.0000

Table 8-8: Linear regression without outlier forced through zero

	Benzene	Toluene	Ethylbenzene	o-Xylene
Slope	847 847	869 136	864 126	949 896
p-value slope	0.0000	0.0000	0.0000	0.0000
R squared	0.9986	0.9985	0.9983	0.9989

8.3 FEP/Glass

Peak area at each sampling time and average peak area measured for BTEX negative control samples taken from glass tubes are shown in Table 8-9. Calculated ratio between average peak area for negative control samples from FEP tubes and glass tubes are shown for 1 bar, 80 bar, 170 bar and 340 bar in respectively Table 8-10, Table 8-11, Table 8-12 and Table 8-13.

Table 8-9: Peak area for negative control samples from glass tubes

Time [d]	Benzene	Toluene	Ethylbenzene	o-Xylene
16.3	4 104 821	4 029 633	3 633 460	4 386 014
20.1	3 883 074	3 762 792	3 162 532	3 909 495
28.0	3 778 912	3 624 111	3 158 114	3 906 050
35.1	3 743 540	3 658 125	3 244 649	3 970 383
38.9	3 969 668	3 833 514	3 353 517	4 155 155
Average	3 896 668 ± 65 633	3 781 635 ±72 325	3 310 454 ± 88 206	4 065 419 ± 92 080

Table 8-10: Ratio between average area measured in negative control samples from FEP tubes at 1 bar and glass tubes

Time [d]	Benzene	Toluene	Ethylbenzene	o-Xylene
16.3	0.93 ± 0.02	0.79 ± 0.02	0.70 ± 0.02	0.79 ± 0.02
20.1	0.83 ± 0.02	0.68 ± 0.02	0.54 ± 0.02	0.64 ± 0.01
28.0	0.82 ± 0.01	0.65 ± 0.01	0.54 ± 0.02	0.64 ± 0.01
35.1	0.80 ± 0.03	0.62 ± 0.02	0.52 ± 0.02	0.61 ± 0.02
38.9	0.83 ± 0.01	0.65 ± 0.02	0.53 ± 0.02	0.63 ± 0.02

Table 8-11: Ratio between average area measured in negative control samples from FEP tubes at 80 bar and glass tubes

Time [d]	Benzene	Toluene	Ethylbenzene	o-Xylene
17.0	0.96 ± 0.03	0.82 ± 0.03	0.74 ± 0.03	0.79 ± 0.03
28.1	0.90 ± 0.08	0.72 ± 0.06	0.62 ± 0.05	0.67 ± 0.05
35.2	0.90 ± 0.03	0.72 ± 0.02	0.61 ± 0.02	0.68 ± 0.02
41.9	0.96 ± 0.02	0.76 ± 0.02	0.63 ± 0.02	0.71 ± 0.02
52.1	0.90 ± 0.02	0.69 ± 0.02	0.57 ± 0.02	0.66 ± 0.02

Table 8-12: Ratio between average area measured in negative control samples from FEP tubes at 170 bar and glass tubes

Time [d]	Benzene	Toluene	Ethylbenzene	o-Xylene
17.1	1.06 ± 0.02	0.92 ± 0.02	0.86 ± 0.03	0.88 ± 0.02
28.1	0.89 ± 0.03	0.75 ± 0.03	0.67 ± 0.03	0.71 ± 0.03
35.2	1.00 ± 0.02	0.83 ± 0.02	0.73 ± 0.02	0.79 ± 0.02
42.1	1.00 ± 0.02	0.81 ± 0.02	0.70 ± 0.02	0.76 ± 0.02
56.0	0.91 ± 0.04	0.73 ± 0.03	0.63 ± 0.02	0.69 ± 0.03

Table 8-13: Ratio between average area measured in negative control samples from FEP tubes at 340 bar and glass tubes

Time [d]	Benzene	Toluene	Ethylbenzene	o-Xylene
20.0	0.99 ± 0.02	0.89 ± 0.02	0.83 ± 0.02	0.88 ± 0.02
35.3	0.99 ± 0.02	0.86 ± 0.02	0.77 ± 0.02	0.82 ± 0.02
45.1	0.93 ± 0.03	0.81 ± 0.03	0.74 ± 0.03	0.80 ± 0.03
55.9	0.95 ± 0.02	0.80 ± 0.02	0.71 ± 0.02	0.79 ± 0.02
60.0	0.92 ± 0.02	0.78 ± 0.02	0.70 ± 0.02	0.78 ± 0.02

8.4 Example chromatogram BTEX

Example of chromatograms obtained for a BTEX sample and BTEX negative control samples are shown in respectively Figure 8-2 and Figure 8-3. The BTEX sample chromatogram shown is from a sampling time in the lag phase.

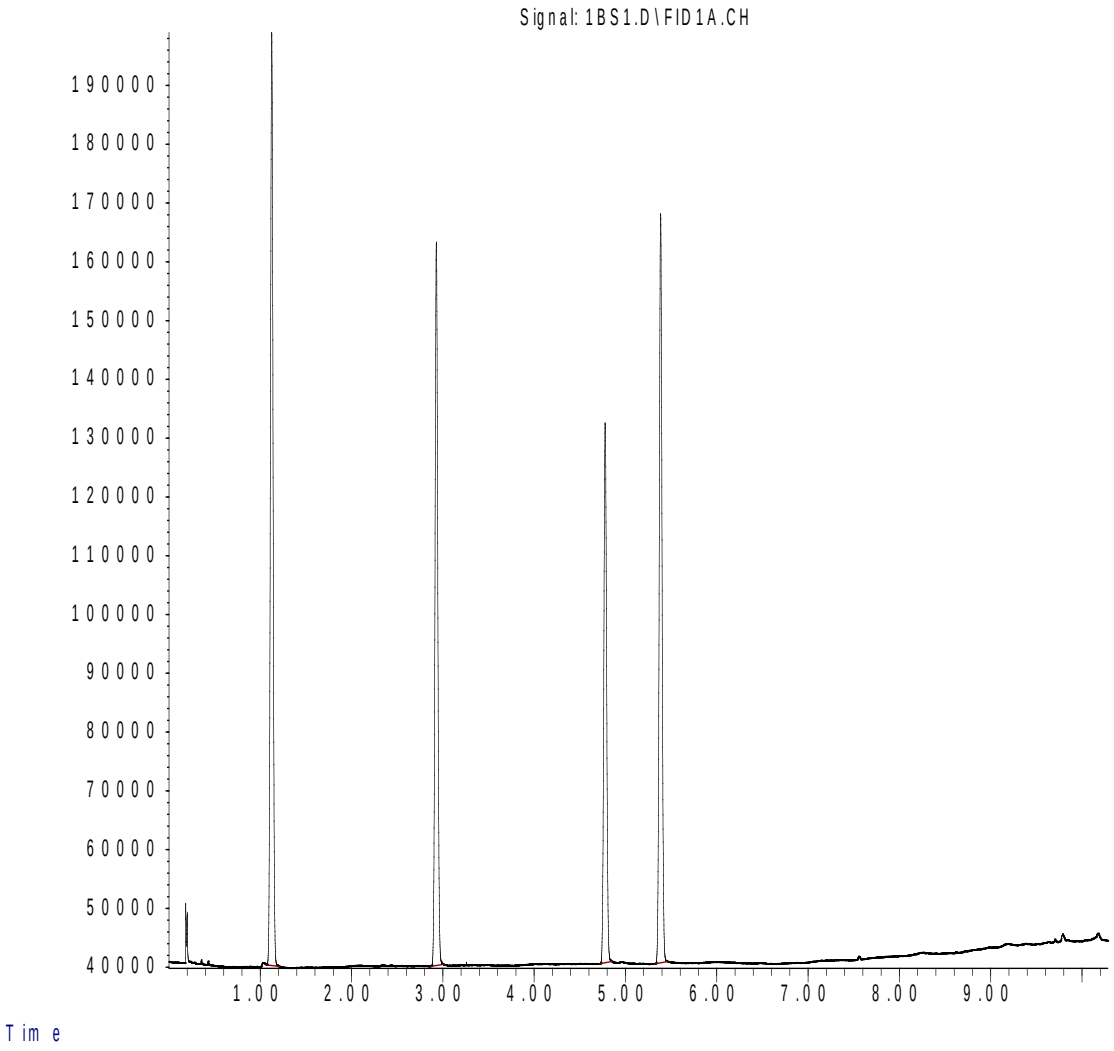

Figure 8-2: BTEX chromatogram from lag phase

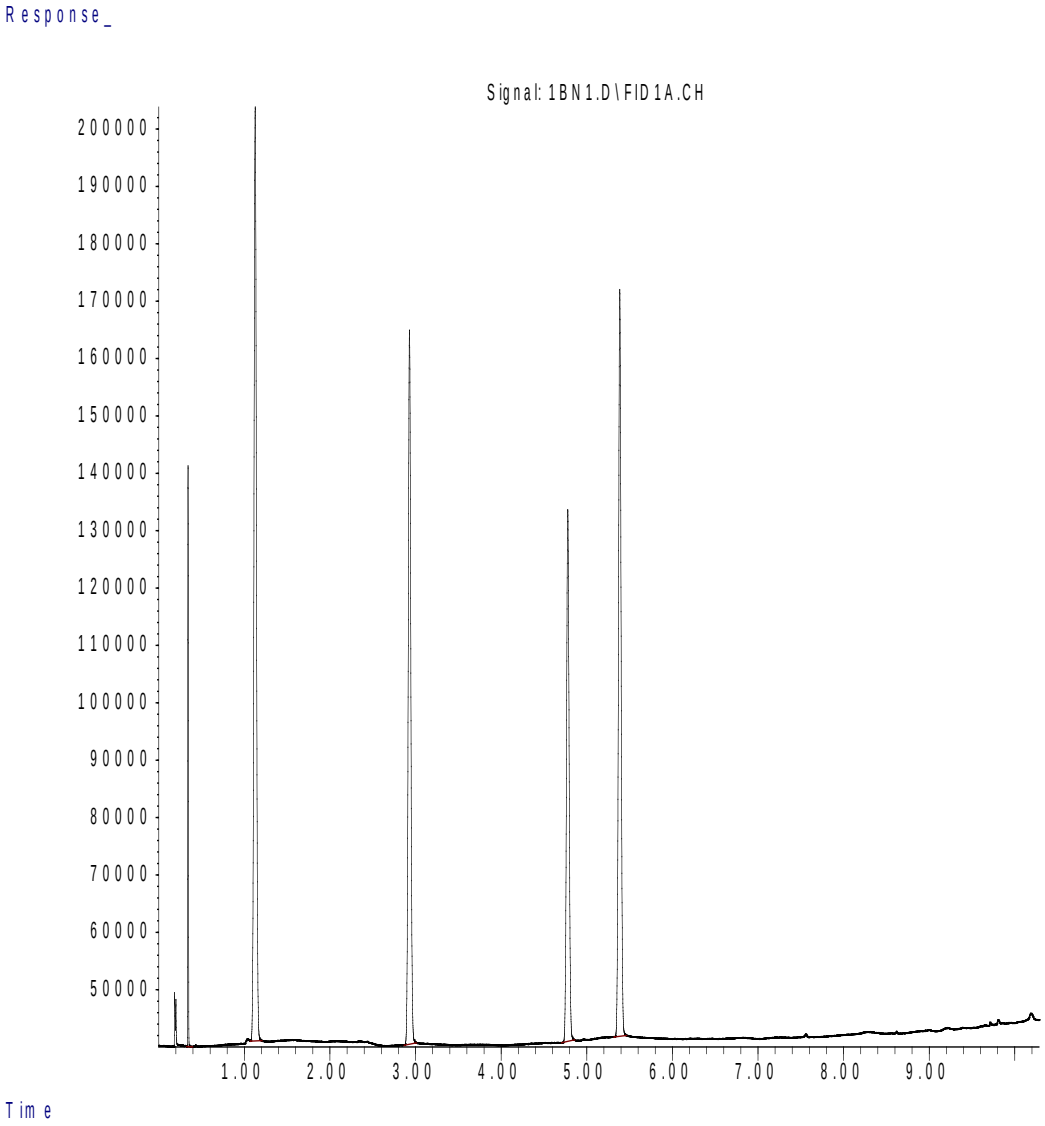

Figure 8-3: BTEX negative control chromatogram